Ethylene Receptor Gain- and Loss-of-function Mutants Reveal an ETR1-dependent Transcriptional Network in Roots

Running head: ETR1-dependent gene regulatory networks in roots

Maleana G. Khoury[1*], Alexandria F. Harkey[1*], Joëlle K. Mühlemann[1,4], Amy L. Olex[2], Maarten Houben[1,4], Brad M. Binder[3], Gloria K. Muday[1]

[1] Wake Forest University, Winston-Salem, NC

[2] Virginia Commonwealth University, Richmond, VA

[3]University of Tennessee, Knoxville, TN

[4]Current Address: KU Leuven, Belgium

*Co-first authors

One sentence summary: Transcriptional responses in *etr1* LOF and GOF mutants reveal an ethylene-mediated ETR1- and EIN3 dependent gene regulatory network that modulates ethylene signaling and synthesis and root development.F

Abstract

In Arabidopsis, a family of five receptors mediates ethylene responses in roots, with Ethylene Response 1 (ETR1) controlling increases in root hair proliferation and decreases in lateral root formation. To define the ETR1-dependent gene regulatory network (GRN) controlling root development, we profiled the root transcriptome from Col-0 and the *etr1-3* gain-of-function and *etr1-7* loss-of-function mutants in the presence and absence of ethylene or the ethylene precursor aminocyclopropane-1-carboxylic acid (ACC). We identified 4,522 differentially expressed (DE) transcripts in Col-0 roots with altered abundance in response to ethylene and/or ACC treatment, most with larger magnitude changes induced by ethylene. These included 553 DE transcripts that were ETR1-dependent, defined by a lack of response to treatment with ethylene and/or ACC in ethylene-insensitive *etr1-3* and constitutively altered in *etr1-7* in the presence and absence of treatment relative to untreated Col-0. Within these ETR1 dependent transcripts were ethylene biosynthesis genes and transcription factors. *ACC OXIDASE 2* (*ACO2)* and *ACO3* convert ACC to ethylene and were ETR1-dependent, and *ACO* promoter fusions were ACC regulated in root tissues in appropriate locations to control root development, with *ACO5* localized to root hairs. Abundance of ETR1-dependent transcripts that were predicted to encode transcription factors and ACOs were examined in Col-0 and an *ein3eil1* mutant with and without ACC treatment, revealing that the ETR1 and EIN3/EIL1 canonical ethylene signaling pathway regulated some, but not all, of these transcriptional responses. Together, these findings reveal features of an ETR1-dependent GRN that controls both ethylene synthesis and root growth and development.

41 **Introduction**

42 Ethylene is a gaseous hormone that modulates growth and development throughout a
43 plant's life cycle, from seed germination to senescence, and controls responses to both biotic and
44 abiotic stress (Abeles et al., 1992; Van de Poel et al., 2015). In young, etiolated seedlings, ethylene
45 induces a triple response: reduced hypocotyl and root elongation, thickening of the hypocotyl, and
46 exaggeration of the apical hook. This triple response phenotype has been the basis of mutant
47 screens in *Arabidopsis thaliana* that have identified key components of the ethylene signaling
48 pathway with ethylene-insensitive or constitutive ethylene signaling phenotypes (Azhar et al.,
49 2020; Schaller and Kieber, 2002). Ethylene also has profound effects on root development,
50 including inhibition of primary root elongation and lateral root formation and stimulation of root
51 hair initiation and elongation (Feng et al., 2017; Harkey et al., 2018; Lewis et al., 2011; Negi et
52 al., 2008; Qin et al., 2019). Many of the proteins that were identified based on their functions in
53 ethylene signaling in etiolated hypocotyls also modulate root development (Khoury et al., 2024b),
54 but with distinct developmental effects downstream of each receptor (Harkey et al., 2018).

55 Ethylene functions through direct binding to members of a family of transmembrane
56 receptors localized to the endoplasmic reticulum and the Golgi apparatus (Azhar et al., 2020;
57 Binder, 2020; Schaller and Kieber, 2002). These receptors are negative regulators of the pathway,
58 such that binding of ethylene to these receptors removes repression of the pathway, which initiates
59 a signaling cascade that upregulates or downregulates genes with distinct transcriptional responses
60 depending on the tissue type and growth conditions (Chang et al., 2013; Harkey et al., 2018, 2019;
61 Stepanova et al., 2007). In Arabidopsis, five receptor isoforms have been identified: Ethylene
62 Response 1 (ETR1), ETR2, Ethylene Insensitive 4 (EIN4), Ethylene Response Sensor 1 (ERS1),
63 and ERS2 (Binder, 2020; Chang et al., 1993; Hua et al., 1998; Hua and Meyerowitz, 1998; Sakai

et al., 1998; Schaller and Bleecker, 1995). Unlike most canonical signaling pathways, however, ethylene receptors are active in the unbound state. In the absence of ethylene, these receptors activate the Raf-like serine/threonine protein kinase Constitutive Triple Response 1 (CTR1), destabilizing EIN3 and EIN3-like (EIL) transcription factors (TFs) and blocking changes in gene expression downstream of these TFs (An et al., 2010; Binder, 2020; Dolgikh et al., 2019; Kieber et al., 1993). In the bound state, however, the ethylene receptors lead to stabilization of EIN3 and EIL TFs in an EIN2-dependent manner (Alonso et al., 1999; An et al., 2010; Huang et al., 2003; Kieber et al., 1993; Qiao et al., 2009), leading to genome-wide changes in transcript abundance (Chang et al., 2013; Harkey et al., 2018). Downstream of EIN3/EIL are ethylene response factors (ERFs) and ethylene response DNA-binding factors (EDFs) that further mediate transcription, consistent with the existence of tissue-specific gene regulatory networks (GRNs) (Wang et al., 2002).

The function of ethylene signaling proteins in controlling root architecture has been examined (Khoury et al., 2024b). EIN2 is required for root developmental responses to ethylene and its immediate precursor 1-aminocyclopropane-1-carboxylic acid, or ACC (Alonso and Stepanova, 2004; Negi et al., 2008). The *ctr1-1* mutant was demonstrated to have constitutive-ethylene-signaling root phenotypes, with this mutant having shorter primary roots and increased root hair proliferation compared to Col-0 seedlings in the absence of ethylene (Hua and Meyerowitz, 1998; Kieber et al., 1993; Masucci and Schiefelbein, 1996; Rahman et al., 2000), suggesting its presence is required to suppress the pathway in the absence of ethylene. EIN3 and EIL1 TFs function in ethylene-dependent root hair formation, with the *ein3eil1* double mutant having reduced ACC-induction of root hair proliferation (Feng et al., 2017). However, root developmental responses to ethylene can still be observed in the *ein3* and *ein3eil1* mutants (Chang

87 et al., 2013; Harkey et al., 2018), suggesting that additional TFs may participate in these ethylene
88 responses.

89 The five ethylene receptors in Arabidopsis each elicit distinct ethylene responses (Shakeel
90 et al., 2013), partially due to differences in receptor subunit structure and receptor dimerization
91 (Berleth et al., 2019). ETR1 was found to be the main receptor controlling inhibition of ethylene
92 perception by silver nitrate, nutational bending of hypocotyls, and remodeling of root architecture
93 (Harkey et al., 2018; McDaniel and Binder, 2012). In Arabidopsis, ETR1 positively regulates
94 nutational bending (Binder et al., 2006), while the other four receptors negatively regulate this
95 process (Kim et al., 2011). In roots, using a series of single and multiple loss-of-function (LOF)
96 and gain-of-function (GOF) mutants, only ETR1 was needed for the inhibition of lateral root
97 formation by ACC (Harkey et al., 2018). The inhibition of lateral root formation by ACC was lost
98 in the GOF, ethylene-insensitive mutant *etr1-3,* which had significantly more lateral roots than
99 wild type in the presence and absence of ACC. The LOF, constitutive-signaling mutant *etr1-7* had
100 significantly fewer lateral roots than wild type in the presence and absence of ACC. ETR1 also
101 has a central role in the inhibition of primary root elongation and stimulation of root hair formation
102 by ACC, consistent with ETR1 playing the most substantial role in modulating ethylene-mediated
103 root remodeling (Harkey et al., 2018). Nevertheless, while it has been demonstrated that elevated
104 levels of ethylene remodel the root transcriptome (Harkey et al., 2018, 2019; Stepanova et al.,
105 2007), the GRN downstream of the ETR1 receptor has not yet been identified in roots.

106 To identify the ETR1-dependent GRN controlling root growth and development, we
107 performed an RNA-Seq analysis in roots from light-grown seedlings using Col-0 and ETR1
108 receptor GOF (*etr1-3*) and LOF (*etr1-7*) mutants treated with ethylene and ACC for one, four, and
109 24 hours. We identified a core set of genes regulated by both ethylene and ACC in Col-0. We also

110 identified a subgroup of these transcripts that were mis-regulated in the mutants which we defined
111 as ETR1 dependent, as they had constitutively altered expression in untreated *etr1-7* (as compared
112 to Col-0) and their responses to ACC and/or ethylene were lost in both *etr1-3* and *etr1-7* mutants.
113 We examined transcripts encoding the ACC oxidases (ACOs), which are the enzymes that convert
114 ACC to ethylene, in our dataset, finding transcriptional controls of some, but not all of these genes,
115 with a subset that were ETR1 dependent. Analysis of verified ACO transcriptional reporters driven
116 by the native ACO promoters revealed overlapping and distinct root tissue expression patterns
117 among this protein family. Finally, we explored the ETR1-dependent GRN through the lens of
118 ETR1-dependent transcripts predicted to encode TFs, building a network model that revealed TF-
119 encoding transcripts with common temporal and ETR1-regulated responses. We identified those
120 TFs that are targets of EIN3 and tested whether these transcriptional responses required functional
121 copies of EIN3/EIL1. This work sheds light on the ETR1 and EIN3-dependent GRNs that mediate
122 the transcriptional responses to elevated levels of ACC and its ethylene product.
123
124

Results

Previous experiments revealed time points and treatment doses for transcriptome analyses

Previous experiments have revealed the profound effects of elevated levels of ethylene and ACC on root architecture (Khoury et al., 2024b), with the ETR1 receptor controlling many aspects of these developmental changes (Harkey et al., 2018). The goal of this work was to define the genes that depend upon ETR1 for their regulation by ethylene In Arabidopsis, a family of five receptors mediates ethylene responses in roots, with Ethylene Response 1 (ETR1) controlling increases in root hair proliferation and decreases in lateral root formation. To define the ETR1-dependent gene regulatory network (GRN) and downstream target genes that control root development, we profiled the root transcriptome from Col-0 and the *etr1-3* gain-of-function and *etr1-7* loss-of-function mutants in the presence and absence of ethylene or the ethylene precursor aminocyclopropane-1-carboxylic acid (ACC). We identified 4,522 differentially expressed (DE) transcripts in Col-0 roots with altered abundance in response to ethylene and/or ACC treatment, most with larger magnitude changes induced by ethylene. These included 553 DE transcripts that were ETR1-dependent, defined by a lack of response to treatment with ethylene and/or ACC in ethylene-insensitive *etr1-3* and constitutively altered in *etr1-7* in the presence and absence of treatment relative to untreated Col-0. Within these ETR1 dependent transcripts were ethylene biosynthesis genes and transcription factors. *ACC OXIDASE 2* (*ACO2)* and *ACO3* convert ACC to ethylene and were ETR1-dependent, and *ACO* promoter fusions were ACC regulated in root tissues in appropriate locations to control root development, with *ACO5* localized to root hairs. Abundance of ETR1-dependent transcripts that were predicted to encode transcription factors and ACOs were examined in Col-0 and an *ein3eil1* mutant with and without ACC treatment, revealing that the ETR1 and EIN3/EIL1 canonical ethylene signaling pathway regulated some, but not all,

148 of these transcriptional responses. Together, these findings reveal features of an ETR1-dependent
149 GRN that controls both ethylene synthesis and root growth and development, which we determined
150 by examining changes in the transcriptome in *etr1* loss-of-function and gain-of-function mutants.
151 We examined transcriptional response to both ethylene and its immediate precursor ACC to
152 compare their GRNs, as previous work suggested that ACC and ethylene act through distinct
153 signaling pathways in some tissues (Mou et al., 2020; Yin et al., 2019). As a first step, we
154 determined the concentration of ethylene that yielded moderate root hair proliferation like that
155 induced by 0.75 µM ACC (Martin et al., 2022), by examining root hairs in Col-0 seedlings treated
156 with a range of ethylene levels for 24 hours (Supplemental Figure 1). The 0.3 ppm ethylene
157 concentration appeared to induce root hair proliferation to a similar degree as 0.75 µM ACC, so
158 we selected 0.3 ppm ethylene and 0.75 µM ACC for this RNA-Seq analysis.

159 The *etr1-3* and *etr1-7* mutants have aberrant ethylene signaling as summarized in Figure
160 1A that leads to altered root development and responses to elevated ethylene (Harkey et al., 2018).
161 An important goal of this work was to examine the changes in the transcriptome profiles of
162 ethylene- and ACC-treated roots of Col-0, *etr1-3,* and *etr1-7* seedlings to determine the extent of
163 overlap between the receptor-mediated transcriptional responses to these molecules. We compared
164 the effects of 24 hours of treatment with ethylene or ACC at these doses on the proliferation of
165 root hairs in the *etr1-3* and *etr1-7* mutants (Figure 1B). Consistent with our previous results
166 (Harkey et al., 2018), *etr1-3* was less sensitive than Col-0 to the effects of ACC and ethylene,
167 forming fewer and shorter root hairs in the presence of either treatment. The *etr1-7* mutant had
168 larger numbers and longer root hairs in the absence of ACC, although it still responded to ACC
169 and ethylene treatments, a role of additional ethylene receptors in the formation and elongation of
170 root hairs. Intriguingly, *etr1-7* appeared to be more sensitive to ethylene than to ACC, as only

171 ethylene induced the formation of a dense cluster of root hairs at the root tip under these treatment
172 conditions.

173 We used our published ACC time-course microarray dataset to determine the best time
174 points for the RNA-Seq analysis (Harkey et al., 2018). We searched for time points that had large
175 numbers of differentially expressed (DE) genes that were not found in other time points and
176 overlapped with the early, middle, and late root hair developmental responses (for details, see
177 Methods). Supplemental Figure 2 displays a pairwise comparison between DE transcripts at each
178 time point. We selected 1 hour as it corresponded to a robust early response and 4 hours as, in our
179 prior experiment, it had 87% of the transcripts that were also DE at 2 hours and 60% of the
180 transcripts that were also DE at 8 hours. This time point is also where ACC began to significantly
181 induce root hair formation (Harkey et al., 2018). This comparison revealed that 1, 4, and 24 hours
182 of ACC treatment yielded large numbers of unique (i.e., not found in other time points) DE
183 transcripts while also overlapping with the root hair developmental responses, so these time points
184 were used in this study.

185

186 ***Principal component analysis and Pearson's correlation reveal genotype and treatment***
187 ***difference in the root transcriptome***

188 We performed this RNA-Seq analysis in triplicate with three genotypes (Col-0, *etr1-3*, and
189 *etr1-7*), two treatments (0.75 µM ACC and 0.3 ppm ethylene gas), and four time points (0, 1, 4,
190 and 24 hours). Roots were collected from these samples, and mRNA was isolated and used for
191 RNA-Seq sample preparation. After sequencing and quality control, principal component analysis
192 (PCA) plots were created using 1000 genes with the most variance between samples. Figure 2A
193 shows the PCA plot for all samples, which highlights differences between genotypes across PC1

194 (*etr1-7* is distinct from the other two genotypes), and there is a clear difference across PC2 between
195 ethylene- and ACC-treated samples at time points other than 0. Additionally, one Col-0 control
196 separated from other controls along the vertical axis, which led us to analyze samples within
197 genotypes to further investigate differences between them. These analyses (Supplemental Figure
198 3; described further in Methods) led us to remove this ethylene time-zero sample as an outlier.

199 We used the three genotype-specific PCA plots (Figure 2B-D) to assess whether there was
200 variation between the type and duration of treatments. All three plots showed separation of ACC
201 and ethylene samples across the PC1 axis. Meanwhile, the PC2 axis separated samples by time of
202 ethylene or ACC treatment, generally moving from time 0 to time 24 hours from bottom to top.
203 The variation was greater in Col-0 in both PC1 and PC2, consistent with maximal ethylene- and
204 ACC-induced transcriptional responses in Col-0 as opposed to the dampened transcriptional
205 changes in the *etr1-3* mutant due to its reduced ethylene signaling and the *etr1-7* mutant due to its
206 elevated ethylene signaling in the presence and absence of ACC. The diminished response in *etr1-*
207 *7* was consistent across most of the time points; only the 24-hour time point showed a major
208 change. These patterns suggested that after genotype, treatment accounted for the largest variance
209 among samples followed by treatment duration.

210 Plots of Pearson's correlation (Figure 2E and Supplemental Figure 4A) and of Euclidean
211 distance (Supplemental Figure 4B and C), with and without hierarchical clustering, were generated
212 to uncover similarities in expression patterns between samples. The scale of the correlation plots
213 suggested that, overall, samples were highly similar, as all correlation values were 0.94 or higher,
214 representing a minimum similarity of 94%. However, some differences were seen in both plots.
215 The *etr1-7* samples tended to cluster primarily with one another, consistent with *etr1-7* having a
216 constitutive transcriptional response to elevated ethylene signaling, while Col-0 and *etr1-3*

217 samples were interspersed with one another, especially in the absence of treatment or at early time
218 points after treatment, consistent with the absence of ethylene responses under those conditions
219 (Figure 2E). To provide additional insight into expression patterns, we also prepared manually
220 arranged plots in which the samples were grouped by genotype, and then the responses to ACC
221 and ethylene were arranged by time within each genotype (Supplemental Figure 4A and B;
222 described further in Methods). These plots also revealed that Col-0 and *etr1-3* showed greater
223 similarity to each other than to *etr1-7*. This separation of *etr1-7* from Col-0 and *etr1-3* was striking,
224 but another pattern also emerged. Replicate 3 of the ethylene-treated samples were consistently
225 different from their matching samples in other replicates, leading to a regular "striping" pattern.
226 This was most obvious in Col-0, slightly less so in *etr1-3*, and although more subtle, also evident
227 in *etr1-7*. This suggested that this third replicate may have had some difference in part of the
228 process such as treatment, sample collection, or sequencing that changed its composition.

229 We performed ACC treatments at Wake Forest University and ethylene treatments at the
230 University of Tennessee. Therefore, to determine if these samples were similar, we first compared
231 the controls from each location for each genotype, as detailed in Methods and in Supplemental
232 Table 1. Since the controls for Col-0 and *etr1-3* were well matched between the two locations, and
233 the PCAs suggested differences in *etr1-7* were not location dependent (Figure 2D), we combined
234 the six untreated (0-hour) samples for each genotype, or the five untreated samples for Col-0,
235 excluding the outlier sample described above, to use as the baseline for comparisons for the
236 remaining analyses.

237

238 ***Ethylene treatment stimulated more dramatic transcriptional changes than ACC treatment in***
239 ***Col-0***

240 To summarize how the abundance of transcripts was affected by ethylene and ACC
241 treatment, we first examined the hormone-induced responses in Col-0. For both treatments, every
242 time point was compared back to the same set of combined Col-0 controls, defined above. We
243 created a density plot depicting the number of transcripts as a function of their $\log_2$FC using those
244 transcripts with a significant adjusted p-value < 0.01 as determined by DESeq2 (Figure 3A). We
245 observed a bimodal distribution at each time point, showing one group of transcripts that increased
246 in abundance and another that decreased in abundance because of these treatments. This pattern
247 was found in response to both ethylene and ACC, although there were larger numbers of DE
248 transcripts and greater magnitude changes in response to ethylene than ACC treatment, especially
249 at one hour. Both treatments resulted in more down-regulated than up-regulated genes at the 4-
250 and 24-hour time points. The bimodal pattern and higher number of down-regulated genes in
251 response to ACC at the four- and 24-hour time points were similar to our previous microarray
252 study (Harkey et al., 2018). In contrast, we observed more up-regulated genes in our RNA-Seq
253 study at the 1-hour time point for both treatments, while the microarray study detected more down-
254 regulated genes at this time point (Harkey et al., 2018). At the 1-hour time point, the bimodal
255 distribution in response to ACC was not observed in the microarray study, likely due to the lower
256 sensitivity of microarrays compared to RNA-Seq, which allows detection of more subtle changes
257 in transcript abundance. In all treatments and time points, the bimodal peaks representing the
258 increases and decreases in transcript abundance relative to untreated Col-0 were centered on or
259 near -0.5 and 0.5 $\log_2$FC.

260 To identify genes with the most robust changes, we utilized a $|\log_2 FC| > 0.5$ and adjusted
261 p-value < 0.01 for the following analyses. Using DESeq2, we identified 4,522 transcripts that were
262 DE using both the $\log_2$FC and p-value cutoffs in response to ethylene and/or ACC in at least one

263 time point in Col-0 (Figure 3B-D). These transcripts and their log_2FCs (Col-0 treated over Col-0
264 untreated) are listed in Supplemental File 1. More transcripts responded to ethylene treatment and
265 had a greater log_2FC than to ACC treatment. This log_2FC cutoff eliminated more genes whose
266 transcripts decreased after treatment, which resulted in a similar number of up- and down-regulated
267 transcripts passing the log_2FC cutoff, despite there being more down-regulated genes in the larger
268 set of those with a p-value < 0.01 (Figure 3A). Many genes showed similar trends in response to
269 ACC and ethylene treatment: 1,493 and 1,657 genes were down- and up-regulated, respectively,
270 by ethylene only, and 182 and 213 genes were down- and up-regulated, respectively, by ACC only
271 as summarized in Supplemental Table 2. Strikingly, only 16 genes had opposite responses to the
272 two treatments: three were down-regulated in ethylene and up-regulated in ACC, and 13 were up-
273 regulated in ethylene and down-regulated in ACC.

274 This analysis also revealed that 457 and 504 transcripts were up- and down- regulated,
275 respectively, by both ACC and ethylene, with heatmaps illustrating the transcript abundance over
276 time in Figure 3C and D. One pattern that became apparent was that for transcripts whose
277 abundance decreased after both treatments, the 1- and 24-hour ACC-treated samples did not
278 respond as strongly as the time-matched ethylene-treated samples, while in the 4-hour ACC
279 treatment, the number of transcripts changed more dramatically than time-matched ethylene
280 treatment. This finding suggested the possibility that the rate of conversion of ACC to ethylene
281 resulted in varied ethylene concentrations across this time course. Indeed, of the 457 transcripts
282 upregulated by both ACC and ethylene, 258 had a larger magnitude change in response to ACC
283 treatment at the 4-hour time point, but when these 258 transcripts were examined at the 1-hour
284 time point, 181 or 70% of them had a larger response to ethylene treatment. Similarly, of the 504
285 transcripts downregulated by both ACC and ethylene, 245 had a larger magnitude change in

286 response to ACC treatment at the 4-hour time point, but 213 or 87% of them responded more
287 strongly to ethylene treatment at the 1-hour time point. These results suggested that ACC induced
288 maximal transcriptional responses more slowly than ethylene, likely due to the time required to
289 convert ACC to ethylene. Intriguingly, the pattern of highest absolute $\log_2$FC at the 4-hour time
290 point was also apparent in the transcripts that were DE only in response to ACC treatment.
291
292 ***Transcripts regulated by ethylene and ACC were enriched in functions related to root***
293 ***development***
294 To determine which biological processes were enriched among the transcripts whose
295 abundance changed after ethylene or ACC treatment in Col-0, we performed Gene Ontology (GO)
296 analysis using AgriGO (Du et al., 2010; Tian et al., 2017) and reported the results in Supplemental
297 Table 3. Genes whose transcripts had increased abundance in both treatments were enriched in
298 functional annotations including "negative regulation of the ethylene-mediated signaling
299 pathway," which is consistent with previous findings that both ethylene and ACC transcriptionally
300 regulate components of the ethylene signaling pathway in a negative feedback loop, and response
301 to auxin stimulus, consistent with crosstalk between ethylene and auxin. Several groups of genes,
302 both up- and down-regulated, were enriched in lipid localization and transport annotations.
303 Transcripts whose abundance decreased after ethylene and/or ACC treatment were
304 enriched in gene annotations including lignin biosynthetic process and cell wall loosening, while
305 transcripts that decreased after only ethylene treatment were enriched in secondary cell wall
306 biogenesis, plant-type cell wall organization, and lignin metabolic process. These results were not
307 surprising given the importance of cell wall remodeling in cell expansion during apical root
308 growth, lateral root emergence, and root hair development.

309 Interestingly, genes whose transcripts decreased in abundance with ethylene treatment only
310 were enriched in annotations of root hair cell differentiation or root hair development, including
311 two myosin genes (*XIB* and *XIK*), *MORPHOGENESIS OF ROOT HAIR 1, 2*, and *6*, *ROOT HAIR*
312 *DEFECTIVE 4* (*RHD4*), *BRISTLED 1*, *CAN OF WORMS 1* (*COW1*), and *SHAVE 2* and *3*. No
313 annotations were significantly enriched in genes down-regulated by ACC only, likely due to the
314 smaller size of this group.

315 We were interested in further examining the identities of the transcripts that were regulated
316 by ACC only, as these might reveal ACC-regulated transcripts that are not ethylene-regulated. The
317 213 transcripts that we upregulated by just ACC included genes encoding two mitogen-activated
318 protein (MAP) kinases MAPKKK13 and MEK1, enzymes that remodel the cell wall including
319 EXPANSIN A17 (EXPA17) and PECTIN METHYLESTERASE 3 (PME3), and RHO OF
320 PLANTS GUANINE NUCLEOTIDE EXCHANGE FACTOR 12 (ROPGEF12) and ROOT HAIR
321 DEFECTIVE 6-LIKE 5 (RSL5), which function in root hair development. We also identified
322 upregulation of transcripts involved in auxin signaling and jasmonic acid metabolism and
323 signaling, indicative of hormonal crosstalk. The 182 transcripts that were downregulated by only
324 ACC encoded enzymes that remodel the cell wall including EXPANSIN A4 (EXPA4) and
325 EXPANSIN-LIKE A2 (EXLA3), and an enzyme involved in the synthesis of ACC, 1-AMINO-
326 CYCLOPROPANE-1-CARBOXYLATE SYNTHASE 7 (ACS7), which converts S-Adenosyl
327 methionine to ACC. This latter finding was quite interesting as it suggested that ACC might
328 negatively regulate its own synthesis in a negative feedback loop when ACC levels are high.

329

330 ***Transcriptional responses are accentuated in constitutive-signaling* etr1-7 *and reduced in***
331 ***ethylene-insensitive* etr1-3**

332 We next asked how the transcriptional responses to ethylene and ACC varied in the *etr1-3*
333 and *etr1-7* mutants compared to Col-0. Using a cutoff of $|\log_2 FC| > 0.5$ and adjusted p-value <
334 0.01, we compared each time point for each treatment and genotype to the Col-0 control and found
335 8,323 transcripts that were DE in at least one of these genotype comparisons, and these transcripts
336 and their $\log_2 FC$ values relative to untreated Col-0 are listed in Supplemental File 1. A heatmap
337 displaying the changes in abundance of these transcripts in all three genotypes and both treatments
338 is shown in Figure 4. All $\log_2 FC$ values represented here were relative to Col-0 at time zero to
339 accurately reflect the changes in baseline levels in *etr1-7*.

340 The heatmap in Figure 4 suggested that the $\log_2 FC$ filter eliminated transcripts that
341 responded to ACC but had smaller magnitude changes in response to ACC than ethylene. As the
342 density plots showed, many transcripts had a $|\log_2 FC|$ between 0.25 and 0.5, so we examined
343 transcriptional responses using a less stringent cutoff. When the cutoff was changed to $|\log_2 FC| >$
344 0.25, we identified 7,104 DE genes in at least one comparison of ethylene and ACC in Col-0,
345 compared to 4,522 with a cutoff of $|\log_2 FC| > 0.5$ (Supplemental Table 3). Regardless of cutoff,
346 the number of transcripts that only responded to ethylene was greater than those only responding
347 to ACC, with approximately 20% of genes regulated by both ACC and ethylene, 70% by ethylene
348 only, and 10% by ACC only. Therefore, we used the more stringent logFC cutoff of 0.5 for the
349 remaining analyses.

350 We compared baseline levels of expression in untreated samples between genotypes
351 (Figure 5A), identifying 2,562 genes that were DE (p-value < 0.01) in at least one of these
352 comparisons (these transcripts and their $\log_2 FC$ values relative to other genotypes are listed in
353 Supplemental File 1). Consistent with our expectations, *etr1-3* and Col-0 were nearly identical in
354 the absence of elevated ethylene; only 49 out of 2,562 genes were found to be DE between them.

355 However, when we compared *etr1-7* with either Col-0 or *etr1-3*, we found a dramatic difference:
356 1,941 genes were DE between *etr1-7* and Col-0, and 2,078 genes were DE between *etr1-7* and
357 *etr1-3*. A large number (1,458) of the genes were DE in both comparisons with *etr1-7,* including
358 genes enriched in the "response to ethylene" annotation (Fig. 5B).

359 One very interesting group of transcripts were the 1,941 transcripts that were DE in *etr1-7*
360 as compared to Col-0, in the absence of hormone treatment. The large number and magnitude
361 change of these genes is consistent with the *etr1-7* mutation being sufficient to lead to large
362 changes in abundances transcripts with endogenous levels of ethylene. Under these conditions, the
363 *etr1-7* mutant has increased root hair formation relative to Col-0. Consistent with this group of
364 genes having an important function in ethylene response, it is enriched in annotations pertaining
365 to the ethylene signaling pathway. Similar annotations were also found in the group of transcripts
366 that responded to ethylene and/or ACC treatment in Col-0, including "response to ethylene"
367 (Supplemental Table 3). These results are consistent with *etr1-7* having constitutive ethylene
368 signaling and therefore a different transcriptional landscape than the other genotypes in the absence
369 of exogenous ethylene or ACC. This group of transcripts is consistent with the *etr1-7* mutation
370 being sufficient to induce transcript abundance changes that overlap with the treatment of Col-0
371 with ACC or ethylene.

372

373 ***A subset of ACC- and ethylene-regulated transcript responses appear to be dependent on ETR1***
374 ***signaling***

375 We developed a more rigorous set of criteria to determine which ethylene- and/or ACC-
376 regulated transcripts were dependent on ETR1 for transcriptional response. For this analysis, we
377 defined a transcript as ETR1-dependent based on the following criteria, with a significant change

378 or response designated as a $|\log_2 FC| > 0.5$ and a p-value < 0.01: 1) transcript showed a significant
379 response to ethylene and/or ACC treatment in at least one time point in Col-0; 2) transcript showed
380 no significant change in any *etr1-3* samples compared to Col-0 time 0; and 3) transcript showed a
381 change in *etr1-7* relative to Col-0 in the baseline and showed similar abundance in ACC- and
382 ethylene-treated *etr1-7* samples. Since *etr1-7* has constitutive ethylene signaling, it should have
383 had transcriptional responses that differed from Col-0 in the absence of either ACC or ethylene
384 treatment and were unchanged by ACC or ethylene treatment. Therefore, we compared *etr1-7*
385 treated samples to *etr1-7* control samples, and only those that did not change with treatment in
386 *etr1-7* qualified as ETR1-dependent.

387 With this strict criteria, 553 transcripts were identified as ETR1-dependent (listed in
388 Supplemental File 1 with their $\log_2 FC$ values relative to untreated Col-0). A subset of 292
389 transcripts met these criteria in ethylene treatment only, another 191 in ACC only, and 70 genes
390 were classified as ETR1-dependent in both treatments. The heatmap in Figure 6 shows all the
391 transcripts that were ETR1-dependent using these criteria. The $\log_2 FC$ values in this table are
392 reported relative to untreated Col-0 samples. It is clear from this heatmap that even though not all
393 of these were DE in both ACC and ethylene treatments, the difference may simply be tied to a
394 smaller magnitude of ACC response that was below the $\log_2 FC$ cutoffs, suggesting that these
395 transcripts are ETR1-dependent regardless of treatment. We also examined the transcripts filtered
396 to have a $|\log_2 FC| > 0.25$, which yielded many more transcripts in each group, but did not change
397 the overall ratios of transcripts in those groups.

398 We generated a network of the 553 ETR1-dependent transcripts using Partitioned Local
399 Depths (PaLD) analysis (Berenhaut et al., 2022; Khoury et al., 2024a), which grouped transcripts
400 together based on their similar responses to ACC and ethylene in Col-0, *etr1-3*, and *etr1-7*

401 (Berenhaut et al., 2022; Khoury et al., 2024a). The $\log_2$FC values of treated samples relative to
402 Col-0 untreated were fed into PaLD, revealing two large groups of up- and down-regulated
403 transcripts (Supplemental Figure 5). We further divided these groups based on transcripts with the
404 strongest ties using the Louvain method for community detection, and these groups were depicted
405 in different colors on the network (Supplemental Figure 5) with the identities of the transcripts in
406 each of these groups provided in Supplemental File 1. This network revealed the complexity of
407 the transcriptional responses of the ETR1-dependent transcripts.

408 Out of the 553 genes which qualified as ETR1-dependent in one or both treatments, 31
409 overlapped with a set of core ethylene-responsive genes identified by a comparison of three
410 transcriptome studies of ethylene- or ACC-treated roots (Harkey et al., 2018). These genes
411 included *ACC OXIDASE 2* (*ACO2*), *ETHYLENE RESPONSE SENSOR* (*ERS)1* & *2*, and
412 *ETHYLENE AND SALT INDUCIBLE 3* (*ESE3*). This finding suggested there were ETR1-
413 dependent transcriptional responses to ACC and ethylene in this core group. Other ethylene-related
414 genes that did not overlap with this group but were identified as ETR1-dependent here included
415 *ACO3*, several *ERFs*, and *PINOID*, a kinase that is a positive regulator of auxin transport (Sukumar
416 et al., 2009) and a negative regulator of root hairs (Lee and Cho, 2008). The 553 ETR1-dependent
417 transcripts were enriched in GO annotations including lipid transport, response to ABA, and
418 regulation of transcription (Supplemental Table 4).

419 We tested an additional set of less stringent criteria, where response to treatment was
420 evaluated by comparing treated samples to the control samples within each genotype, but only
421 required presence or absence of treatment response regardless of the control sample abundance. In
422 this case, ETR1 dependence was defined by a response in Col-0 but not in the mutants, and ETR1
423 independence was defined as a response in all three genotypes. This analysis allowed for a larger

424 set of transcripts to be included in both groups (Supplemental Figure 6), but ultimately the changes
425 in abundance of the additional transcripts were not as strong as those seen with the more stringent
426 criteria, so we focused our analysis on the transcripts that met the more stringent criteria. We
427 continued to calculate, and report in heatmaps, the *etr1-3* and *etr1-7* $\log_2$FC values relative to Col-
428 0 untreated but used the comparison of *etr1-7* to its own untreated sample for defining ETR1
429 dependence in the *etr1-7* samples.
430
431 ***Other transcripts appear to be regulated by ACC and/or ethylene in an ETR1-independent***
432 ***manner***
433 Next, we defined ETR1-independent responses for each treatment as having a response to
434 treatment in all genotypes and no altered response in the mutants at baseline (compared to
435 untreated Col-0). Again, we compared the *etr1-7* treated samples to the *etr1-7* control samples to
436 determine whether a gene responded to treatment in this genotype relative to baseline transcript
437 levels, but in this case a response to treatment was required to qualify as ETR1-independent.
438 The search for ETR1-independent genes resulted in a slightly smaller set of genes: 481
439 genes qualified as ETR1-independent in ethylene only, 95 in ACC only, and 117 qualified in both
440 treatments (listed in Supplemental File 1 with their $\log_2$FC values relative to Col-0 untreated).
441 These ETR1-independent transcripts are shown in the heatmap in Figure 7, where the $\log_2$FC
442 relative to untreated Col-0 was reported. Unlike the ETR1-dependent genes, these genes showed
443 different patterns depending on whether they met ETR1-independent criteria in ethylene- or ACC-
444 treated samples; genes which were ETR1-independent in one treatment had a reduced response to
445 the other treatment. GO annotations enriched in this group of genes included several stress-

446 response annotations, as well as “root hair cell differentiation” and “unidimensional cell growth”
447 (Supplemental Table 4).
448
449 ***The largest set of genes had complex, but more muted responses to ethylene and/or ACC***
450 After identification of genes with ETR1-dependent and -independent responses, an
451 additional 7,077 genes were left with differential expression in at least one sample (listed in
452 Supplemental File 1 with their $\log_2$FC values relative to untreated Col-0). These genes did not
453 meet the strict criteria defined for ETR1-dependent or -independent genes above, showing patterns
454 of response inconsistent with either definition. We divided these “complex” transcripts based on
455 their general patterns across genotypes relative to Col-0 control. A transcript was counted as DE
456 in a genotype if it passed p-value and $\log_2$FC cutoffs in at least one sample of that genotype as
457 compared to Col-0 control, including control samples for *etr1-3* and *etr1-7* (Supplemental Figure
458 7). The largest group consisted of genes that were DE in *etr1-7* only (2,974 genes). However, many
459 of these were DE only in one or two samples. The same is true for the 508 and 357 genes which
460 were DE only in Col-0 or *etr1-3*, respectively. The next largest group of 1,068 transcripts had at
461 least one DE sample in each genotype. These transcripts had some response to treatment in all
462 genotypes, so they looked like the ETR1- independent genes but failed the strict filtering used for
463 that group. Similarly, the 1,020 genes that were DE in Col-0 in response to treatment with ACC
464 and/or ethylene and DE between *etr1-7* and Col in the absence of treatment looked like the ETR1-
465 dependent group of genes. Perhaps most puzzling were transcripts which were DE in *etr1-3* and
466 one other genotype, as these did not behave as expected for either ETR1-independent or -
467 dependent genes. In these groups of genes with complex behavior, a wide variety of GO terms
468 were enriched, including response to light stimulus, phenylpropanoid biosynthetic process,

469 response to abscisic acid stimulus, cell wall modification, regulation of transcription, response to
470 ethylene stimulus, and cell wall macromolecule metabolic process (Supplemental Table 4).
471
472 ***Several ACOs are transcriptionally regulated by ACC and ethylene via the ETR1 receptor***

473 An important action of both ACC and ethylene is to positively regulate the synthesis of
474 more ethylene. In particular, the ACC oxidase (ACO) enzyme catalyzes the oxidation of ACC to
475 ethylene as the final step of ethylene biosynthesis. Transcripts encoding ACO enzymes are
476 positively regulated by ACC levels (Harkey et al., 2018), which then drives ethylene synthesis.
477 Included in the ETR1-dependent dataset were transcripts encoding several of the five genes
478 encoding ACOs (*ACO1* through *ACO5*), which synthesize ethylene from both endogenously
479 produced and exogenously supplied ACC. The abundance of transcripts from these genes varied
480 in untreated Col-0 roots with TPM values of 8, 313, 6, 39, and 315 for *ACO1-5*, respectively. We
481 found that both ethylene and ACC treatment of Col-0 significantly increased the transcript
482 abundance of four *ACO*s (*ACO1*, *ACO2*, *ACO3*, and *ACO5*) in at least one time point after
483 treatment. The transcript levels of *ACO1*, *ACO2*, and *ACO3* in each genotype and treatment are
484 shown in Fig. 8. For these genes, there was a greater magnitude increase in transcript abundance
485 in response to ACC than to ethylene treatment in at least one time point for each transcript. This
486 difference in response is striking as most of the upregulated DE transcripts in our dataset had larger
487 magnitude changes in response to ethylene than to ACC treatment. This finding suggests that
488 exogenous ACC may be a stronger signal to promote transcript accumulation of *ACO*s than
489 ethylene gas itself.

490 According to our strict criteria for ETR1 dependence, detailed above, *ACO2* and *ACO3*
491 were ETR1-dependent in response to ethylene treatment, with uniform reductions in transcript

492 abundance in *etr1-3* and increases in *etr1-7* compared to Col-0 (Fig. 8D, F). While *ACO2* and
493 *ACO3* passed the criteria for ETR1 dependence in Col-0 and *etr1-3* in response to ethylene
494 treatment, ACC induced significant increases in transcript abundance at one time point in the *etr1-*
495 *7* mutant relative to the *etr1-7* untreated control and therefore these *ACOs* did not pass the criteria
496 for ETR1 dependence in the presence of ACC. *ACO1*, *ACO4,* and *ACO5* did not meet our criteria
497 for ETR1 dependence in the presence of either ACC or ethylene (Figure 8A, B; Supplemental
498 Figure 8). *ACO5* appeared to be ETR1-dependent based on p-value, but it failed the $\log_2$FC cutoff
499 for having a smaller magnitude change than required for our stringent requirement. It is clear from
500 the graphs that reduced or constitutive ethylene signaling in the *etr1-3 and etr1-7* mutants,
501 respectively, altered the transcriptional response of each *ACO* to ACC and/or ethylene, consistent
502 with the importance of the ETR1 receptor in regulating *ACO* transcript abundance, even for *ACO*s
503 that do not meet our stringent ETR1-dependent criteria.

504

505 ***ACC-induced transcript accumulation of ACO1, ACO2, and ACO4 is mediated by EIN3/EIL1***

506 To extend our understanding of the regulation of *ACO*s, we asked if their changes in
507 transcript abundance in roots were regulated by both ETR1- and EIN3-mediated GRNs. We
508 quantified the transcript abundance of the *ACO*s in roots of Col-0 and *ein3eil1* using RT-qPCR in
509 the presence and absence of 0.75 µM ACC. We treated these samples with ACC for 4 hours, as
510 this was the time point that yielded the largest increases in *ACO* transcript abundance (relative to
511 untreated Col-0) in our RNA-Seq data. For *ACO1*, *ACO2*, and *ACO4*, we found significant
512 increases in transcript levels with ACC treatment in Col-0, including 2-fold increases in *ACO1* and
513 *ACO2* and a 1.5-fold increase in *ACO4* (Fig. 8G-I). These ACC-induced increases were lost in the
514 *ein3eil1* mutant, consistent with these transcripts being ACC-regulated through the canonical

515 ethylene signaling pathway (Fig. 8G-I). Consistent with our RT-qPCR results, the promoters of
516 *ACO2 and ACO4* were found to be directly bound by EIN3 in a DAP-Seq (O'Malley et al., 2016)
517 and/or ChIP-Seq dataset (Chang et al., 2013) as summarized in Harkey et al. 2019, but the absence
518 of *ACO1* as an EIN3 target is surprising and is consistent with an EIN3-regulated TF binding to
519 and controlling *ACO1* transcription, rather than being a direct EIN3 target.

520 In contrast, we did not detect significant increases in *ACO3* and *ACO5* transcripts in
521 response to ACC treatment in Col-0 in our RT-qPCR (Supplemental Figure 9). *ACO3* transcript
522 levels in *ein3eil1* did not differ from those in Col-0 in the presence or absence of ACC, while
523 *ACO5* transcript levels in Col-0 ACC-treated samples were significantly higher than those in
524 *ein3eil1* in the presence and absence of ACC (Supplemental Figure 9). For both *ACOs*, these
525 findings were consistent with localized changes in abundance in specific tissues that cannot be
526 consistently detected by RT-qPCR using whole roots. Therefore, to gain further insight into where
527 these genes are expressed and to reveal localized change in response to ACC, we examined
528 reporters consisting of green fluorescent protein driven by the *ACO* promoters (Houben et al. 2024)
529 treated with and without ACC.

530

531 ***ACO transcription increases in distinct root cell types in response to ACC treatment***

532 To determine which of the *ACO*s might control ACC- and ethylene-induced changes in
533 root development, we queried the *ACO*s in a root cell-type-specific dataset (Brady et al., 2007) to
534 identify the tissues where these transcripts were most highly enriched. We searched for transcripts
535 that were localized in the appropriate tissues to mediate ACC- and ethylene-induced root
536 responses, including stimulation of root hair initiation (Harkey et al., 2018), inhibition of lateral

537 root emergence (Negi et al., 2008), and inhibition of root elongation at the root tip (Qin et al.,
538 2019). *ACO5* was identified as a candidate for the control of root hair growth because, like *ETR1*,
539 its transcripts were highly enriched in cells expressing root hair markers, while the other *ACOs*
540 had low transcript abundance in this cell type (Fig. 9A).

541 To provide additional insight into the effect of ACC treatment on tissue-specific
542 localization and abundance of *ACO* transcripts, we examined a fluorescent reporter driven by each
543 of the native *ACO* promoters (Houben et al., 2024). To validate the root hair cell specific *ACO5*
544 accumulation in the microarray described above, we examined fluorescence of a *pACO5*::GFP-
545 GUS reporter in roots. We observed fluorescence in hair cells and root hairs in the absence of
546 ACC. Consistent with ACC-induced increases in *ACO5* transcript levels, fluorescence at the tips
547 of root hairs was brighter in the presence of ACC (Fig. 9B), suggesting that *ACO5* is expressed in
548 the appropriate position for its protein product to synthesize ethylene to drive root hair elongation.
549 Laser scanning confocal microscope (LSCM) images of root tips of 10-day-old seedlings revealed
550 brighter fluorescence in hair cells than non-hair cells, consistent with cell-type-specific expression
551 patterns (Fig. 9C; Figure 10). In contrast, *pACO5*::GFP-GUS fluorescence was at low levels in the
552 root tip in both the presence and absence of ACC in five-day-old seedlings, with higher signal in
553 the elongation zone (EZ) and differentiation zone (DZ) than other *ACO*s (see below) (Fig. 9B).

554 We found shared and distinct expression patterns in roots of 10-day-old seedlings in the
555 presence and absence of 0.75 μM ACC after five days of treatment (Figure 10). The *pACO1*::GFP-
556 GUS reporter had a fluorescent signal in the lateral root cap and the columella of primary and
557 lateral root tips, where this signal was increased in response to ACC treatment. The *pACO3*::GFP-
558 GUS reporter exhibited a fluorescent signal in the primary root columella and the inner tissues of
559 primary and lateral roots, where this signal was increased in response to ACC treatment.

560 Interestingly, the *pACO4*::GFP-GUS reporter had a fluorescent signal in the columella of
561 elongated lateral roots that was increased after ACC treatment, but this signal was not detected in
562 the columella of primary root tips in the presence or absence of ACC. We identified weak ACC-
563 induced changes for some of the reporters in the root tissues of interest, although there appeared
564 to be moderate basal levels of expression consistent with the cell type data (Figure 10). The
565 fluorescence of the *pACO2*::GFP-GUS reporter was low and did not show induction by ACC in
566 root tissues of interest (Supplemental Figure 10).

567

568 ***Identification of EIN3-regulated transcripts predicted to encode TFs within the ETR1-***
569 ***dependent GRN***

570 One goal of this study was to gain additional insight into the transcriptional regulators
571 downstream of ETR1 whose abundance changed in response to ACC and ethylene treatment.
572 Consistent with a global remodeling of the transcriptome, a GO analysis revealed that the ETR1-
573 dependent transcripts were significantly enriched in genes that function in the regulation of
574 transcription (Supplemental Table 4). We identified 60 ETR1-dependent transcripts predicted to
575 encode TFs using the AGRIS database (Palaniswamy et al., 2006). The expression patterns of
576 these TF-encoding transcripts were calculated and the $\log_2$FC relative to Col-0 untreated is
577 shown in Figure 11A. Note the larger number of downregulated than upregulated transcripts and
578 the distinct temporal responses, with some transcripts changing rapidly after ACC and/or
579 ethylene treatment and other transcripts responding more slowly to these treatments.

580 To better visualize groups of TFs that have similar expression patterns in response to
581 treatments and in the *etr1* mutants, we employed a PaLD analysis (Berenhaut et al., 2022;

582 Khoury et al., 2024a) using the $\log_2$FC values relative to Col-0 time 0 for each transcript to
583 generate a network of the 60 ETR1-dependent TFs (Fig. 11B). This analysis results in a network
584 with each node representing one of the 60 TF-encoding transcripts and the edges connecting
585 transcripts with the most similar responses to ACC and ethylene over time in the different
586 genotypes.

587 To sort these transcripts into distinct groups with the most similar responses, we used the
588 Louvain method, which identifies communities in large networks (Blondel et al., 2008). The
589 network yielded a structure consisting of six groups containing two or more transcripts.
590 Transcripts belonging to the same group as indicated by their matching colors are those with the
591 most similar transcript abundance patterns across the time course of ACC and ethylene treatment
592 in Col-0, *etr1-3*, and *etr1-7*. As EIN3 is a transcription factor that is downstream of ETR1 in the
593 canonical ethylene signaling pathway (Dolgikh et al., 2019), we used publicly available data on
594 the genes to which EIN3 binds revealed by DAP-Seq (O'Malley et al., 2016) or ChIP-Seq
595 (Chang et al., 2013). We highlighted on the PaLD network in large, bold font the direct targets of
596 EIN3. Consistent with EIN3 functioning to primarily increase transcript abundance (Harkey et
597 al., 2018), most of the targets were found in the upregulated groups of genes (Fig. 11B). We also
598 calculated the percent of genes in each Louvain group that are direct EIN3 targets. The pink and
599 yellow groups making up the upregulated transcripts consisted of 71% and 31% EIN3 targets,
600 respectively. These numbers are substantially higher than the 4% of the whole genome
601 containing EIN3 targets as noted by Harkey et al. (2018). In contrast, the green, blue, orange, and
602 red-orange groups consisting of down-regulated transcripts included 25%, 8%, 0%, and 0%
603 EIN3 targets, respectively. The upregulated EIN3 targets had diverse expression patterns, with
604 some being rapidly induced by ACC/ethylene treatment (e.g., *ERF2*) and others being more

605 slowly induced (e.g., *RSL5*). The downregulated EIN3 targets were also diverse in their patterns,
606 with AT1G08320 being rapidly downregulated and *MYB9* and *MYB107* being more slowly
607 downregulated.

608 To validate whether both upregulated and downregulated ETR1-dependent transcripts that
609 are EIN3 targets by ChIP-Seq and DAP-Seq showed altered transcript abundance in the *ein3eil1*
610 mutant, we quantified the transcript abundance of several genes in roots of five-day-old Col-0 and
611 *ein3eil1* seedlings in the presence and absence of ACC after 4 hours. We were interested in *ROOT*
612 *HAIR DEFECTIVE 6-LIKE 5* (*RSL5*), as this TF was previously demonstrated to be involved in
613 root hair development (Pires et al., 2013). Intriguingly, in our RNA-Seq dataset, *RSL5* transcript
614 levels were significantly upregulated by ACC at the four- and 24-hour time points but were not
615 significantly regulated by ethylene (Fig. 11C, D). Consistent with these data, we found a
616 significant increase in *RSL5* transcripts in the presence of ACC and demonstrated the dependence
617 of this change on EIN3, as this induction was lost in the *ein3eil1* mutant (Fig. 11E). This result
618 suggested that although *RSL5* was more strongly regulated by ACC, this regulation depended upon
619 the canonical ethylene signaling pathway. We also observed a significant increase in *RAP2.6L*
620 transcript levels and a significant decrease in *MYB9* transcript levels in the presence of ACC, and
621 both changes were lost in the *ein3eil1* mutant (Fig. 11F, G). We also examined transcript
622 abundance of an additional gene (*LRP1*) whose promoter was targeted by EIN3, and three genes
623 (*ANAC058*, *MYB52*, and *MYB93*) that were not identified as direct targets of EIN3 by ChIP-Seq
624 and DAP-Seq (Chang et al., 2013; O'Malley et al., 2016). However, the levels of these transcripts
625 were not significantly altered by ACC in our RT-qPCR data, although there were trends consistent
626 with the patterns observed in the RNA-Seq data (Supplemental Figure 11). This example further
627 validates the ability of this RNA-Seq dataset to identify additional root-specific genes that are

628 dependent upon ETR1 and EIN3 for altered transcript accumulation in response to ACC and/or
629 ethylene treatment.

630 ***The proLRP1::GUS reporter exhibited increased amounts of GUS product in lateral root***
631 ***primordia in the presence of ACC***

632 We were interested in exploring the roles of several of these ETR1-dependent TFs in root
633 development and how they were modulated by ACC. One gene, *LRP1*, stood out since it had
634 previously been demonstrated to function in lateral root primordium (LRP) development , as *LRP1*
635 overexpression lines had increased numbers of stage I, IV, and V LRP, but reduced numbers of
636 emerged lateral roots (Singh et al., 2020). Since *LRP1* transcripts were induced in whole roots in
637 response to ethylene and ACC treatment (Fig. 12A, B), we next asked in which root tissues these
638 transcripts were synthesized. We used the *proLRP1*::GUS transcriptional reporter (Estornell et al.,
639 2018) treated with ACC for five days and visualized GUS product in roots using a
640 stereomicroscope. In 10-day-old seedlings, we found the GUS product accumulated in the central
641 root tissues in both the presence and absence of ACC, beginning at the root elongation zone (Fig.
642 12C). We observed increased GUS activity in the presence of ACC in lateral root primordia at all
643 primordia stages and in emerged lateral roots, consistent with *LRP1* transcripts being synthesized
644 in these tissues and having increased expression in response to ACC treatment.

645 We also quantified the number of lateral roots and the lateral root density in the region of
646 new root growth in the *lrp1-1* and *lrp1-2* mutants in the presence and absence of ACC, with
647 representative images shown in Supplemental Figure 12A. Based on a prior report that examined
648 *LRP1* overexpression lines and identified a 2.5-fold decrease in lateral root density in these lines
649 compared to Col-0 (Singh et al., 2020), we expected to see a large phenotypic difference in these

650 mutants. We quantified the number of lateral roots in the region of root formed after transfer to
651 control or ACC media, as we previously demonstrated a negative effect of ACC on lateral root
652 formation in this region (Negi et al., 2008). We found that in untreated roots, there was a small
653 and significant increase in the number of emerged lateral roots in *lrp1-1* with a non-significant
654 increase in *lrp1-2* (Supplemental Figure 12C). We found that these small differences were lost in
655 the presence of ACC, which had equivalent inhibition of lateral root formation as Col-0. We also
656 quantified lateral root density in the region of new root growth (5 days of ACC treatment) and
657 found no significant difference in lateral root density in *lrp1-1* and *lrp1-2* in the absence of ACC
658 (Supplemental Figure 12D). The reduction in lateral root density by ACC significantly differed
659 from Col-0 in *lrp1-2* and not *lrp1-1*, with less inhibition of lateral root formation in *lrp1-2*
660 compared to Col-0. Consistent with the weak accumulation and the absence of changes with ACC
661 of the *proLRP1*::GUS reporter in the primary root tip (Fig. 12C), there were subtle changes in
662 primary root elongation in the mutants (Supplemental Figure 12B). We observed a small but
663 statistically significant increase in primary root growth in *lrp1-1* in the absence of ACC and no
664 significant increase in *lrp1-2* compared to Col-0.

665

666 ***Several ETR1-dependent TF mutants show subtle differences in root hair initiation, lateral root***
667 ***formation, and root elongation***

668 We screened mutants in a small set of ETR1-dependent TFs for root phenotypes in the
669 presence and absence of ACC. We selected several genes that were also regulated by ACC over a
670 time course of ACC treatment (Harkey et al., 2018). These included *RAP2.6-L*, *ANA058*, *MYB9*,
671 and *MYB52*, some of which were also found to be direct targets of EIN3. To illustrate how these
672 genes responded to ethylene and ACC treatment in Col-0, *etr1-3*, and *etr1-7* in this RNA-Seq

673 study, we reported the fold change in transcript abundance relative to untreated Col-0
674 (Supplemental Figure 13). These transcripts were also expressed in various root tissues, including
675 lateral roots, pericycle cells, xylem pole pericycle cells, hair cells, and non-hair cells to varying
676 degrees (Supplemental Figure 14A).

677 We found that in the region of new root growth, *myb52-1* had significantly fewer lateral
678 roots than Col-0 in the absence of ACC, but it showed wild-type inhibition of lateral root formation
679 in the presence of ACC (Supplemental Figure 14B). The *anac058-1*, *myb52-1*, and *rap2.6l-1*
680 mutants all had lower lateral root densities in this region in the presence of ACC compared to Col-
681 0, suggesting they may function to promote lateral root formation (Supplemental Figure 14C).
682 These results were consistent with *MYB52* and *ANAC058* being downregulated by ACC, but not
683 with *RAP2.6L* being upregulated by ACC. The *myb9-1* mutant was also found to have a longer
684 primary root growth phenotype in the absence of ACC compared to Col-0, and no difference was
685 observed in the presence of ACC (Supplemental Figure 14D), suggesting MYB9 may inhibit
686 primary root growth, although this was not consistent with MYB9 being downregulated by ACC.
687 We also examined the effects of these mutants on root hair number in the absence and presence of
688 four hours of ACC treatment. Only the *myb52-1* mutant had aberrant root hair formation with
689 reduced root hairs compared to Col-0 in both the presence and absence of ACC, suggesting it
690 functions to promote root hair formation (Supplemental Figure 15). These subtle phenotypes were
691 likely due to functional redundancy, as many of the proteins encoded by these transcripts belonged
692 to extensive TF families.

693 We also compared the growth response of the light-grown seedlings described above to
694 dark-grown seedlings (Supplemental Figure 16). In 10-day-old light-grown seedlings, the *lrp1-1*
695 and *myb9-1* mutants exhibited more primary root growth, yet the ability of ACC to inhibit

696 elongation was like that observed in Col-0, with other mutants having Col-0 levels of root
697 elongation in the absence of treatment (Supplemental Figure 12B; Supplemental Figure 14B).
698 When these same mutants were etiolated on ACC (or untreated) plates for four days, we found that
699 *lrp1-1* had significantly shorter roots than Col-0 at 0.2 µM ACC, while *myb9-1* behaved like Col-
700 0 at all doses of ACC we tested. We also found that *rap2.6l-1*, which did not have a primary root
701 growth phenotype when grown under continuous light, displayed shorter roots than Col-0 at
702 multiple lower doses of ACC (<0.5 µM) after etiolation. However, *lrp1-1* and *rap2.6l-1* did not
703 differ from Col-0 at ACC doses of 0.5 µM and higher. The *myb52-1* mutant displayed longer roots
704 than Col-0 under control conditions at five days of age, although the primary root growth did not
705 differ from Col-0 at 10 days of age when lateral roots were measured. In contrast, etiolated *myb52-*
706 *1* seedlings displayed longer roots than Col-0 in the absence of ACC treatment but shorter roots
707 than Col-0 in the presence of 0.2 µM ACC. The *anac058-1* mutant was not significantly different
708 from Col-0 at any of the doses of ACC we tested. These differences in light- and dark-grown
709 seedlings suggested that perhaps some of the ETR1-dependent TFs were more important for light-
710 dependent root responses than light-independent ones (Harkey et al., 2019).

711 **Discussion**

712 The Arabidopsis genome encodes five ethylene receptors that have distinct and overlapping
713 functions in the regulation of plant growth. The specific roles of individual receptors in controlling
714 ethylene-regulated development have been examined only in a few tissues (Binder, 2020; Cancel
715 and Larsen, 2002; Harkey et al., 2018; Ma and Dong, 2021). These receptors negatively regulate
716 the ethylene signaling pathway and are turned off by the binding of ethylene, inducing downstream
717 changes in transcription. In roots, ETR1 is the ethylene receptor that is most strongly linked to the
718 inhibition of both lateral root formation and primary root elongation and the stimulation of root

719 hair growth (Harkey et al., 2018). To understand the transcripts whose synthesis is regulated by
720 ETR1 to control root development, we identified genome-wide changes in transcript abundance in
721 roots in response to treatment with ethylene or its precursor, ACC, using Col-0 and LOF and GOF
722 *etr1* receptor mutants. We examined the GRNs that are turned on by ethylene and ACC and are
723 dependent on ETR1 signaling, revealing transcripts encoding enzymes of ethylene synthesis and
724 TFs that drive transcriptional responses downstream of ethylene.

725 To identify the transcriptional changes in the presence and absence of ethylene and ACC
726 in Col-0, we began by determining the doses of ethylene and ACC that had similar root
727 developmental responses. The transcript abundance in the presence of ACC and ethylene treatment
728 was quantified at each time point relative to untreated Col-0 to identify DE transcripts and the
729 direction and magnitude change of abundance of these transcripts in response to elevated levels of
730 ethylene or ACC. Ethylene induced a greater number of DE genes than ACC at all time points
731 after treatment and yielded larger magnitude changes in transcript abundance for most transcripts.
732 The most likely explanation for this result was that ethylene gas used in our treatments elevated
733 ethylene levels more than ACC, while ACC needed to be converted to ethylene to induce
734 transcriptional responses. The differences in the magnitude of transcript abundance changes
735 between the treatments were likely due to limitations in cellular uptake of ACC and the additional
736 step required to convert ACC to ethylene by ACO (Houben and Van de Poel, 2019), resulting in
737 reduced and delayed ethylene signaling in the ACC-treated seedlings than in seedlings directly
738 treated with ethylene gas. It is also worth noting that in response to ACC and ethylene treatments,
739 most transcriptional changes were decreases in abundance, especially at the 4- and 24-hour time
740 points. This observation is in alignment with our previous finding that ACC treatment led to a

741 greater number of transcripts with decreased abundance than increased abundance relative to
742 untreated controls (Harkey et al., 2018).

743 Several reports have suggested that ACC may act as a signal independently of its
744 conversion to ethylene, especially at high concentrations where ACO-dependent conversion of
745 ACC to ethylene becomes rate limiting (Althiab-Almasaud et al., 2021; Houben and Van de Poel,
746 2019; Li et al., 2020, 2022; Mou et al., 2020; Polko and Kieber, 2019; Tsang et al., 2011;
747 Tsuchisaka et al., 2009; Van de Poel, 2020; Van de Poel and Van Der Straeten, 2014;
748 Vanderstraeten et al., 2019; Xu et al., 2008; Yin et al., 2019). At concentrations of 10 μM and
749 above, ACC inhibits rosette size and growth across all tissues in seedlings (Vanderstraeten et al.,
750 2019). However, in roots at lower doses of ACC (less than or equal to 1 μM), both the ethylene-
751 insensitive *ein2-1* and *ein2-5* mutants do not respond to treatment with 1 μM ACC (Harkey et al.,
752 2018; Ivanchenko et al., 2008; Muday et al., 2012; Negi et al., 2008; Růžička et al., 2007),
753 suggesting that ACC is either completely converted to ethylene at this dose or that in these tissues
754 under these growth conditions ACC does not control development independent of its conversion
755 to ethylene. Our finding that most of the transcripts that were DE in response to ACC were also
756 DE in response to ethylene is consistent with these possibilities. There were only 395 transcripts,
757 or 9% of all ethylene- and/or ACC-regulated transcripts, that were DE in response to ACC and not
758 ethylene. This small group of ACC-regulated transcripts may result from direct ACC signaling
759 rather than signaling after its conversion to ethylene. We found that several transcripts regulated
760 by ACC only included those encoding MAP kinases, enzymes that remodel the cell wall, and
761 proteins involved in root hair development, as well as ACO enzymes who regulation we
762 characterized. We found that ACC downregulated *ACS7*, which might suggest a negative feedback

763 of ACC synthesis in response to elevated levels of ACC, while *ACO* transcripts increase to
764 facilitate conversion to ethylene.

765 We identified ETR1-regulated genes using two *etr1* mutant alleles: *etr1-3*, which is a GOF
766 receptor mutant with a constitutively active receptor that turns off ethylene signaling, resulting in
767 an ethylene-insensitive phenotype, and *etr1-7*, which is a LOF receptor mutant that has an inactive
768 receptor, resulting in constitutive ethylene signaling. The combination of GOF and LOF receptor
769 mutants served as a powerful approach to identify ETR1-dependent transcriptional responses. This
770 is clear from the earliest steps of the analysis; comparison of all samples by a PCA plot, Pearson's
771 correlation, and Euclidean distance plots led to the separation of *etr1-7* samples from Col-0 and
772 *etr1-3* on the PC1 axis (Figure 2A). This pattern was also observed in the Pearson's correlation
773 and Euclidean distance plots, which showed that *etr1-7* samples were more like each other than to
774 either Col-0 or *etr1-3* (Figure 2E and Supplemental Figure 4). When we examined transcripts that
775 were DE when comparing baseline differences between the genotypes, most transcripts were found
776 DE in comparisons of *etr1-7* to Col-0 or *etr1-3*. In contrast, in the absence of ACC or ethylene,
777 Col-0 and *etr1-3* had nearly identical transcriptional profiles (Figure 5). In a heatmap of all
778 transcripts that changed in Col-0 and the *etr1* mutants in response to ACC and/or ethylene (Figure
779 4), many of the transcripts that changed in *etr1-7* had transcript abundances that changed in the
780 same direction upon ACC or ethylene treatment. Together, these data demonstrated the dramatic
781 effect that constitutive signaling by ETR1 had on the transcriptional profile of Arabidopsis.

782 We compared the transcriptional profiles of the *etr1* mutants to Col-0 in the presence and
783 absence of ethylene or ACC to identify transcripts whose changes in abundance were tied to ETR1
784 functionality. The criteria by which we determined whether a transcript was ETR1 dependent
785 were: 1) if it had a significant change in response to ethylene and/or ACC treatment in at least one

786 time point in Col-0; 2) if it showed no significant change in all treatment samples in *etr1-3*
787 compared to untreated Col-0; and 3) if it showed a significant change in *etr1-7* relative to Col-0 in
788 the baseline with no further changes across the time points. We organized transcripts by their
789 responses, classifying them as ETR1-dependent, ETR1-independent, or complex. ETR1
790 dependency was defined using stringent criteria to identify only those transcripts that clearly
791 required this receptor for transcriptional response to ACC and/or ethylene. The strict ETR1-
792 dependent group was enriched in transcripts annotated to function in "ethylene mediated signaling
793 pathway." We also compared our ETR1 dependent genes to a conserved group of ethylene-
794 responsive genes from a meta-analysis of three root ACC and ethylene response datasets finding
795 31 transcripts that were ETR dependent in the overlap of these groups.

796 An unexpected finding in this study was that there were nearly as many transcripts that
797 responded in an ETR1-independent fashion as those that were ETR1-dependent. Transcripts were
798 defined as ETR1-independent if they responded to ACC or ethylene treatment in all three
799 genotypes. If the abundance of these transcripts increased and decreased in *etr1-7* and *etr1-3*,
800 respectively, and changed with hormone treatment, this might suggest two receptors control their
801 activity with hormone-dependent changes being mediated by a second receptor.

802 In a prior study we found ETR1 to be essential in some root developmental responses and
803 identified roles for other ethylene receptors in other responses (Harkey et al., 2018). ACC effects
804 on lateral root development were completely lost in the ethylene-insensitive mutant *etr1-3* and not
805 induced by addition of ACC in the constitutively signaling mutant *etr1-7*, suggesting inhibition of
806 lateral root formation by ethylene signaling had strong dependence on ETR1. In contrast, inhibition
807 of primary root elongation and stimulation of root hair growth by ACC were less dependent on
808 ETR1 as they showed attenuated responses to ACC in *etr1-7* (Harkey et al., 2018), suggesting a

809 role of other ethylene receptors in these root processes. Perhaps some of the transcripts which were
810 ETR1 independent were involved in root elongation or root hair initiation. Indeed, when we
811 examined genes that were ETR1-independent by the strictest criteria, they were enriched in the
812 annotation "root hair cell differentiation" and several other related annotations.

813 We had identified a small subset of transcripts that were regulated only by ACC in Col-0,
814 suggesting responses that may be driven by ACC signaling independently of its conversion to
815 ethylene. Therefore, we were interested in further analyzing the transcripts that encode ACC
816 oxidases, which convert ACC to ethylene, as this might provide insight into understanding how
817 ACC may regulate its conversion to ethylene. In our dataset, we found that *ACO* transcripts were
818 themselves regulated by ACC and ethylene in a positive feed forward loop, where application of
819 ethylene and/or ACC induced transcript accumulation of all *ACO*s in at least one time point after
820 treatment. We found that *ACO2* and *ACO3* met our strict criteria for ETR1 dependence in response
821 to ethylene but not ACC. This suggests that ACC may be able to regulate transcripts in ways above
822 and beyond the function of ETR1, consistent with the possibility of an ACC-independent signaling
823 pathway. Among these results, we found it most intriguing that *ACO2* and *ACO3* were ETR1-
824 dependent in response to ethylene but not ACC treatment, which would suggest that ACC may act
825 through different molecular machinery than ethylene to regulate the levels of these transcripts.
826 However, for *ACO2*, perhaps the most puzzling of the *ACO*s, ACC-mediated changes in transcript
827 abundance were completely lost in *ein3eil1*, suggesting that ACC activates the canonical ethylene
828 signaling pathway to control *ACO2* levels. It is not clear how ACC both activates the canonical
829 ethylene signaling pathway and induces changes in the *etr1* mutants that were not induced by
830 ethylene. Perhaps ACC can work through a non-canonical ethylene signaling pathway or directly
831 bind to a different ethylene receptor, as this might be required when ACC levels become too high,

832 and the plant needs a mechanism to rapidly convert ACC to ethylene. There is evidence that
833 glucose can signal to EIN2 and subsequently EIN3/EIL1 through the target of rapamycin pathway
834 (Fu et al., 2021), so it is possible that ACC could activate this pathway resulting in transcriptional
835 changes that are not dependent on ETR1 but require the EIN3/EIL1 machinery.

836 To provide more information on the localization of changes in *ACO* transcript abundance,
837 we examined the root cell-type-specific localization of *ACO* transcripts in untreated roots using
838 publicly available transcriptome data and *in planta* using ACO promoter-driven fluorescent protein
839 reporters to inform our understanding of the tissues that express the machinery to convert ACC to
840 ethylene under our treatment conditions. We found that each *ACO* had a distinct tissue expression
841 pattern, and many of these were enhanced in the presence of ACC treatment in 10-day-old
842 seedlings. These findings were consistent with *ACO*s being expressed in root hairs, lateral roots,
843 pericycle cells, and the root elongation zone where their protein products convert ACC to ethylene
844 to signal root responses in these tissues. The most striking observation was that *ACO5* transcripts
845 were the only *ACO* accumulating to high levels in hair cells and root hairs, including the root hair
846 tips, and this expression was induced upon ACC treatment in young seedlings, consistent with a
847 role for ACO5 in driving root hair elongation. On the other hand, the other *pACO*::GFP reporters
848 were not detected or had low fluorescence in root hairs.

849 We were interested in mapping the GRN downstream of ETR1 and EIN3 by examining
850 transcripts predicted to encode TFs using the Agris database (Davuluri et al., 2003). We identified
851 60 TF-encoding transcripts in the ETR1-dependent list of genes and found some that were rapidly
852 upregulated and a greater number that were downregulated by ACC and ethylene treatment with a
853 range of different kinetic responses to these treatments. We also generated a network using PaLD,
854 which groups transcripts together with the most similar temporal responses. This network allows

855 us to visualize connections among transcripts with the most similar responses to ACC and ethylene
856 across time and genotypes and to partition transcripts into groups of like responding genes. We
857 found that the upregulated genes clustered into two groups, one consisting of transcripts with rapid
858 and strong induction in response to treatment, and another consisting of transcripts with more
859 muted up-regulatory patterns, and both groups were enriched in direct targets of EIN3. In contrast,
860 the downregulated genes clustered into four groups containing two or more transcripts with distinct
861 expression patterns, and few of the transcripts in these groups were direct targets of EIN3. These
862 results raise the interesting question of what is the regulatory mechanism by which so many
863 transcripts are decreased in abundance in response to ACC and ethylene treatment.

864 We asked whether three of the TF encoding genes that were found to be EIN3 targets in
865 DAP-Seq or ChIP-Seq datasets (Chang et al. 2013; O'Malley et al. 2016) lost their ACC-regulated
866 expression in an *ein3eil1* mutant, focusing on *ROOT HAIR DEFECTIVE 6-LIKE 5* (*RSL5*),
867 *RELATED TO AP2 6L (RAP2.L)*, and *MYB9*. We found that the ACC-mediated increase in *RSL5*
868 and *RAP2.6L* transcripts and the decrease in *MYB9* transcripts were both lost in *ein3eil1*. It was
869 previously reported that an *rsl5* mutant exhibited normal root hair development in the absence of
870 treatment (Pires et al. 2013), which is not surprising due to the low levels of transcript abundance
871 in untreated roots, suggesting that RSL2 might function in ACC- and ethylene-stimulated root hair
872 formation (2 TPM). One future direction would be to determine whether there is a root hair
873 phenotype in this mutant in the presence of ACC to test the role of *RSL5* in ethylene regulated root
874 hair formation.

875 ETR1 is important in ethylene's ability to inhibit lateral root formation in the region of new
876 root growth formed after exposure to ACC. *LRP1* was identified as ETR-dependent in our dataset;
877 this gene encodes a TF that has previously been shown to function in inhibiting lateral root

878 emergence downstream of ARF7/ARF19, LATERAL ROOT PRIMORDIA 1 (LRP1) (Singh et
879 al., 2020). LRP1 overexpression lines had fewer emerged lateral roots, suggesting that LRP1
880 functions to inhibit lateral root emergence. By examining a *proLRP1*::GUS reporter, we found that
881 *LRP1* expression was increased by ACC in lateral root primordia at all stages of primordia
882 development, and in emerged lateral root tips and in the innermost root cells of primary and lateral
883 roots. However, we examined two *lrp1* mutant alleles in the presence and absence of ACC we
884 observed that one mutant had reduced inhibition of lateral root formation in response to ACC,
885 while the other allele did not, which is inconsistent with the wild-type gene functioning to control
886 lateral root development under our growth conditions.

887 We examined mutants in several other TFs that were selected based on their transcriptional
888 responses to ACC in both this dataset and our prior ACC time course dataset (Harkey et al., 2018),
889 including ANAC058, MYB9, MYB52, and RAP2.6L. We found subtle but statistically significant
890 root phenotypes in these mutants, with *anac058-1*, *myb52-1*, and *rap2.6l-1* having reduced lateral
891 root densities in the presence of ACC compared to Col-0, and *myb9-1* having increased primary
892 root growth compared to Col-0 in the absence of ACC. We also found that *myb52-1* had fewer
893 root hairs than Col-0 in both the presence and absence of ACC. We also examined these mutants
894 for triple response phenotypes in the presence and absence of several concentrations of ACC,
895 finding differences in phenotypes between seedlings grown under continuous light conditions and
896 those grown in the dark for four days prior to exposure to light. These findings suggested that some
897 of these TFs could be involved in the light-dependent pathway downstream of ethylene (Harkey
898 et al., 2019).

899 This study provides insight into the ETR1-mediated GRN controlling root growth and
900 development, identifying genes that are regulated by ETR1 and/or EIN3 and the networks of

901 transcriptional responses that may mediate ethylene dependent root development. We examined
902 the transcriptional regulation of genes encoding ACC oxidases to understand this final step in
903 ethylene synthesis, which controls the balance of accumulation of the ACC precursor and the
904 ethylene product. We find that the *ACO* transcript abundance is regulated more strongly by ACC
905 than ethylene consistent with feed forward synthesis of ethylene when ACC accumulates, which
906 hints at an ethylene-independent role in the regulation of this gene family. This study also provides
907 a valuable dataset to allow researchers to further dissect the role of ETR1 in controlling root
908 responses to changes in both ethylene and the ethylene precursor, ACC.

909

910

Methods

Genotypes and plant growth conditions

All mutants used in this study were in the Col-0 background. Both the *etr1-3* and *etr1-7* alleles have been described previously (Guzmán and Ecker, 1990; Harkey et al., 2018; Hua and Meyerowitz, 1998). The *etr1-7* (AT1G66340) mutant was obtained from Elliot Meyerowitz (Hua and Meyerowitz, 1998). T-DNA insertion mutants were obtained from the Arabidopsis Biological Resource Center for AT3G18400 (SALK_049205C), AT5G12330 (SAIL_402_G06/CS873836 and SALK_201247C), AT5G16770 (SALK_149765C), AT1G17950 (SALK_138624C), and AT5G13330 (SALK_051006C); see Supplemental Table 5 for more information on these lines. The *pACO*::GFP-GUS reporters were prepared by Dr. John Vaughan-Hirsh and shared by Dr. Bram Van de Poel (Houben et el. 2024). The *proLRP1*::GUS reporter was obtained from ABRC (Estornell et al., 2018).

Plants were grown on 1× Murashige and Skoog medium (Caisson Laboratories), pH 5.6, Murashige and Skoog vitamins, and 0.8% agar, buffered with 0.05% MES (Sigma), and supplemented with 1% sucrose. After stratification for 72 h at 4°C, plants were grown under 100-130 μmol m^{-2} s^{-1} continuous cool-white light.

For selecting a dose of ethylene for the RNA-Seq, Col-0 seedlings were treated on day five after germination. For ACC treatment, the seedlings were transferred to a growth medium containing 0 or 0.75 μM ACC for 24 hours before imaging. For ethylene treatment, plates were placed in clear treatment tanks with constant flow-through of the indicated concentration of ethylene for 24 hours before imaging.

Method for selecting time points for RNA-Seq analysis using a previous microarray study

934 We developed an analysis approach to identify the subset of time points that contained the
935 most unique (i.e., not found in other time points) DE genes in response to ACC treatment using
936 our previously published time-course microarray study with ACC treated Col-0 roots (Harkey et
937 al. 2018). In that prior study, we examined transcriptional responses to 1 μM ACC after 0, 0.5, 1,
938 2, 4, 8, 12, and 24 hours of treatment, which overlaid the timeline for ACC-induced root hair
939 initiation. To inform the selection of time points for the present study, we first analyzed the prior
940 microarray data to find DE genes for each individual time point compared to time zero. We then
941 performed a pairwise comparison of time points to determine the number of overlapping DE genes
942 between each time point (Supplemental Figure 1B) and the percent of DE genes in a time point
943 that overlapped with another time point (Supplemental Figure 1A). These results revealed that
944 treatment times of 1, 4, and 24 hours contained the most unique sets of transcripts while also
945 overlapping with the timing of root hair formation to capture early, middle, and late developmental
946 responses. Therefore, we chose to perform RNA-Seq using samples treated with ACC or ethylene
947 at three time points: 1 hour, to monitor rapid transcriptional responses that precede developmental
948 changes; 4 hours, where the most unique transcripts are DE and root hair initiation and primary
949 root elongation are increasing and decreasing, respectively, in response to treatment; and 24 hours
950 to identify transcripts linked to ethylene-modulated lateral root regulation.

951 Microarray data (Harkey et al., 2018) was analyzed using limma (Ritchie et al., 2015).
952 Probes were first filtered for interquartile range (IQR), with anything less than 0.1 excluded from
953 further analysis. Time points were then compared to their time-matched controls; p-values were
954 adjusted using a Benjamini-Hochberg correction. Genes with an absolute $\log_2$FC greater than 0.5
955 and an adjusted p-value less than 0.05 were considered to be DE at that time point. The overlap
956 matrix was created by comparing the DE genes across the time points in a pair-wise manner.

957 Supplemental Figure 1A graphically illustrates the results of this analysis. For each
958 column, the percentage of DE genes at that time point (column) that are also DE in the time point
959 to which it was compared (row) is shown. The number of genes in each comparison that was used
960 to calculate the percentages can be seen in Supplemental Figure 1B. For example, the 2-hour time
961 point showed considerable overlap with the four-hour time point; 87% of all 2-hour DE genes were
962 also DE at 4 hours. The reverse comparison of the four-hour genes that were also DE at 2 hours
963 yielded only 32% of the four-hour genes that were DE at two hours because there were more DE
964 genes in this 4-hour sample. Therefore, the four-hour time point identified nearly all the same DE
965 genes as the 2-hour time point, as well as many more unique genes, so we selected the 4-hour time
966 point over the 2-hour for this RNA-Seq analysis. We also examined the overlaps of the 4- and 8-
967 hour time points and the 12- and 24-hour time points, finding more unique DE transcripts in the
968 8- and 24-hour time points for each of these overlaps. However, as root hairs had already begun to
969 initiate by 4 hours (Harkey et al., 2018), and the ethylene-dependent inhibition of lateral root
970 initiation had begun by 24 hours, these time points also represented important developmental
971 milestones. Ultimately, this analysis informed our choice to do the present experiment with time
972 points 0, 1, 4, and 24 hours.
973
974 ***ACC and ethylene treatment of seedlings for RNA isolation for sequencing***
975 Plants were grown on media as described above on top of a nylon filter (03-100/32; Sefar
976 Filtration) pressed against the plate, as described previously (Harkey et al., 2018; Levesque et al.,
977 2006). Approximately 100 sterilized seeds were placed on each filter; 2 plates were combined for
978 each biological replicate. ACC-treated samples were grown and harvested at Wake Forest
979 University and ethylene-treated samples were grown and harvested at the University of Tennessee

980 Knoxville utilizing a gas flow-through system to treat with constant levels of ethylene gas. The
981 same researchers prepared both sets of samples and identical reagents and light treatments were
982 used in both laboratories. Time 0 controls were prepared in both locations to account for any
983 location-specific effects on baseline expression.

984 Plants were treated on day five after germination. For untreated samples, the nylon filter
985 containing five-day-old plants was transferred to a new control medium and root tissue was
986 immediately harvested. For ACC treatment, the plants on nylon were transferred to growth
987 medium with 1 μM ACC for the given treatment time (1, 4, and 24 h) and then root tissue was
988 harvested. For ethylene treatment, the nylon was transferred to new control medium, and plants
989 were placed in clear treatment tanks with constant flow-through of 0.3 ppm ethylene gas for the
990 given treatment time (1, 4, and 24 h) and then root tissue was harvested. At time of harvesting,
991 roots were cut from seedlings and flash frozen in liquid nitrogen. Frozen samples were ground in
992 liquid nitrogen, and RNA isolation was performed according to the Qiagen plant RNeasy kit
993 protocol, with the addition of the Qiagen RNase-free DNase treatment (Qiagen). After RNA
994 isolation, samples were quantified by A260 using a Nanodrop spectrophotometer (Nanodrop
995 Technologies). Each sample yielded at least 3 μg, and on average 15 μg, of RNA. One Col-0
996 sample which had a 4-hour ethylene treatment had an RNA integrity number (RIN) less than 6 and
997 was not sequenced. Sequencing was performed by GENEWIZ, LLC using the Illumina HiSeq
998 platform.

999

1000 ***RNA-Seq preprocessing and quality control***

1001 FastQC v0.11.8 (Wingett and Andrews, 2018) and MultiQC v1.7 (Ewels et al., 2016) were
1002 used for assessing read quality, which identified adaptor contamination and a bimodal GC Content

1003 distribution. Adaptors were trimmed from reads using CutAdapt v1.18 (Martin, 2011), and reads
1004 trimmed to less than 25 bp were removed. Trimmed reads were then processed with the BBMap
1005 tool BBDuk (Bushnell 2014) to identify and remove rRNA contamination. Running
1006 FastQC/MultiQC over the trimmed and filtered reads revealed the identified quality issues had
1007 been mitigated. Read quantification was performed directly on the processed fastq files with the
1008 Salmon v0.12.0 (Patro et al., 2017) "quant" algorithm in mapping mode using the "--
1009 validateMapping" flag, setting the library type to "IU", and using the TAIR10 reference
1010 transcriptome (NCBI ID: GCF_000001735.3). Counts were imported into R v3.6.0 using the
1011 tximport R package v1.12.3 (Soneson et al., 2016) and summarized to the gene level.
1012
1013 ***Differential expression and visualization***
1014 For visualization and sample comparisons, raw read counts were normalized using the
1015 Variant Stabilizing Transformation method from the R package DESeq2 v1.24.0 (Love et al.,
1016 2014). Sample-wise comparison heatmaps were generated using Pearson's correlation and
1017 Euclidean distance as the distance metrics, respectively. PCA analyses were performed by
1018 DESeq2's plotPCA method using the top 1000 most variable genes for all genotypes together, and
1019 on a per-genotype basis.
1020 All sample-wise comparisons were performed using the DESeq2 package and ashr v2.2-
1021 47 (Stephens et al., 2020). Density plots were generated using ggplot2 v3.3.0 (Wickham, 2016),
1022 and heatmaps of sample-wise comparisons were generated using ComplexHeatmap v.2.3.4 (Gu et
1023 al., 2016). For DE transcripts used in heatmaps and GO analyses, we considered a transcript to be
1024 DE if it had a p-value < 0.01, $|\log FC| > 0.5$, and baseMean > 10.
1025

1026 ***Method to identify and remove outlier control sample***

1027 To determine if all the control samples could be pooled for calculation of logFC of samples,
1028 we generated a PCA plot using only the Col-0 samples (Supplemental Figure 3). This revealed that
1029 one control (an ethylene time 0 sample) did not cluster with the 5 other control samples. This single
1030 sample showed separation on the PC1 axis, which represents over 50% of the variance across all
1031 the Col-0 samples. This sample was found to have far lower RNA yield than the other 71 samples
1032 prepared. This analysis suggested that this sample should be removed from the rest of our analyses.
1033 We generated a new PCA plot without it present revealing much great consistency.

1034 To further validate this method, we performed a differential expression analysis to look for
1035 differences in transcripts between locations with all six Col-0 control samples (three from each
1036 location) and with the outlier sample removed. When all six samples were included, 693 genes
1037 were found to be DE (adjusted p-value < 0.01, $|\log_2 FC| > 0.5$) between the ACC and ethylene
1038 controls performed at these two locations (Supplemental Table 1). When the outlier sample
1039 identified by the PCA plot was removed from the analysis, only 34 genes were found to be DE
1040 between the Col-0 samples (Supplemental Table 1). This removal also affected the model
1041 generated by DESeq2, resulting in subtle effects on the *etr1-3* and *etr1-7* comparisons
1042 (Supplemental Table 1). In the model with the outlier Col-0 removed, 121 and 763 genes were DE
1043 between the controls compared at each location in *etr1-3* and *etr1-7*, respectively (Supplemental
1044 Table 1). The untreated *etr1-7* samples had more DE genes between locations than had been
1045 expected, but there were two controls that were quite different than other samples (as evident in
1046 the PCA analysis in Figure 2D), which suggested that this is a character of two samples rather than
1047 a difference in samples because of location (Supplemental Table 1). We ultimately decided to
1048 combine the control samples for each genotype from both locations.

1049 ***PaLD analysis***

1050 A newly developed tool called Partitioned Local Depths (PaLD) was used to generate
1051 networks of the 553 ETR1-dependent transcripts and the 60 ETR1-dependent transcription factors,
1052 with application of this algorithm to gene expression and time course datasets described previously
1053 (Berenhaut et al., 2022; Khoury et al., 2024a). We sorted genes based on their transcript abundance
1054 patterns in response to ACC and ethylene over time in Col-0, *etr1-3*, and *etr1-7*. We used the
1055 $\log_2$FC values relative to untreated Col-0 as input for the PaLD analysis. We further divided the
1056 networks using the Louvain method for community detection (Blondel et al., 2008). Relevant R
1057 code can be found at https://github.com/moorekatherine/pald.

1058 ***RT-qPCR***

1059 RNA was extracted from roots using the RNeasy Plant Mini Kit (Qiagen) according to the
1060 manufacturer's protocol, with buffer RLT selected as the extraction buffer for roots. RNA with
1061 A260/230 values less than 1.5 were re-isolated using isopropanol. DNA was removed using the
1062 RapidOut DNA Removal Kit (ThermoScientific) according to the manufacturer's instructions.
1063 Complementary DNA was synthesized using the Superscript III First-Strand Synthesis System for
1064 RT-PCR (Invitrogen) with RNA template primed with random hexamers according to the
1065 manufacturer's instructions. PowerUp SYBR Green Master Mix (Applied Biosystems) was used
1066 for quantitative PCR on a QuantStudio 3 Real-Time PCR System (Applied Biosystems). Primer
1067 efficiency and transcript abundance values were calculated using the standard curve method and
1068 primer sequence is reported in Supplemental Table 1.

1069 ***Fluorescence and brightfield imaging***

1070 For high resolution imaging of all *pACO*::GFP-GUS reporters, a Zeiss LSM 880
1071 microscope was used. Roots were first stained with propidium iodide (PI) diluted in water to a
1072 final concentration of 0.01 mg/mL for 2 min before being washed briefly in DI water and mounted
1073 on slides in DI water with #1.5 coverslips. Confocal images were acquired with a 488 nm excitation
1074 laser for imaging GFP and the 561 nm laser for imaging PI with emission ranges of 490-552 nm
1075 and 56-696 nm, respectively. To minimize light scatter and improve image resolution, the pinholes
1076 for imaging GFP and PI were adjusted to slightly less than 1 Airy Unit. Images were taken with a
1077 Plan-Apo 20x/0.8NA objective and field size of 2048 x 2048 pixels. For Z-stacks, pixel dwell time
1078 was 0.26 µs and line averaging was set to 4. Z-stacks were obtained with 2.9 µm intervals between
1079 optical slices. For single-slice, high-resolution images, pixel dwell time was 1.02 µs and line
1080 averaging was set to 8.

1081 For epifluorescence imaging of the *pACO5*::GFP-GUS reporter, a Zeiss Axio Zoom.V16
1082 equipped with a PlanNeoFluar Z 1.0x (0.25NA) objective was used. An excitation range of 430-
1083 495 nm and emission range of 495-575 nm was employed with a Zeiss 38HE fluorescence filter
1084 cube. Images were captured with an Axiocam 506 monochrome camera with an exposure time of
1085 around 500 ms.

1086 For imaging *proLRP1*::GUS, the Zeiss Axio Zoom.V16 equipped with a PlanNeoFluar Z
1087 2.3x (0.75NA) objective was used. Images were captured with an AxioCam HR R3 color camera
1088 with an exposure time of around 10 ms.

1089 ***GUS staining procedure***

1090 Fresh X-Gluc (GoldBio) was dissolved on ice in N,N-Dimethylformamide immediately
1091 before incubating samples. For GUS staining, ten-day-old seedlings were vacuum infiltrated with

1092 GUS buffer containing X-Gluc (100 mM phosphate buffer pH 7, 0.5 mM $K_4Fe(CN)_6$, 0.5 mM,
1093 $K_3Fe(CN)_6$, 0.5 mM, 10 mM EDTA, 0.1% Triton X-100, and 2 mM X-Gluc) for five minutes, then
1094 incubated in the buffer and X-Gluc mixture for 1.5 hours at 37°C. Following product formation,
1095 seedlings were washed in 70% EtOH for 10 min. then fixed overnight in 3:1 EtOH:acetic acid at
1096 4°C in the dark prior to imaging.

1097 ***PCR genotyping***

1098 The primers used for genotyping are reported in Supplemental Table 5. Young leaf tissue
1099 was homogenized in a microcentrifuge tube using a micropestle that was dipped in liquid nitrogen.
1100 Edwards Solution (Edwards et al., 1991) was added to the homogenized leaf tissue and samples
1101 were incubated at room temperature for at least one hour before being spun down. Supernatant
1102 was carefully transferred to a new tube containing an equal volume of isopropanol. Samples were
1103 washed with EtOH and air dried in a sterile hood for approximately 30 minutes before being
1104 resuspended in molecular biology grade H_2O. Genotype was determined using wild-type primers
1105 that flanked the T-DNA insert (the wild-type reaction) to amplify the gene, and right border
1106 primers with T-DNA primers (the T-DNA reaction) to amplify the T-DNA insert (O'Malley et al.,
1107 2015), with primer sequences listed in Supplemental Table 5. DreamTaq DNA Polymerase
1108 (ThermoFisher) was used according to the manufacturer's instructions.

1109 ***Root development analysis***

1110 For analysis of root hair and lateral root phenotypes, five-day-old seedlings were
1111 transferred to plates containing 0 or 0.75 μM ACC for 4 hours or 5 days before imaging root hairs
1112 and lateral roots, respectively. For the root length analysis of dark grown seedlings, seeds were
1113 germinated in the dark for 4 days on untreated plates or plates containing 0.1, 0.2, 0.5, 1 or 2 μM
1114 ACC, then root lengths were measured. Statistical tests (two-way ANOVA and multiple

comparisons tests) were performed in GraphPad Prism 8.0.2. Outliers were identified using ROUT (Q = 1%).

Acknowledgements

This work was supported by the National Science Foundation Systems and Synthetic Biology (MCB-1716279 to GKM) and the Center for Molecular Signaling Graduate Research Fellowship to MGK and a WFU Provost's Pilot Research grant (to GKM and MGK).

References

Abeles, F. B., Morgan, P. W., and Saltveit, M. E. (1992). *Ethylene in plant biology* (2nd ed). Academic Press.

Alonso, J. M., Hirayama, T., Roman, G., Nourizadeh, S., and Ecker, J. R. (1999). EIN2, a Bifunctional Transducer of Ethylene and Stress Responses in Arabidopsis. *Science*, *284*(5423), 2148–2152. https://doi.org/10.1126/science.284.5423.2148

Alonso, J. M., and Stepanova, A. N. (2004). The Ethylene Signaling Pathway. *Science*, *306*(5701), 1513–1515. https://doi.org/10.1126/science.1104812

Althiab-Almasaud, R., Sallanon, H., Chang, C., and Chervin, C. (2021). 1-Aminocyclopropane-1-carboxylic acid stimulates tomato pollen tube growth independently of ethylene receptors. *Physiologia Plantarum*, *173*(4), 2291–2297. https://doi.org/10.1111/ppl.13579

An, F., Zhao, Q., Ji, Y., Li, W., Jiang, Z., Yu, X., Zhang, C., Han, Y., He, W., Liu, Y., Zhang, S., Ecker, J. R., and Guo, H. (2010). Ethylene-Induced Stabilization of ETHYLENE INSENSITIVE3 and EIN3-LIKE1 Is Mediated by Proteasomal Degradation of EIN3 Binding F-Box 1 and 2 That Requires EIN2 in Arabidopsis. *The Plant Cell*, *22*(7), 2384–2401. https://doi.org/10.1105/tpc.110.076588

Azhar, B. J., Zulfiqar, A., Shakeel, S. N., and Schaller, G. E. (2020). Amplification and Adaptation in the Ethylene Signaling Pathway. *Small Methods*, *4*(8), 1900452. https://doi.org/10.1002/smtd.201900452

Berenhaut, K. S., Moore, K. E., and Melvin, R. L. (2022). A social perspective on perceived distances reveals deep community structure. *Proceedings of the National Academy of Sciences*, *119*(4), e2003634119. https://doi.org/10.1073/pnas.2003634119

Berleth, M., Berleth, N., Minges, A., Hänsch, S., Burkart, R. C., Stork, B., Stahl, Y., Weidtkamp-Peters, S., Simon, R., and Groth, G. (2019). Molecular Analysis of Protein-Protein Interactions in the

Ethylene Pathway in the Different Ethylene Receptor Subfamilies. *Frontiers in Plant Science*, *10*. https://www.frontiersin.org/journals/plant-science/articles/10.3389/fpls.2019.00726

Binder, B. M. (2020). Ethylene signaling in plants. *Journal of Biological Chemistry*, *295*(22), 7710–7725. https://doi.org/10.1074/jbc.REV120.010854

Binder, B. M., O'Malley, R. C., Wang, W., Zutz, T. C., and Bleecker, A. B. (2006). Ethylene Stimulates Nutations That Are Dependent on the ETR1 Receptor. *Plant Physiology*, *142*(4), 1690–1700. https://doi.org/10.1104/pp.106.087858

Blondel, V. D., Guillaume, J.-L., Lambiotte, R., and Lefebvre, E. (2008). Fast unfolding of communities in large networks. *Journal of Statistical Mechanics: Theory and Experiment*, *2008*(10), Article 10. https://doi.org/10.1088/1742-5468/2008/10/P10008

Brady, S. M., Orlando, D. A., Lee, J.-Y., Wang, J. Y., Koch, Dinneny, J. R., Mace, D., Ohler, U., and Benfey, P. N. (2007). A High-Resolution Root Spatiotemporal Map Reveals Dominant Expression Patterns. *Science*, *318*(5851), 801–806. https://doi.org/10.1126/science.1146265

Cancel, J. D., and Larsen, P. B. (2002). Loss-of-Function Mutations in the Ethylene ReceptorETR1 Cause Enhanced Sensitivity and Exaggerated Response to Ethylene in Arabidopsis. *Plant Physiology*, *129*(4), 1557–1567. https://doi.org/10.1104/pp.003780

Chang, K. N., Zhong, S., Weirauch, M. T., Hon, G., Pelizzola, M., Li, H., Huang, S. C., Schmitz, R. J., Urich, M. A., Kuo, D., Nery, J. R., Qiao, H., Yang, A., Jamali, A., Chen, H., Ideker, T., Ren, B., Bar-Joseph, Z., Hughes, T. R., and Ecker, J. R. (2013). Temporal transcriptional response to ethylene gas drives growth hormone cross-regulation in Arabidopsis. *eLife*, *2*, e00675. https://doi.org/10.7554/eLife.00675

Chang, Kwok, S. F., Bleecker, A. B., and Meyerowitz, E. M. (1993). Arabidopsis Ethylene-Response Gene ETR1: Similarity of Product to Two-Component Regulators. *Science*, *262*(5133), 539–544. https://doi.org/10.1126/science.8211181

Davuluri, R. V., Sun, H., Palaniswamy, S. K., Matthews, N., Molina, C., Kurtz, M., and Grotewold, E. (2003). AGRIS: Arabidopsis Gene Regulatory Information Server, an information resource of

1173 Arabidopsis cis-regulatory elements and transcription factors. *BMC Bioinformatics*, *4*(1), 25.
1174 https://doi.org/10.1186/1471-2105-4-25
1175 Dolgikh, V. A., Pukhovaya, E. M., and Zemlyanskaya, E. V. (2019). Shaping Ethylene Response: The
1176 Role of EIN3/EIL1 Transcription Factors. *Frontiers in Plant Science*, *10*.
1177 https://www.frontiersin.org/journals/plant-science/articles/10.3389/fpls.2019.01030
1178 Du, Z., Zhou, X., Ling, Y., Zhang, Z., and Su, Z. (2010). agriGO: a GO analysis toolkit for the
1179 agricultural community. *Nucleic Acids Research*, *38*(suppl_2), W64–W70.
1180 https://doi.org/10.1093/nar/gkq310
1181 Edwards, K., Johnstone, C., and Thompson, C. (1991). A simple and rapid method for the preparation of
1182 plant genomic DNA for PCR analysis. *Nucleic Acids Research*, *19*(6), 1349–1349.
1183 https://doi.org/10.1093/nar/19.6.1349
1184 Estornell, L. H., Landberg, K., Cierlik, I., and Sundberg, E. (2018). SHI/STY Genes Affect Pre- and Post-
1185 meiotic Anther Processes in Auxin Sensing Domains in Arabidopsis. *Frontiers in Plant Science*,
1186 *9*. https://www.frontiersin.org/journals/plant-science/articles/10.3389/fpls.2018.00150
1187 Ewels, P., Magnusson, M., Lundin, S., and Käller, M. (2016). MultiQC: summarize analysis results for
1188 multiple tools and samples in a single report. *Bioinformatics*, *32*(19), 3047–3048.
1189 https://doi.org/10.1093/bioinformatics/btw354
1190 Feng, Y., Xu, P., Li, B., Li, P., Wen, X., An, F., Gong, Y., Xin, Y., Zhu, Z., Wang, Y., and Guo, H.
1191 (2017). Ethylene promotes root hair growth through coordinated EIN3/EIL1 and RHD6/RSL1
1192 activity in Arabidopsis. *Proceedings of the National Academy of Sciences*, *114*(52), 13834–
1193 13839. https://doi.org/10.1073/pnas.1711723115
1194 Fu, L., Liu, Y., Qin, G., Wu, P., Zi, H., Xu, Z., Zhao, X., Wang, Y., Li, Y., Yang, S., Peng, C., Wong, C.
1195 C. L., Yoo, S.-D., Zuo, Z., Liu, R., Cho, Y.-H., and Xiong, Y. (2021). The TOR–EIN2 axis
1196 mediates nuclear signalling to modulate plant growth. *Nature*, *591*(7849), 288–292.
1197 https://doi.org/10.1038/s41586-021-03310-y

1198 Ge, S. X., Jung, D., and Yao, R. (2020). ShinyGO: a graphical gene-set enrichment tool for animals and
1199 plants. *Bioinformatics*, *36*(8), 2628–2629. https://doi.org/10.1093/bioinformatics/btz931
1200 Gu, Z., Eils, R., and Schlesner, M. (2016). Complex heatmaps reveal patterns and correlations in
1201 multidimensional genomic data. *Bioinformatics*, *32*(18), Article 18.
1202 https://doi.org/10.1093/bioinformatics/btw313
1203 Guzmán, P., and Ecker, J. R. (1990). Exploiting the triple response of Arabidopsis to identify ethylene-
1204 related mutants. *The Plant Cell*, *2*(6), 513–523. https://doi.org/10.1105/tpc.2.6.513
1205 Harkey, A. F., Watkins, J. M., Olex, A. L., DiNapoli, K. T., Lewis, D. R., Fetrow, J. S., Binder, B. M.,
1206 and Muday, G. K. (2018). Identification of Transcriptional and Receptor Networks That Control
1207 Root Responses to Ethylene. *Plant Physiology*, *176*(3), 2095–2118.
1208 https://doi.org/10.1104/pp.17.00907
1209 Harkey, A. F., Yoon, G. M., Seo, D. H., DeLong, A., and Muday, G. K. (2019). Light Modulates
1210 Ethylene Synthesis, Signaling, and Downstream Transcriptional Networks to Control Plant
1211 Development. *Frontiers in Plant Science*, *10*. https://www.frontiersin.org/journals/plant-
1212 science/articles/10.3389/fpls.2019.01094
1213 Houben, M., and Van de Poel, B. (2019). 1-Aminocyclopropane-1-Carboxylic Acid Oxidase (ACO): The
1214 Enzyme That Makes the Plant Hormone Ethylene. *Frontiers in Plant Science*, *10*.
1215 https://www.frontiersin.org/articles/10.3389/fpls.2019.00695
1216 Hua, J., and Meyerowitz, E. M. (1998). Ethylene Responses Are Negatively Regulated by a Receptor
1217 Gene Family in Arabidopsis thaliana. *Cell*, *94*(2), 261–271. https://doi.org/10.1016/S0092-
1218 8674(00)81425-7
1219 Hua, J., Sakai, H., Nourizadeh, S., Chen, Q. G., Bleecker, A. B., Ecker, J. R., and Meyerowitz, E. M.
1220 (1998). EIN4 and ERS2 Are Members of the Putative Ethylene Receptor Gene Family in
1221 Arabidopsis. *The Plant Cell*, *10*(8), 1321–1332. https://doi.org/10.1105/tpc.10.8.1321

1222 Huang, Y., Li, H., Hutchison, C. E., Laskey, J., and Kieber, J. J. (2003). Biochemical and functional
1223 analysis of CTR1, a protein kinase that negatively regulates ethylene signaling in Arabidopsis.
1224 *The Plant Journal*, *33*(2), 221–233. https://doi.org/10.1046/j.1365-313X.2003.01620.x
1225 Ivanchenko, M. G., Muday, G. K., and Dubrovsky, J. G. (2008). Ethylene–auxin interactions regulate
1226 lateral root initiation and emergence in Arabidopsis thaliana. *The Plant Journal*, *55*(2), 335–347.
1227 https://doi.org/10.1111/j.1365-313X.2008.03528.x
1228 Khoury, M. G., Berenhaut, K. S., Moore, K. E., Allen, E. E., Harkey, A. F., Mühlemann, J. K., Craven, C.
1229 N., Xu, J., Jain, S. S., John, D. J., Norris, J. L., and Muday, G. K. (2024). Informative community
1230 structure revealed using Arabidopsis time series transcriptome data via partitioned local depth. *In*
1231 *Silico Plants*, *6*(1), diad018. https://doi.org/10.1093/insilicoplants/diad018
1232 Khoury, M. G., Martin, R. E., Houben, M., and Muday, G. K. (2024). Ethylene Regulates Root Growth
1233 and Development. In *Plant Roots: The Hidden Half* (5th ed.). CRC Press. 10.1201/b23126-19
1234 Kieber, J. J., Rothenberg, M., Roman, G., Feldmann, K. A., and Ecker, J. R. (1993). CTR1, a negative
1235 regulator of the ethylene response pathway in arabidopsis, encodes a member of the Raf family of
1236 protein kinases. *Cell*, *72*(3), 427–441. https://doi.org/10.1016/0092-8674(93)90119-B
1237 Kim, H., Helmbrecht, E. E., Stalans, M. B., Schmitt, C., Patel, N., Wen, C.-K., Wang, W., and Binder, B.
1238 M. (2011). Ethylene Receptor ETHYLENE RECEPTOR1 Domain Requirements for Ethylene
1239 Responses in Arabidopsis Seedlings. *Plant Physiology*, *156*(1), 417–429.
1240 https://doi.org/10.1104/pp.110.170621
1241 Lee, S. H., and Cho, H.-T. (2008). Auxin and Root Hair Morphogenesis. In *Plant Cell Monographs* (pp.
1242 1–20). Springer Berlin Heidelberg. https://doi.org/10.1007/7089_2008_16
1243 Levesque, M. P., Vernoux, T., Busch, W., Cui, H., Wang, J. Y., Blilou, I., Hassan, H., Nakajima, K.,
1244 Matsumoto, N., Lohmann, J. U., Scheres, B., and Benfey, P. N. (2006). Correction: Whole-
1245 Genome Analysis of the SHORT-ROOT Developmental Pathway in Arabidopsis. *PLOS Biology*,
1246 *4*(7), e249. https://doi.org/10.1371/journal.pbio.0040249

1247 Lewis, D. R., Negi, S., Sukumar, P., and Muday, G. K. (2011). Ethylene inhibits lateral root development,
1248 increases IAA transport and expression of PIN3 and PIN7 auxin efflux carriers. *Development*,
1249 *138*(16), 3485–3495. https://doi.org/10.1242/dev.065102
1250 Li, D., Flores-Sandoval, E., Ahtesham, U., Coleman, A., Clay, J. M., Bowman, J. L., and Chang, C.
1251 (2020). Ethylene-independent functions of the ethylene precursor ACC in Marchantia
1252 polymorpha. *Nature Plants*, *6*(11), 1335–1344. https://doi.org/10.1038/s41477-020-00784-y
1253 Li, D., Mou, W., Van de Poel, B., and Chang, C. (2022). Something old, something new: Conservation of
1254 the ethylene precursor 1-amino-cyclopropane-1-carboxylic acid as a signaling molecule. *Current*
1255 *Opinion in Plant Biology*, *65*, 102116. https://doi.org/10.1016/j.pbi.2021.102116
1256 Love, M. I., Huber, W., and Anders, S. (2014). Moderated estimation of fold change and dispersion for
1257 RNA-seq data with DESeq2. *Genome Biology*, *15*(12), 550. https://doi.org/10.1186/s13059-014-
1258 0550-8
1259 Ma, Q., and Dong, C.-H. (2021). Regulatory functions and molecular mechanisms of ethylene receptors
1260 and receptor-associated proteins in higher plants. *Plant Growth Regulation*, *93*(1), 39–52.
1261 https://doi.org/10.1007/s10725-020-00674-5
1262 Martin. (2011). Cutadapt removes adapter sequences from high-throughput sequencing reads.
1263 *EMBnet.Journal*, *17*, 10–12.
1264 Martin, R. E., Marzol, E., Estevez, J. M., and Muday, G. K. (2022). Ethylene signaling increases reactive
1265 oxygen species accumulation to drive root hair initiation in Arabidopsis. *Development*, *149*(13),
1266 dev200487. https://doi.org/10.1242/dev.200487
1267 Masucci, J. D., and Schiefelbein, J. W. (1996). Hormones act downstream of TTG and GL2 to promote
1268 root hair outgrowth during epidermis development in the Arabidopsis root. *The Plant Cell*, *8*(9),
1269 1505–1517. https://doi.org/10.1105/tpc.8.9.1505
1270 McDaniel, B. K., and Binder, B. M. (2012). Ethylene Receptor 1 (ETR1) Is Sufficient and Has the
1271 Predominant Role in Mediating Inhibition of Ethylene Responses by Silver in Arabidopsis

1272 thaliana*. *Journal of Biological Chemistry*, *287*(31), 26094–26103.
1273 https://doi.org/10.1074/jbc.M112.383034
1274 Mou, W., Kao, Y.-T., Michard, E., Simon, A. A., Li, D., Wudick, M. M., Lizzio, M. A., Feijó, J. A., and
1275 Chang, C. (2020). Ethylene-independent signaling by the ethylene precursor ACC in Arabidopsis
1276 ovular pollen tube attraction. *Nature Communications*, *11*(1), 4082.
1277 https://doi.org/10.1038/s41467-020-17819-9
1278 Muday, G. K., Rahman, A., and Binder, B. M. (2012). Auxin and ethylene: Collaborators or competitors?
1279 *Trends in Plant Science*, *17*(4), 181–195. https://doi.org/10.1016/j.tplants.2012.02.001
1280 Negi, S., Ivanchenko, M. G., and Muday, G. K. (2008). Ethylene regulates lateral root formation and
1281 auxin transport in Arabidopsis thaliana. *The Plant Journal*, *55*(2), 175–187.
1282 https://doi.org/10.1111/j.1365-313X.2008.03495.x
1283 O'Malley, R. C., Barragan, C. C., and Ecker, J. R. (2015). A user's guide to the Arabidopsis T-DNA
1284 insertion mutant collections. *Methods in Molecular Biology (Clifton, N.J.)*, *1284*, 323–342.
1285 PubMed. https://doi.org/10.1007/978-1-4939-2444-8_16
1286 O'Malley, R. C., Huang, S.-S. C., Song, L., Lewsey, M. G., Bartlett, A., Nery, J. R., Galli, M., Gallavotti,
1287 A., and Ecker, J. R. (2016). Cistrome and Epicistrome Features Shape the Regulatory DNA
1288 Landscape. *Cell*, *165*(5), 1280–1292. PubMed. https://doi.org/10.1016/j.cell.2016.04.038
1289 Palaniswamy, S. K., James, S., Sun, H., Lamb, R. S., Davuluri, R. V., and Grotewold, E. (2006). AGRIS
1290 and AtRegNet. A Platform to Link cis-Regulatory Elements and Transcription Factors into
1291 Regulatory Networks. *Plant Physiology*, *140*(3), 818–829. https://doi.org/10.1104/pp.105.072280
1292 Patro, R., Duggal, G., Love, M. I., Irizarry, R. A., and Kingsford, C. (2017). Salmon provides fast and
1293 bias-aware quantification of transcript expression. *Nature Methods*, *14*(4), 417–419.
1294 https://doi.org/10.1038/nmeth.4197
1295 Pires, N. D., Yi, K., Breuninger, H., Catarino, B., Menand, B., and Dolan, L. (2013). Recruitment and
1296 remodeling of an ancient gene regulatory network during land plant evolution. *Proceedings of the*
1297 *National Academy of Sciences*, *110*(23), 9571–9576. https://doi.org/10.1073/pnas.1305457110

1298 Polko, J. K., and Kieber, J. J. (2019). 1-Aminocyclopropane 1-Carboxylic Acid and Its Emerging Role as
1299 an Ethylene-Independent Growth Regulator. *Frontiers in Plant Science*, *10*.
1300 https://www.frontiersin.org/journals/plant-science/articles/10.3389/fpls.2019.01602
1301 Qiao, H., Chang, K. N., Yazaki, J., and Ecker, J. R. (2009). Interplay between ethylene, ETP1/ETP2 F-
1302 box proteins, and degradation of EIN2 triggers ethylene responses in Arabidopsis. *Genes &*
1303 *Development*, *23*(4), 512–521.
1304 Qin, H., He, L., and Huang, R. (2019). The Coordination of Ethylene and Other Hormones in Primary
1305 Root Development. *Frontiers in Plant Science*, *10*. https://www.frontiersin.org/journals/plant-
1306 science/articles/10.3389/fpls.2019.00874
1307 Rahman, A., Tsurumi, S., Amakawa, T., Soga, K., Hoson, T., Goto, N., and Kamisaka, S. (2000).
1308 Involvement of Ethylene and Gibberellin Signalings in Chromosaponin I-Induced Cell Division
1309 and Cell Elongation in the Roots of Arabidopsis Seedlings. *Plant and Cell Physiology*, *41*(1), 1–
1310 9. https://doi.org/10.1093/pcp/41.1.1
1311 Ritchie, M. E., Phipson, B., Wu, D., Hu, Y., Law, C. W., Shi, W., and Smyth, G. K. (2015). Limma
1312 powers differential expression analyses for RNA-sequencing and microarray studies. *Nucleic*
1313 *Acids Research*, *43*(7), Article 7. https://doi.org/10.1093/nar/gkv007
1314 Růžička, K., Ljung, K., Vanneste, S., Podhorská, R., Beeckman, T., Friml, J., and Benková, E. (2007).
1315 Ethylene Regulates Root Growth through Effects on Auxin Biosynthesis and Transport-
1316 Dependent Auxin Distribution. *The Plant Cell*, *19*(7), 2197–2212.
1317 https://doi.org/10.1105/tpc.107.052126
1318 Sakai, H., Hua, J., Chen, Q. G., Chang, C., Medrano, L. J., Bleecker, A. B., and Meyerowitz, E. M.
1319 (1998). ETR2 is an ETR1-like gene involved in ethylene signaling in Arabidopsis. *Proceedings of*
1320 *the National Academy of Sciences*, *95*(10), 5812–5817. https://doi.org/10.1073/pnas.95.10.5812
1321 Schaller, G. E., and Bleecker, A. B. (1995). Ethylene-Binding Sites Generated in Yeast Expressing the
1322 Arabidopsis ETR1 Gene. *Science*, *270*(5243), 1809–1811. JSTOR.

1323 Schaller, G. E., and Kieber, J. G. (2002). Ethylene. *The Arabidopsis Book*, *2002*(1).
1324 https://doi.org/10.1199/tab.0071
1325 Shakeel, S. N., Wang, X., Binder, B. M., and Schaller, G. E. (2013). Mechanisms of signal transduction
1326 by ethylene: Overlapping and non-overlapping signalling roles in a receptor family. *AoB*
1327 *PLANTS*, *5*, plt010. https://doi.org/10.1093/aobpla/plt010
1328 Singh, S., Yadav, S., Singh, A., Mahima, M., Singh, A., Gautam, V., and Sarkar, A. K. (2020). Auxin
1329 signaling modulates LATERAL ROOT PRIMORDIUM1 (LRP1) expression during lateral root
1330 development in Arabidopsis. *The Plant Journal*, *101*(1), 87–100.
1331 https://doi.org/10.1111/tpj.14520
1332 Soneson, C., Matthes, K. L., Nowicka, M., Law, C. W., and Robinson, M. D. (2016). Isoform prefiltering
1333 improves performance of count-based methods for analysis of differential transcript usage.
1334 *Genome Biology*, *17*(1), 12. https://doi.org/10.1186/s13059-015-0862-3
1335 Stepanova, A. N., Yun, J., Likhacheva, A. V., and Alonso, J. M. (2007). Multilevel Interactions between
1336 Ethylene and Auxin in Arabidopsis Roots. *The Plant Cell*, *19*(7), 2169–2185.
1337 https://doi.org/10.1105/tpc.107.052068
1338 Stephens, M., Carbonetto, P., Gerard, D., Lu, M., Sun, L., Willwerscheid, J., and Xiao, N. (2020).
1339 *Methods for Adaptive Shrinkage, using Empirical Bayes [R package ashr version 2.2-47]*.
1340 https://api.semanticscholar.org/CorpusID:226047420
1341 Sukumar, P., Edwards, K. S., Rahman, A., DeLong, A., and Muday, G. K. (2009). PINOID Kinase
1342 Regulates Root Gravitropism through Modulation of PIN2-Dependent Basipetal Auxin Transport
1343 in Arabidopsis. *Plant Physiology*, *150*(2), 722–735. https://doi.org/10.1104/pp.108.131607
1344 Tian, T., Liu, Y., Yan, H., You, Q., Yi, X., Du, Z., Xu, W., and Su, Z. (2017). agriGO v2.0: A GO
1345 analysis toolkit for the agricultural community, 2017 update. *Nucleic Acids Research*, *45*(W1),
1346 W122–W129. https://doi.org/10.1093/nar/gkx382

1347 Tsang, D. L., Edmond, C., Harrington, J. L., and Nühse, T. S. (2011). Cell Wall Integrity Controls Root
1348 Elongation via a General 1-Aminocyclopropane-1-Carboxylic Acid-Dependent, Ethylene-
1349 Independent Pathway. *Plant Physiology*, *156*(2), 596–604. https://doi.org/10.1104/pp.111.175372
1350 Tsuchisaka, A., Yu, G., Jin, H., Alonso, J. M., Ecker, J. R., Zhang, X., Gao, S., and Theologis, A. (2009).
1351 A Combinatorial Interplay Among the 1-Aminocyclopropane-1-Carboxylate Isoforms Regulates
1352 Ethylene Biosynthesis in Arabidopsis thaliana. *Genetics*, *183*(3), 979–1003.
1353 https://doi.org/10.1534/genetics.109.107102
1354 Van de Poel, B. (2020). Ethylene's fraternal twin steals the spotlight. *Nature Plants*, *6*(11), 1309–1310.
1355 https://doi.org/10.1038/s41477-020-00796-8
1356 Van de Poel, B., Smet, D., and Van Der Straeten, D. (2015). Ethylene and Hormonal Cross Talk in
1357 Vegetative Growth and Development. *Plant Physiology*, *169*(1), 61–72.
1358 https://doi.org/10.1104/pp.15.00724
1359 Van de Poel, B., and Van Der Straeten, D. (2014). 1-aminocyclopropane-1-carboxylic acid (ACC) in
1360 plants: More than just the precursor of ethylene! *Frontiers in Plant Science*, *5*.
1361 https://www.frontiersin.org/journals/plant-science/articles/10.3389/fpls.2014.00640
1362 Vanderstraeten, L., Depaepe, T., Bertrand, S., and Van Der Straeten, D. (2019). The Ethylene Precursor
1363 ACC Affects Early Vegetative Development Independently of Ethylene Signaling. *Frontiers in*
1364 *Plant Science*, *10*. https://www.frontiersin.org/journals/plant-
1365 science/articles/10.3389/fpls.2019.01591
1366 Wang, K. L.-C., Li, H., and Ecker, J. R. (2002). Ethylene Biosynthesis and Signaling Networks. *The*
1367 *Plant Cell*, *14*(suppl_1), S131–S151. https://doi.org/10.1105/tpc.001768
1368 Wickham, H. (2016). *ggplot2: Elegant Graphics for Data Analysis* (2nd ed.). Springer Cham.
1369 https://doi.org/10.1007/978-3-319-24277-4
1370 Wingett, S., and Andrews, S. (2018). FastQ Screen: A tool for multi-genome mapping and quality control
1371 [version 2; peer review: 4 approved]. *F1000Research*, *7*(1338).
1372 https://doi.org/10.12688/f1000research.15931.2

1373 Xu, S.-L., Rahman, A., Baskin, T. I., and Kieber, J. J. (2008). Two Leucine-Rich Repeat Receptor
1374 Kinases Mediate Signaling, Linking Cell Wall Biosynthesis and ACC Synthase in Arabidopsis.
1375 *The Plant Cell*, *20*(11), 3065–3079. https://doi.org/10.1105/tpc.108.063354
1376 Yin, J., Zhang, X., Zhang, G., Wen, Y., Liang, G., and Chen, X. (2019). Aminocyclopropane-1-
1377 carboxylic acid is a key regulator of guard mother cell terminal division in Arabidopsis thaliana.
1378 *Journal of Experimental Botany*, *70*(3), 897–908. https://doi.org/10.1093/jxb/ery413
1379

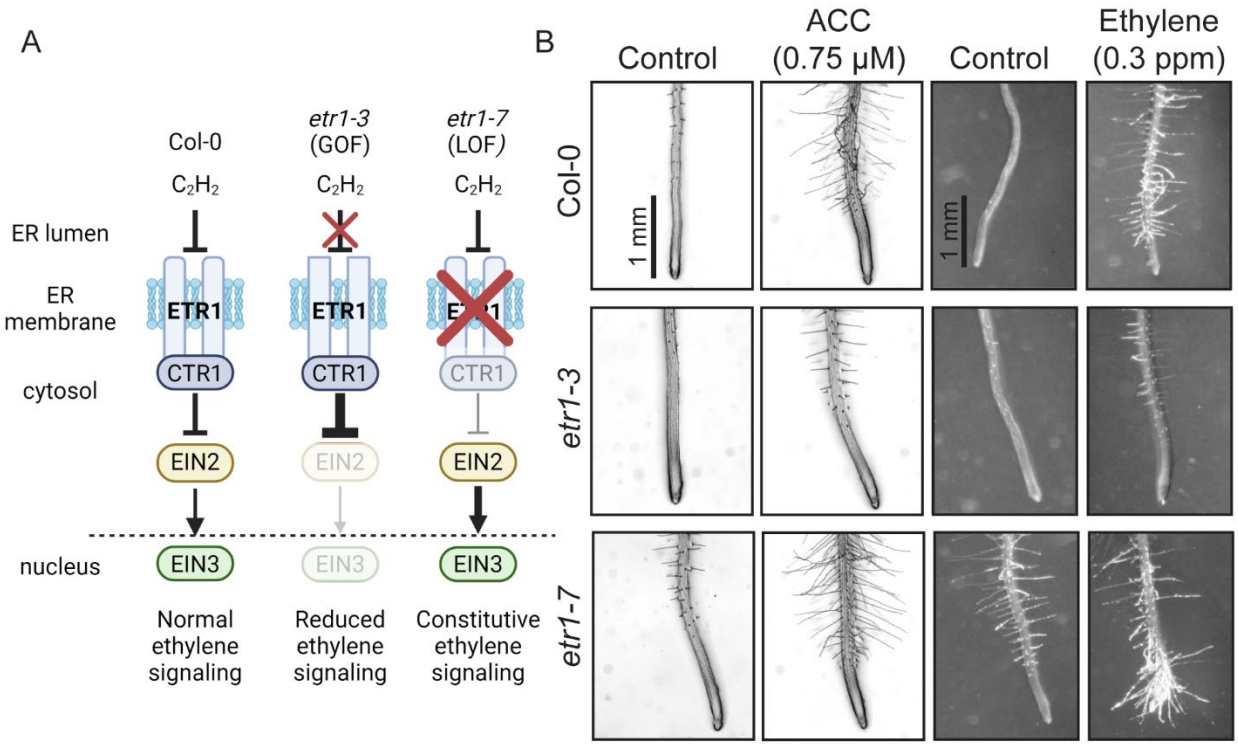

Figure 1. Altered ethylene signaling in the *etr1-3* and *etr1-7* mutants results in aberrant root hair formation. (A) A schematic illustrating the wild-type ethylene signaling pathway and how it is altered in *etr1-3* and *etr1-7* mutants. This image was prepared using Biorender. (B) Representative images of six-day-old Col-0, *etr1-3*, and *etr1-7* seedlings treated with 0.3 ppm ethylene or 0.75 μM ACC for 24 hours, revealing similar developmental responses by these two doses of ethylene and ACC within the different genotypes.

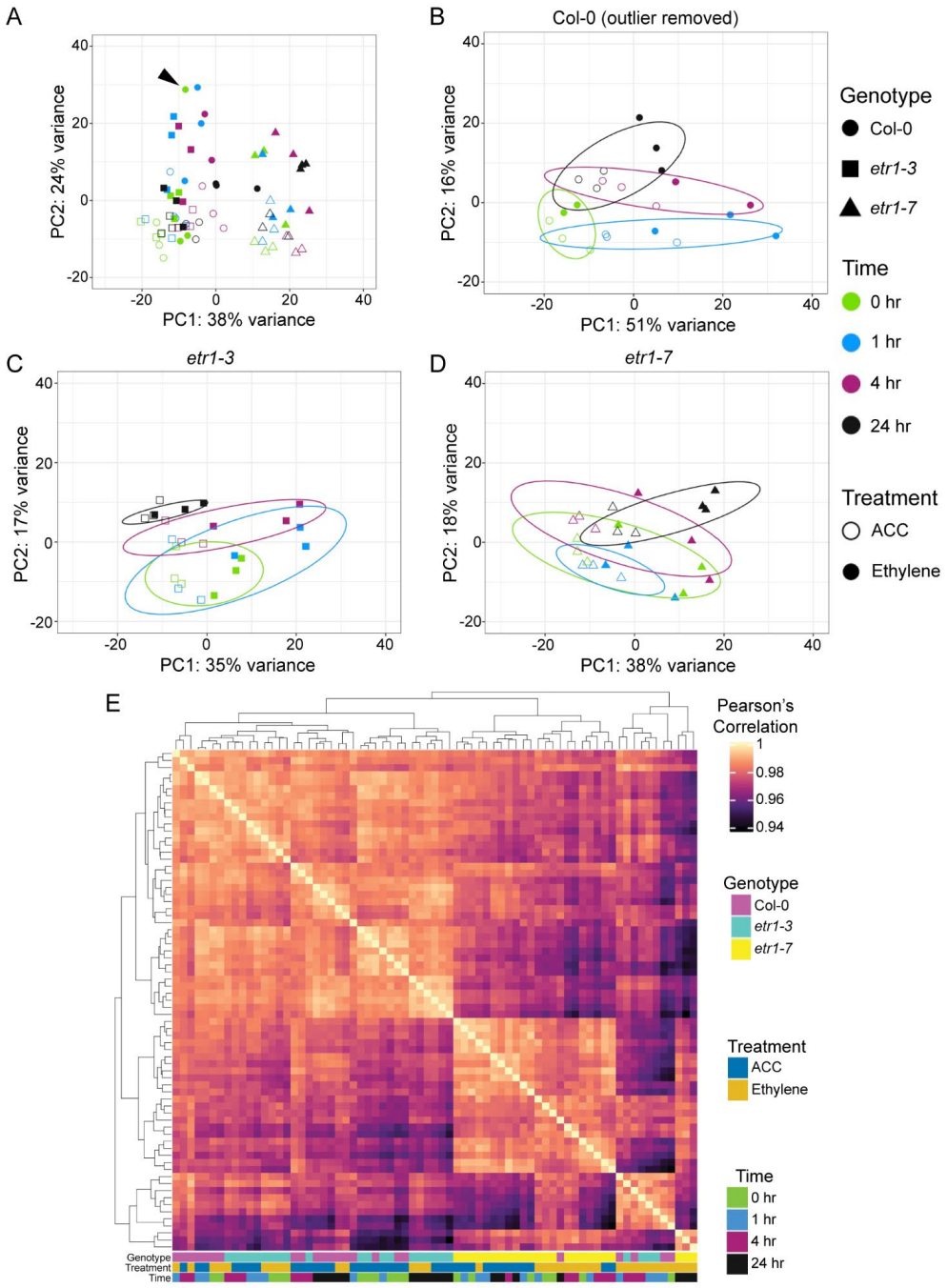

Figure 2. Large-scale transcript abundance patterns in data show *etr1-7* samples are distinctly different from Col-0 and *etr1-3*. (A) PCA plot of all sequenced samples with the genotype indicated by shape of the symbol, the time of treatment indicated by color, and the treatment type ACC or ethylene, indicated by open or filled symbols, respectively. The arrow denotes an untreated Col-0 outlier. PCA plots of (B) Col-0 (with the outlier sample removed), (C) *etr1-3*, and (D) *etr1-7* samples. Circles surround the 80% confidence intervals for each time point. (E) Pearson Correlation plot for all samples.

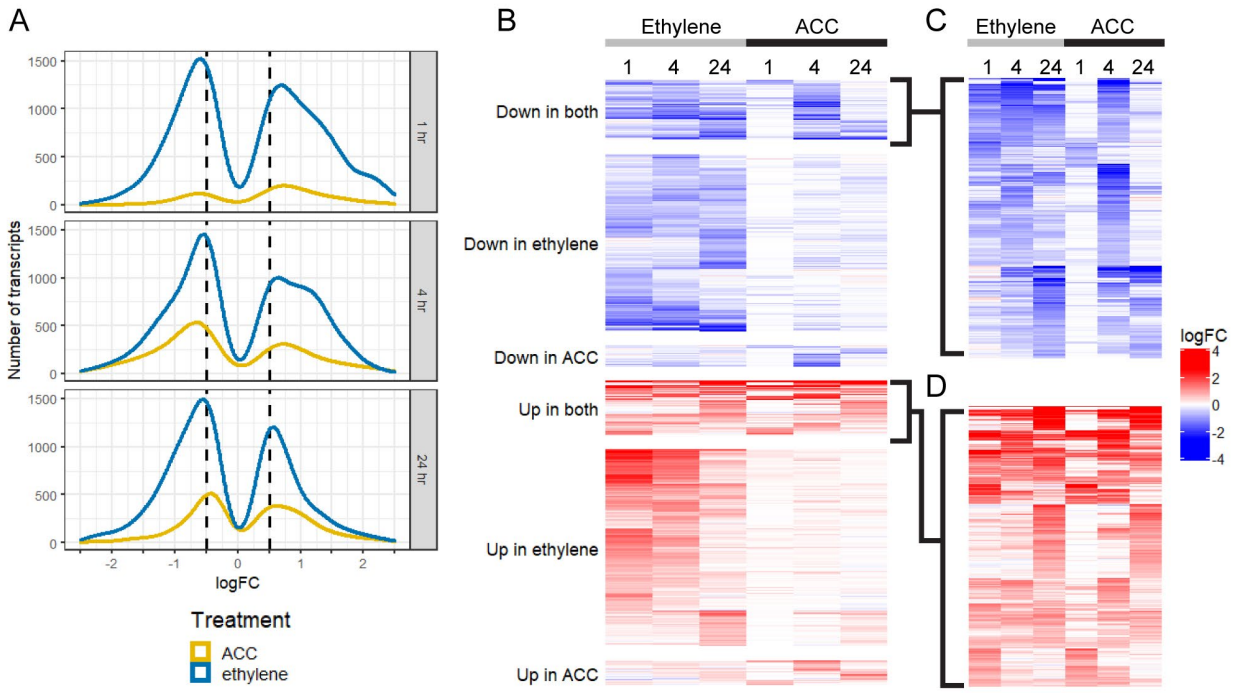

Figure 3. The transcriptional responses to ethylene and ACC treatment revealed more down-regulated genes at 4 and 24 hours and more DE genes by ethylene than ACC. (A) Density plot reporting the number of transcripts across a range of $\log_2$FC values for each treatment and time point in Col-0 samples. The $\log_2$FC is relative to Col-0 control (time 0). For each treatment and time point, only transcripts with an adjusted p-value < 0.01 are shown; no $\log_2$FC cutoff was used. (B) Heatmap showing the $\log_2$FC values of the 4,522 transcripts that were DE relative to untreated Col-0 in at least one Col-0 sample treated with ethylene or ACC based on $|\log_2 FC| > 0.5$ and adjusted p-value < 0.01. (C & D) Transcripts which are DE in at least one time point for both ethylene and ACC, with a (C) negative or (D) positive $\log_2$FC.

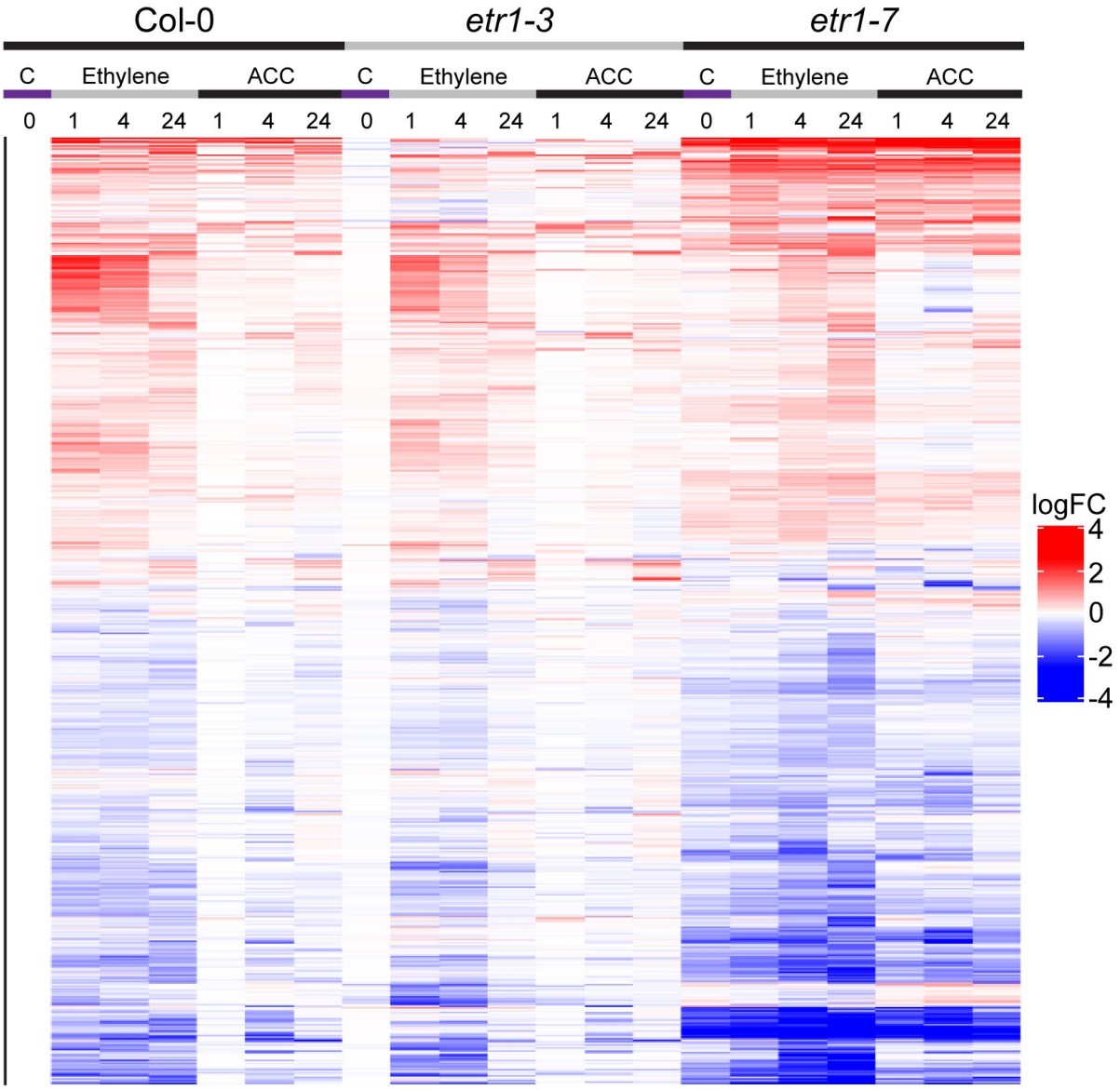

Figure 4. Heatmap of all transcripts that were DE in at least one time point, treatment, or genotype revealed a variety of patterns. This comparison of the transcriptional responses of 8,323 DE transcripts across treatments, time points and genotypes revealed suppressed ethylene signaling in *etr1-3* and enhanced ethylene signaling in *etr1-7*, relative to Col-0 untreated. The heat map includes all 8,323 transcripts that are DE in at least one of the represented groups in comparison with Col-0 control with $|\log_2 FC| > 0.5$ and adjusted p-value < 0.01. $\log_2 FC$ for all columns is relative to untreated Col-0 samples.

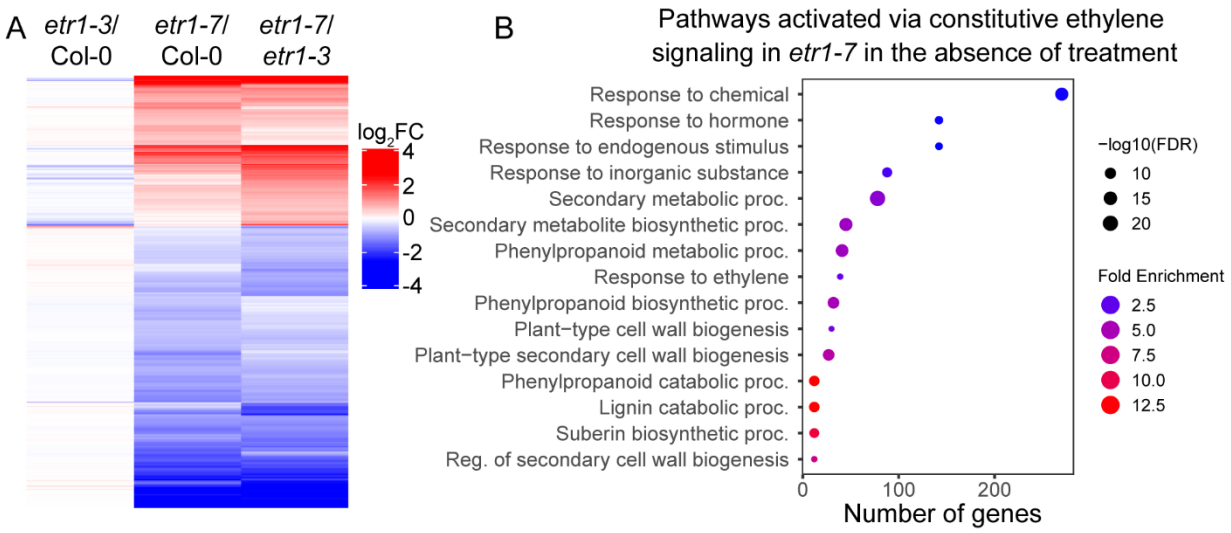

Figure 5. Baseline transcript abundance differences between Col-0 and the *etr1* mutants were consistent with constitutive ethylene signaling in *etr1-7*. (A) All transcripts which are DE in at least one comparison with $|\log_2 FC| > 0.5$ and adjusted p-value < 0.01. $\log_2 FC$ is relative to the second genotype in each comparison. (B) Enriched biological processes among the 1,458 DE genes in the overlap between the *etr1-7* vs. Col-0 comparisons and the *etr1-7* vs. *etr1-3* comparisons as determined by ShinyGO 0.80 (Ge et al., 2020).

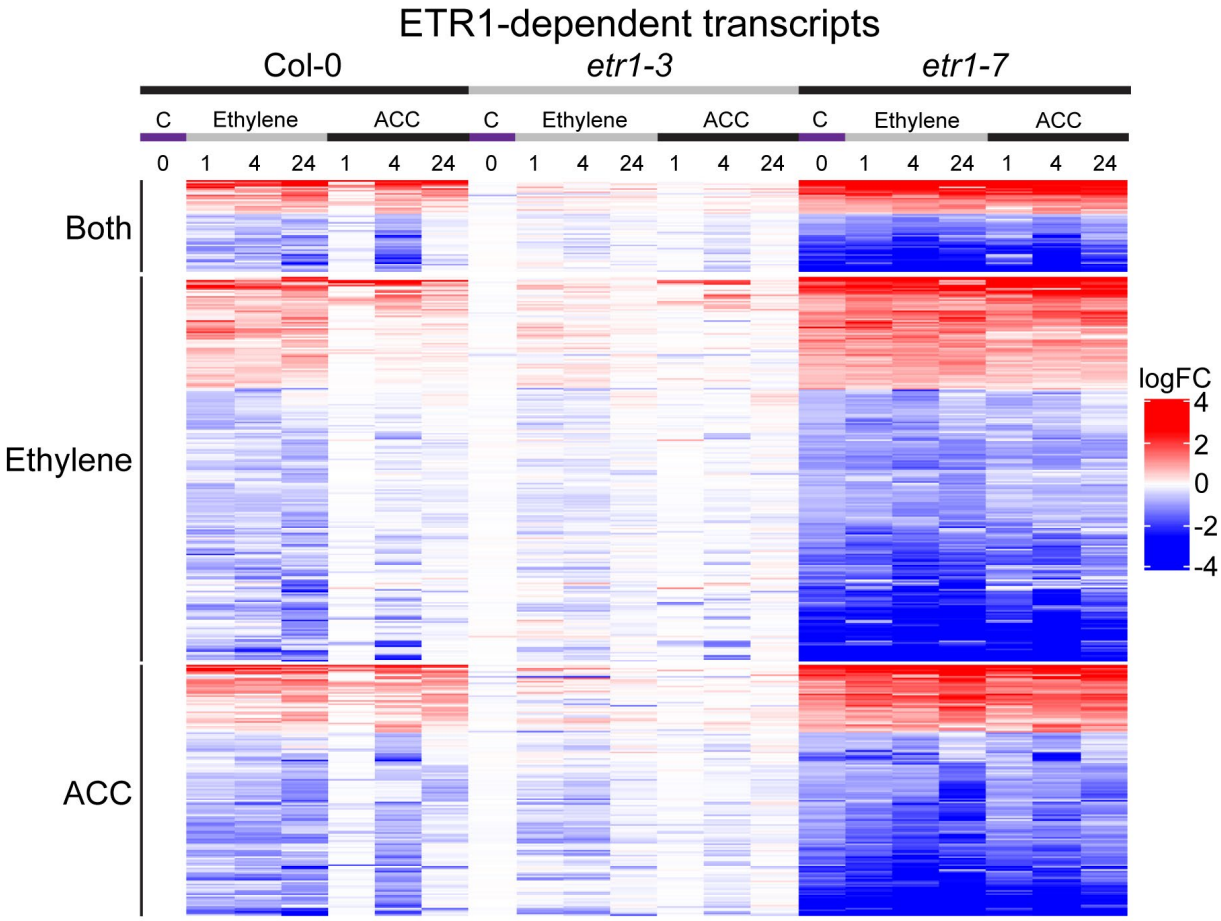

Figure 6. ETR1-dependent transcript heatmap revealed genotype and treatment dependent changes in transcript abundance. This comparison of transcript abundance across treatments and genotypes revealed a set of transcripts that responded to ethylene and/or ACC treatment in Col-0 but not in the mutants. Transcripts which follow a pattern of response that suggests they are ETR1-dependent were selected. These transcripts respond to ACC and/or ethylene treatment in Col-0, do not respond in *etr1-3*, and are constitutively up or down in *etr1-7*, based on $|\log_2 FC| > 0.5$ and adjusted p-value < 0.01. The $\log_2 FC$ reported here was determined relative to untreated Col-0. Genes are split into three groups based on whether they met our ETR1-dependent criteria in ethylene only (292 transcripts), ACC only (191 transcripts), or both treatments (70 transcripts).

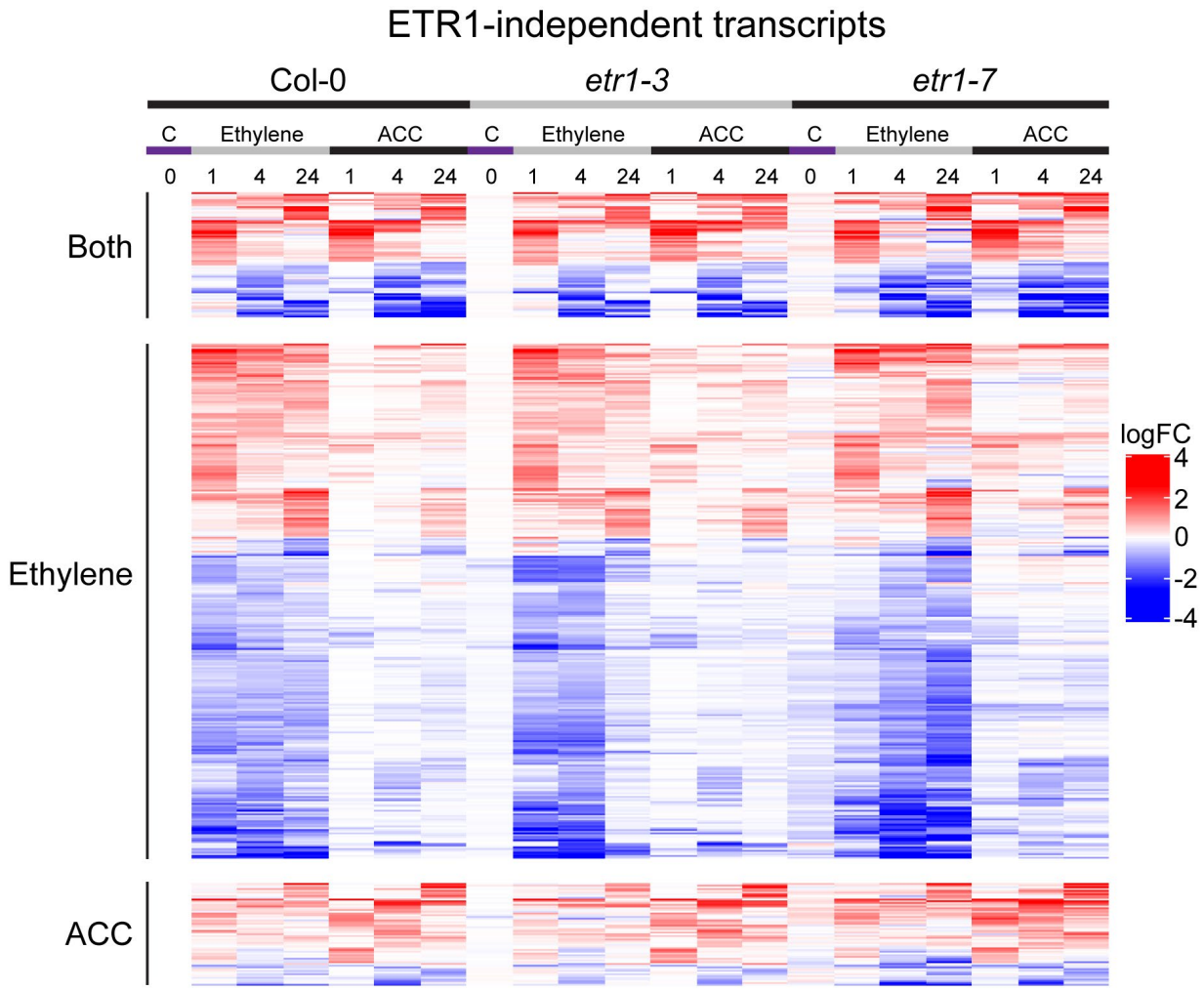

Figure 7. ETR1-independent transcript heatmap revealed genotype and treatment independent changes in transcript abundance. This comparison of transcript abundance across treatments and genotypes revealed a set of genes that responded to ethylene and/or ACC treatment in all genotypes. Genes which respond to ethylene or ACC in all three genotypes were considered receptor-independent (since transcript abundance should have been constant in *etr1-3* and *etr1-7)*. Significant differences were defined as having $|\log_2 FC| > 0.5$ and adjusted p-value < 0.01. Transcripts are divided based on which treatment qualifies as ETR1-independent. $\log_2 FC$ is reported relative to untreated Col-0. Genes are split into three groups based on whether they met our ETR1-independent criteria in ethylene only (488 transcripts), ACC only (95 transcripts), or both treatments (117 transcripts).

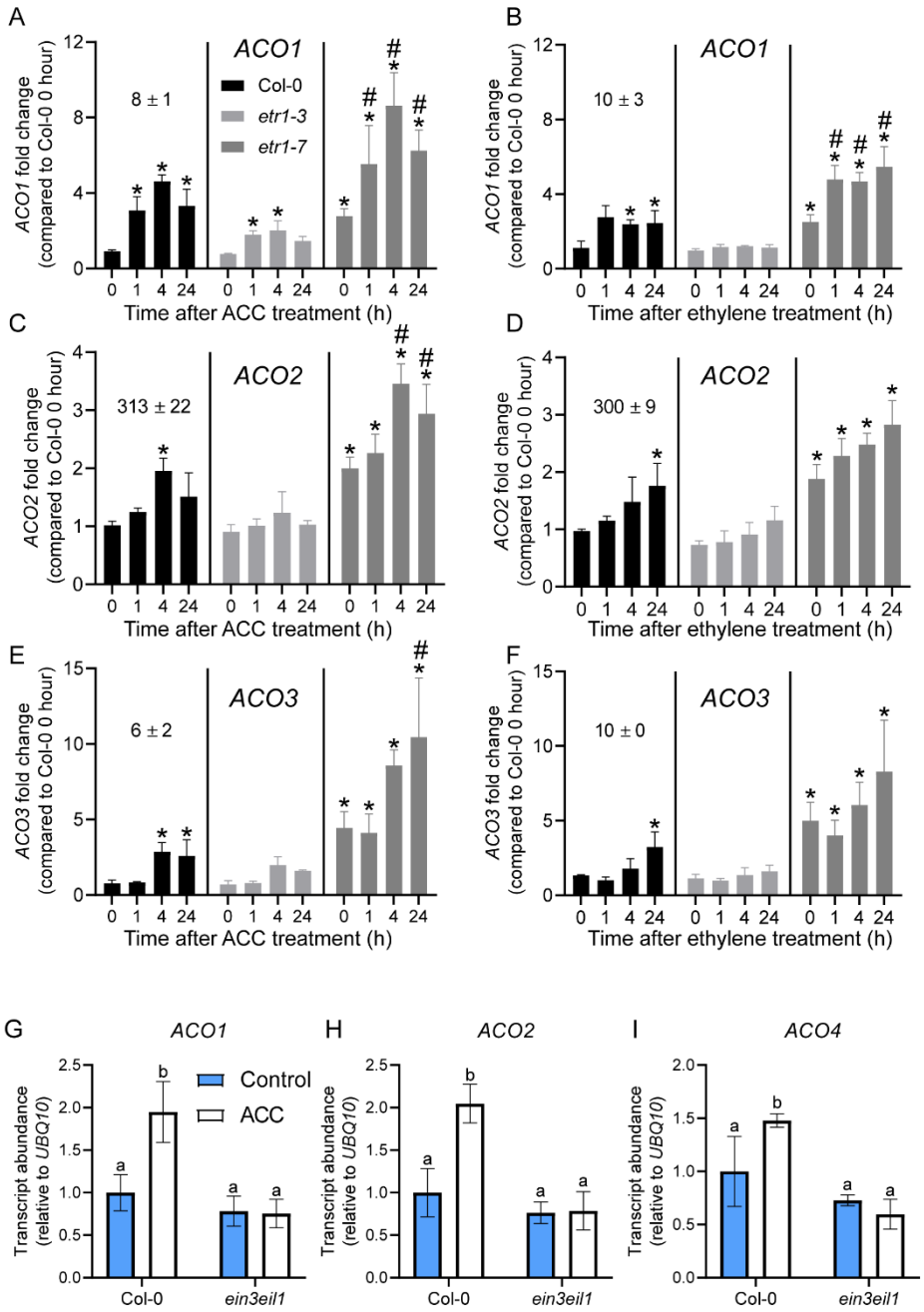

Figure 8. Transcript abundance of ETR1-dependent and/or EIN3/EIL1-regulated *ACO*s. (A-F) Normalized transcript abundance was calculated for *ACO1, ACO2*, and *ACO3* by taking average TPM for each time point and reporting it relative to the average TPM of untreated Col-0. Asterisks indicate statistical significance (p-value < 0.01) compared to Col-0 time zero. Pound symbols indicate statistical significance (p-value < 0.01) compared to *etr1-7* time zero and are displayed only for *etr1-7*. Error bars represent SD. (G-I) Transcript abundance in Col-0 and *ein3eil1* samples treated with and without 0.75 µM ACC for 4 hours was quantified using RT-qPCR. The average of three biological replicates are reported with error bars representing SD. Statistical significance was defined as p-value < 0.05 using Tukey's multiple comparisons test.

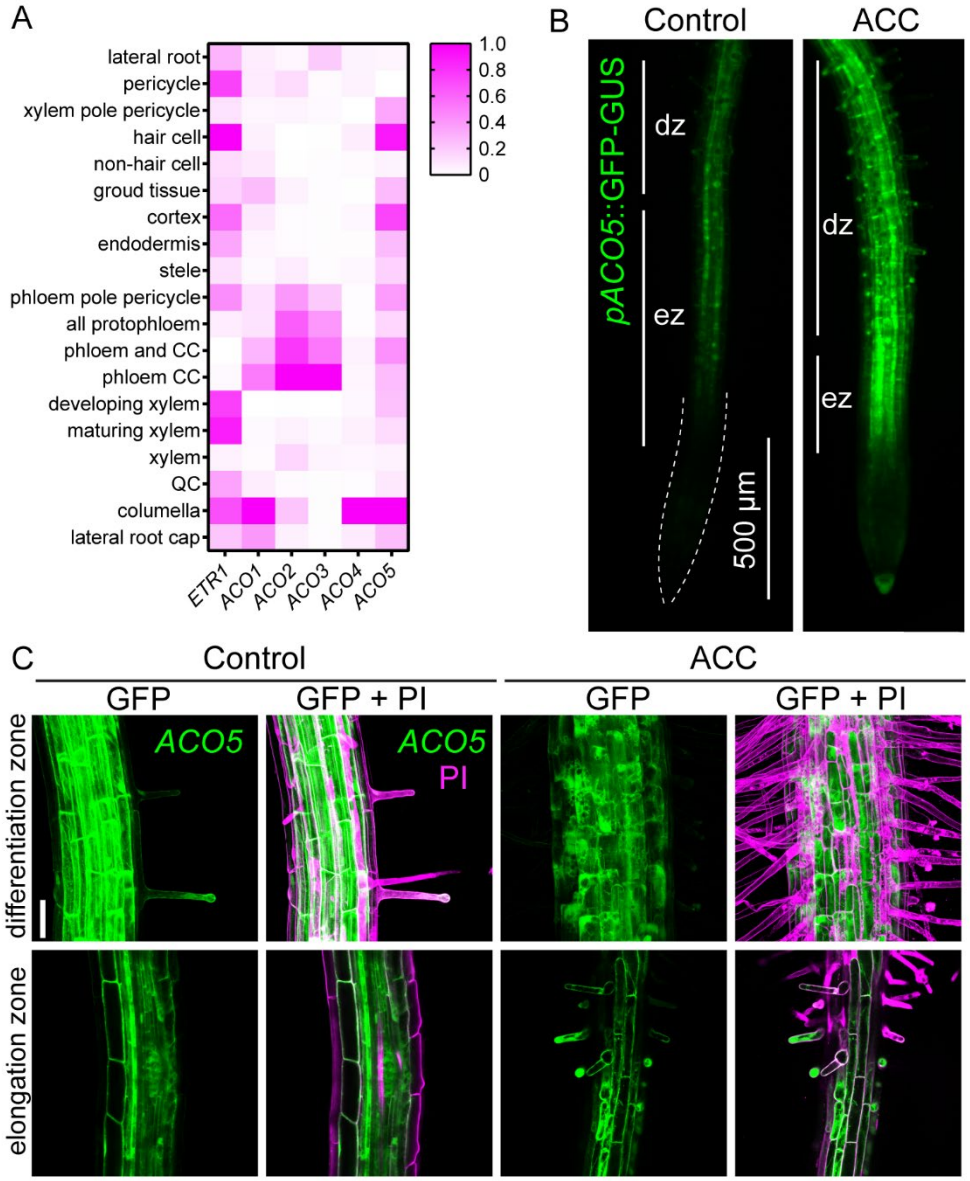

Figure 9. *pACO5*::GFP-GUS fluorescence increased in root tissues including root hairs in response to ACC treatment. (A) Publicly available root cell type data reported as a heatmap (Brady et al., 2007). Data has been scaled and normalized to the tissue with the highest expression for each transcript. (B) Roots of five-day-old *pACO5*::GFP-GUS seedlings treated with and without 0.75 µM ACC for four hours with images captured on a fluorescent stereomicroscope. DZ, differentiation zone. EZ, elongation zone. Scale bar is 500 µm. (C) Roots of 10-day-old *pACO5*::GFP-GUS seedlings treated with 0.75 µM ACC for five days and stained with propidium iodide (PI; magenta) were imaged by laser scanning confocal microscopy. Scale bar= 150 µm.

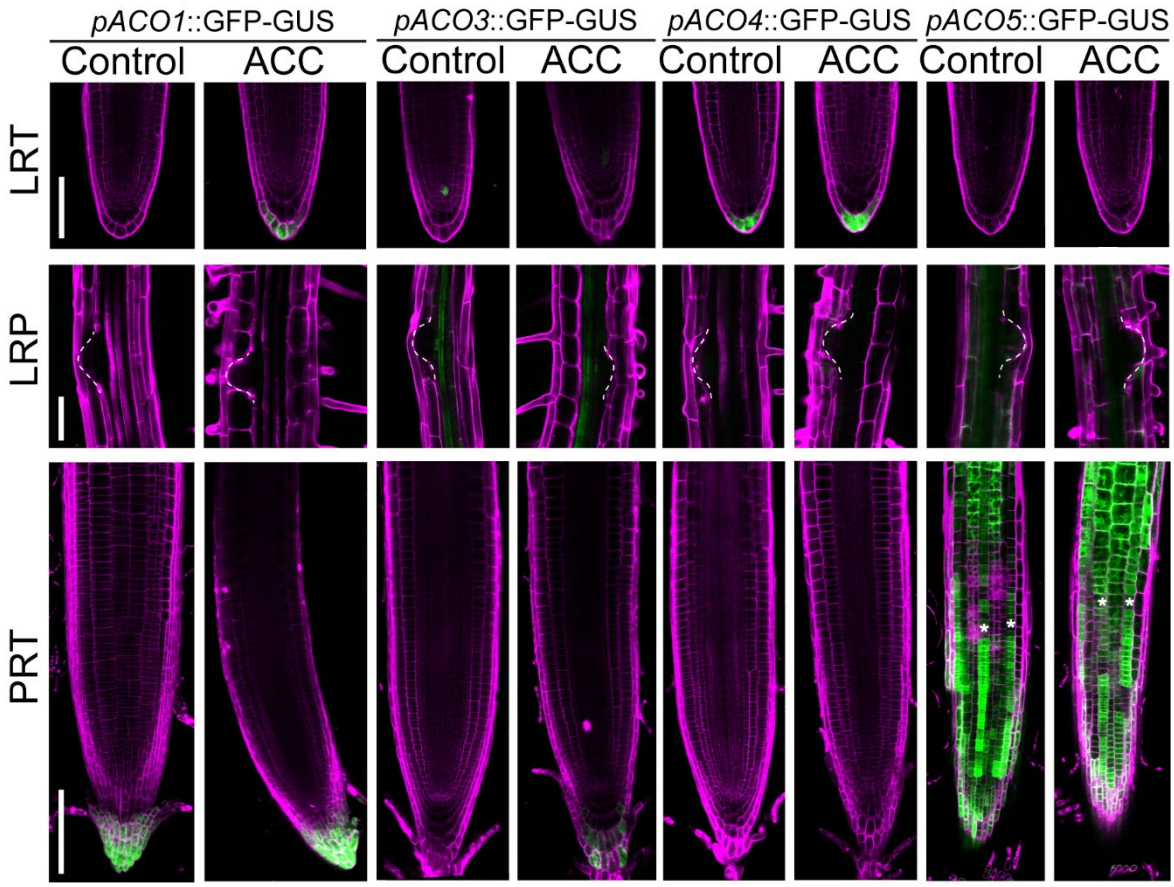

Figure 10. *ACO* transcripts are synthesized in distinct root tissues in response to ACC treatment. 10-day-old *pACO*::GFP-GUS seedlings treated with and without 0.75 µM ACC for five days. Abbreviations for root regions are primary root tip (PRT), lateral root primordium (LRP), and lateral root tip (LRT). Scale bar is 150 µm for PRT and LRT images and 100 µm for LRP images.

.

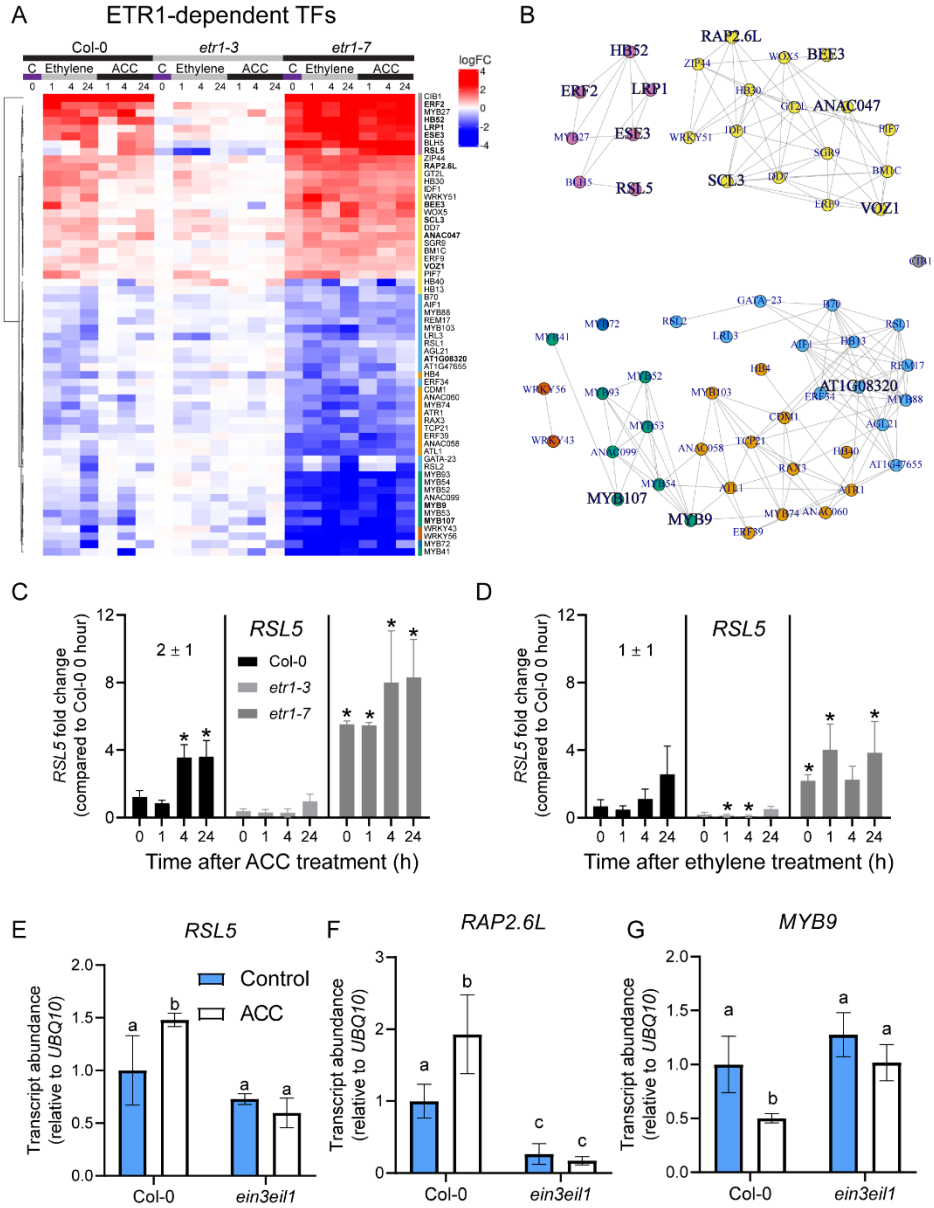

Figure 11. ETR1-dependent transcripts annotated as transcription factors (TFs) exhibit diverse expression patterns. (A) Heatmap of transcript abundance of the 60 ETR1-dependent transcripts that are predicted to encode TFs (reported as $\log_2$FC relative to Col-0 time zero). Colors next to gene names correspond to colors in the PaLD network. (B) PaLD network of the ETR1-dependent TFs, with EIN3 direct targets highlighted on the network in large, bold font. The node for *CIB1* was positioned more closely to the main network to conserve space. (C, D) *RSL5* normalized transcript abundance was calculated by taking average TPM for each time point and reporting it relative to the average TPM of untreated Col-0. (E-G) Transcript abundance in the roots of Col-0 and *ein3eil1* seedlings treated with and without 0.75 µM ACC for four hours. Error bars represent SD. Statistical significance was defined as $P < 0.05$ according to Tukey's multiple comparisons test.

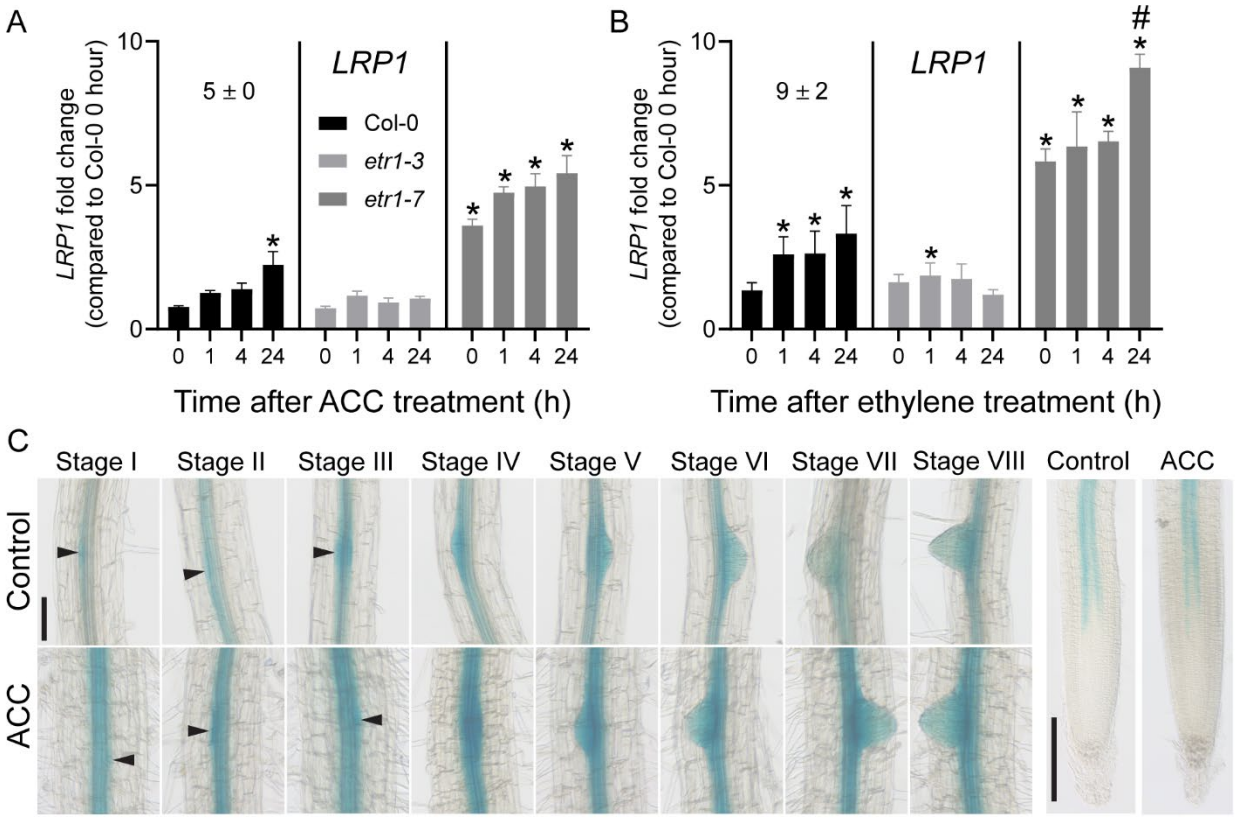

Figure 12. *ProLRP1*::GUS reporter results are consistent with higher *LRP1* expression in lateral root primordia in response to ACC treatment. (A, B) *LRP1* normalized transcript abundance was calculated by dividing the TPM of each time point by the average TPM of untreated Col-0. Error bars are SD. (C) Images of lateral root primordia of 10-day-old GUS-stained *proLRP1*::GUS seedlings in the presence and absence of 0.75 µM ACC after five days. Arrows point to stage I-III primordia. Scale bar is 100 µm.

Supplemental Materials

Supplemental File 1. This file includes a list of genes that were DE in response to ethylene and/or ACC in Col-0 at each time point, a summary of ETR1 dependence, a list of the ETR1-dependent, -independent, and complex DE genes, and a list of the DE genes in the genotype comparisons at baseline. All DE genes are listed with their $\log_2$FC values (relative to Col-0 control samples or other genotype in the genotype comparisons) and p-values.

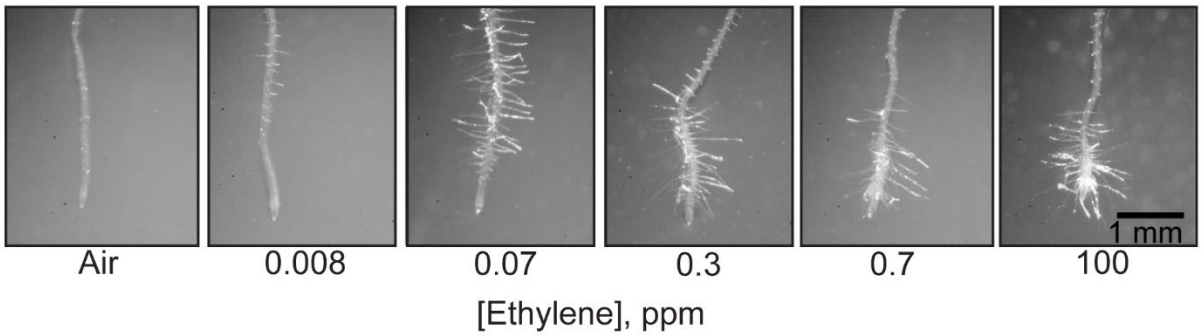

Supplemental Figure 1. Root hair formation in response to increasing concentrations of ethylene gas. Images of the root tips of six-day-old seedlings were captured 24 hours after treatment with ethylene gas at the indicated concentrations.

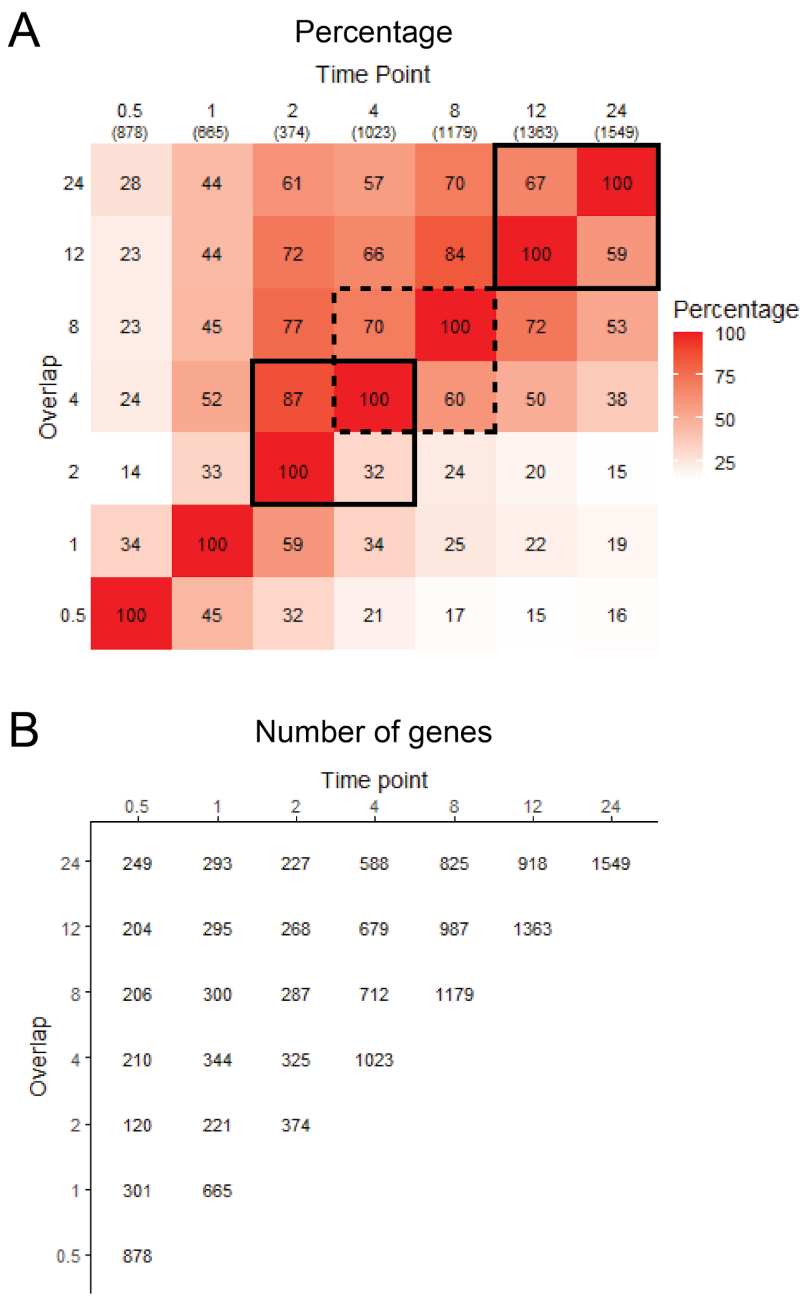

Supplemental Figure 2. Pairwise comparison of the DE genes at each time point in the ACC microarray dataset (Harkey et al., 2018)**.** (A) The percentage of DE genes in one time point (column) which were also DE in the overlap time point (row). The total number of DE genes in each time point is shown in parentheses under the column time point labels. Comparisons highlighted in the text are boxed in black solid or dashed lines. (B) The number of DE genes in one time point (column) which were also DE in the overlap time point (row).

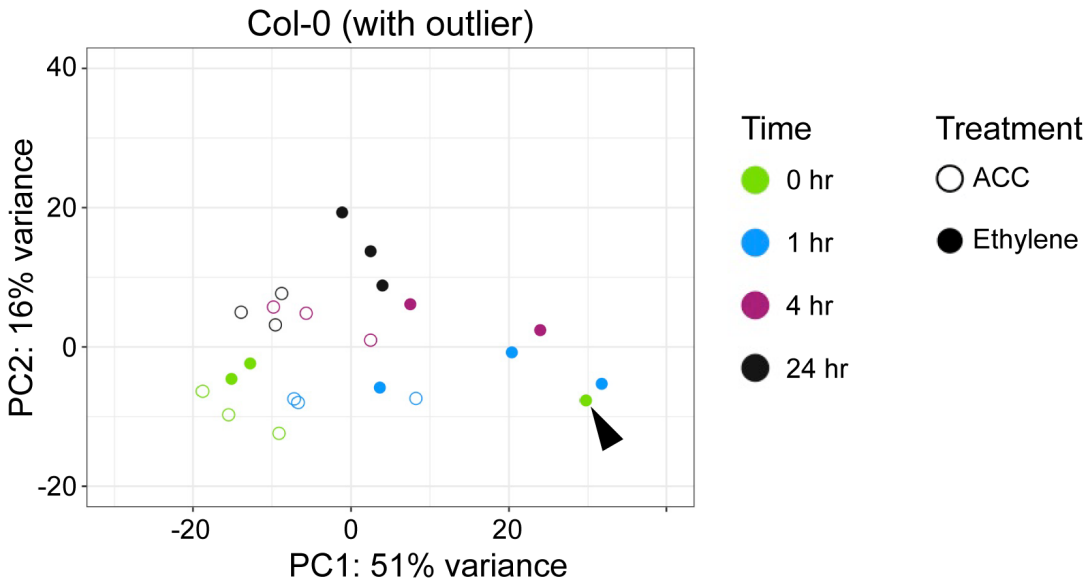

Supplemental Figure 3. Principal component analysis was used in the decision to remove Col-0 outlier. PCA plot of Col-0 samples, with the outlier sample included.

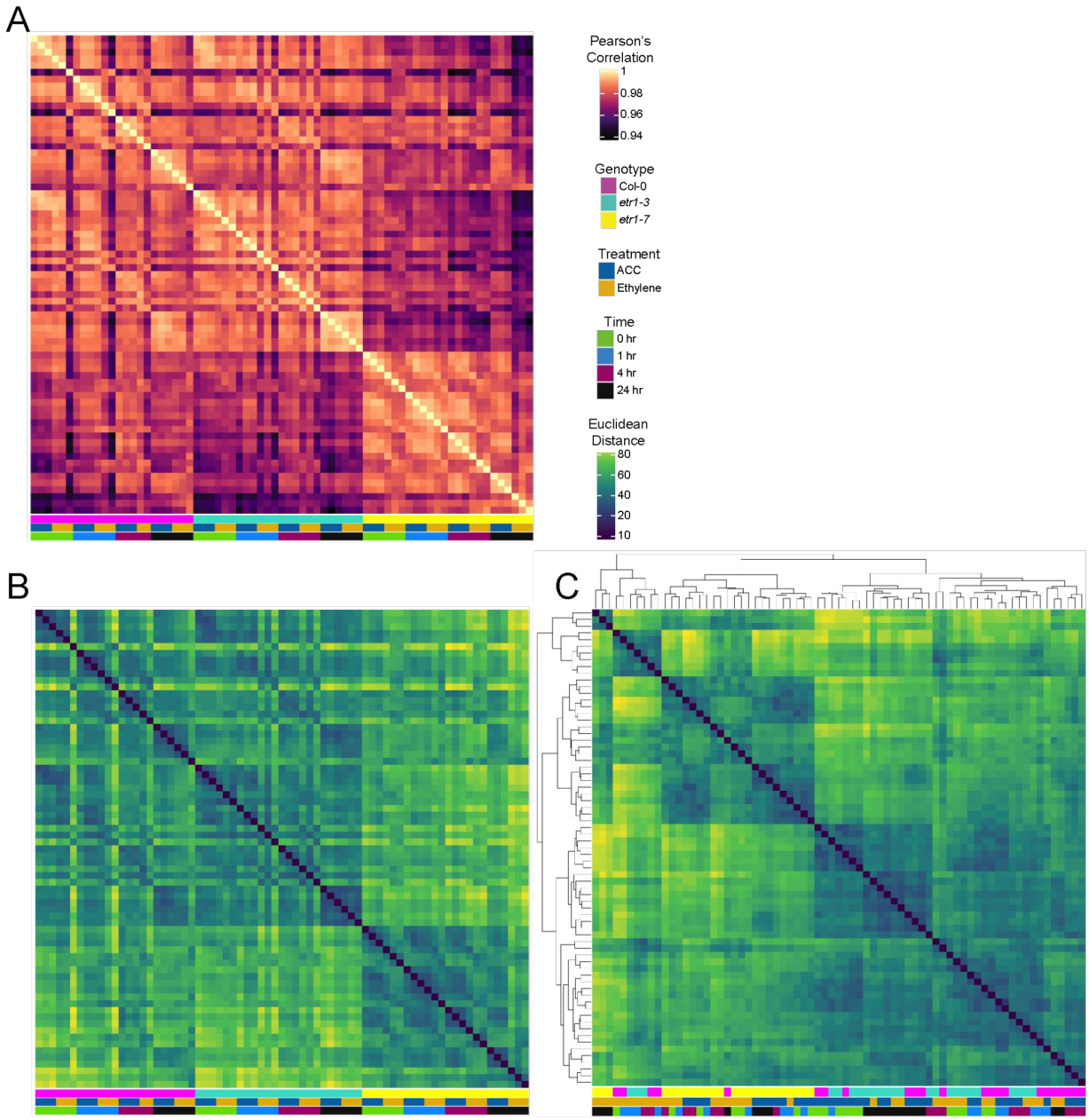

Supplemental Figure 4. Large-scale patterns of data from all samples. Samples were compared in a pair-wise manner using Pearson's correlation (A) or Euclidean distance (B & C), then sorted by genotype and treatment (A and B), which highlights samples that differed from other replicates from the same genotypes and treatment times, or clustered based on greatest similarity between samples (C).

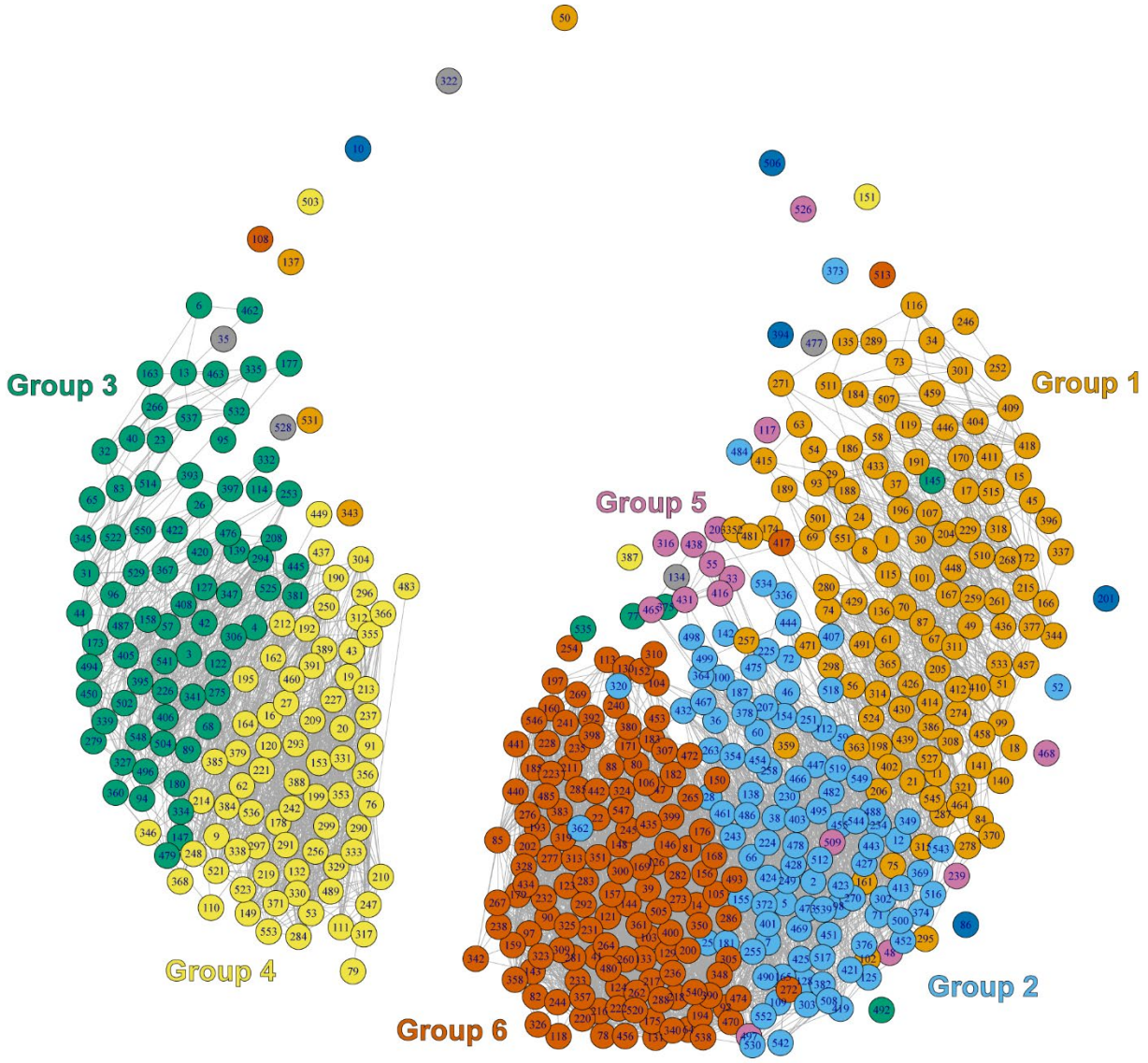

Supplemental Figure 5. PaLD network of the 553 ETR1-dependent transcripts. Nodes represent transcripts, and edges represent connections between transcripts with the most similar temporal response to ACC and ethylene across treatments of Col-0, *etr1-3*, and *etr1-7*. The $\log_2$FC values of treated samples relative to Col-0 untreated were used as input for PaLD. Colors indicate transcripts belonging to communities with the strongest ties as identified by the Louvain method. Numbers correspond to genes listed in Supplemental File 1. The group on the left are transcripts whose abundance increases with ACC and ethylene treatment and the group on the right have transcript levels that decrease with these treatments.

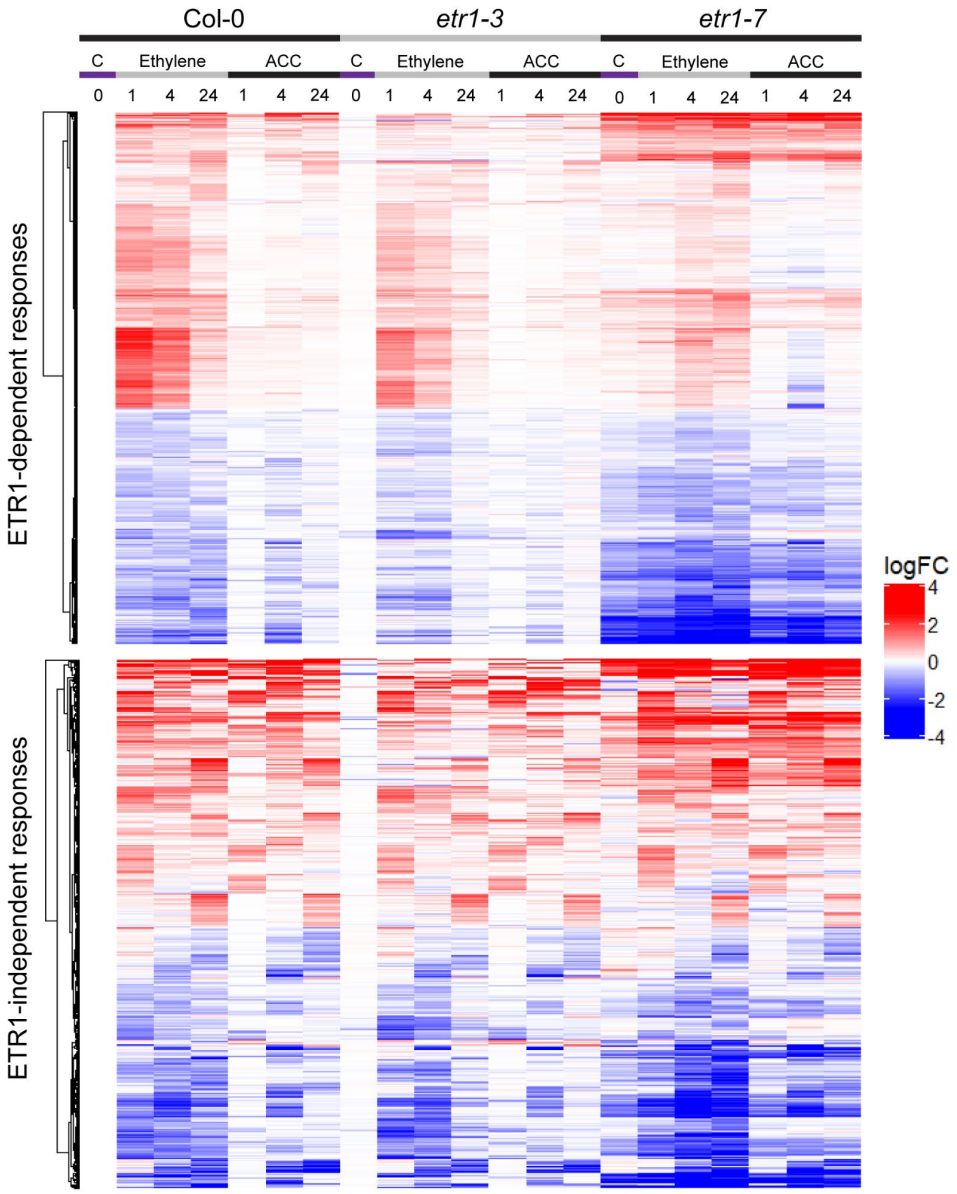

Supplemental Figure 6. Transcripts identified by less stringent criteria for ETR1 dependence or independence. For this analysis, ETR1-dependent transcripts were required to respond to treatment in Col-0, and not respond in the mutants; ETR1-independent transcripts were required to respond to treatment in all three genotypes. Both sets of criteria were evaluated based on comparison of treatment samples to the untreated control samples for the same genotype, regardless of the transcript abundance in that control sample.

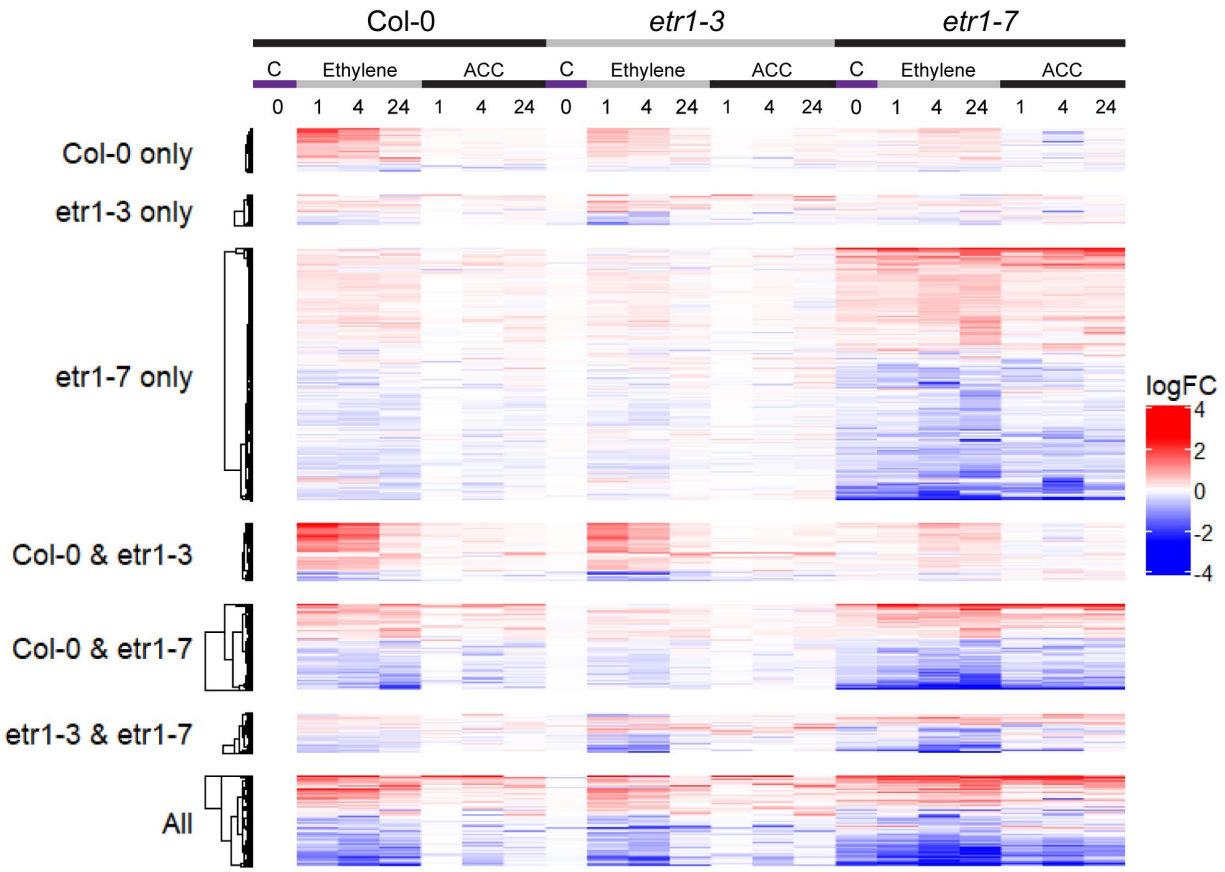

Supplemental Figure 7. Transcripts with complex responses, which responded to ACC or ethylene, but were not consistently regulated by ETR1. Genes with complex responses to ethylene and/or ACC which did not qualify as ETR1-dependent or -independent. Genes were split into groups based on which genotypes had at least one DE sample, based on $|\log_2 FC| > 0.5$ and adjusted p-value < 0.01. Log_2FC was reported relative to untreated Col-0.

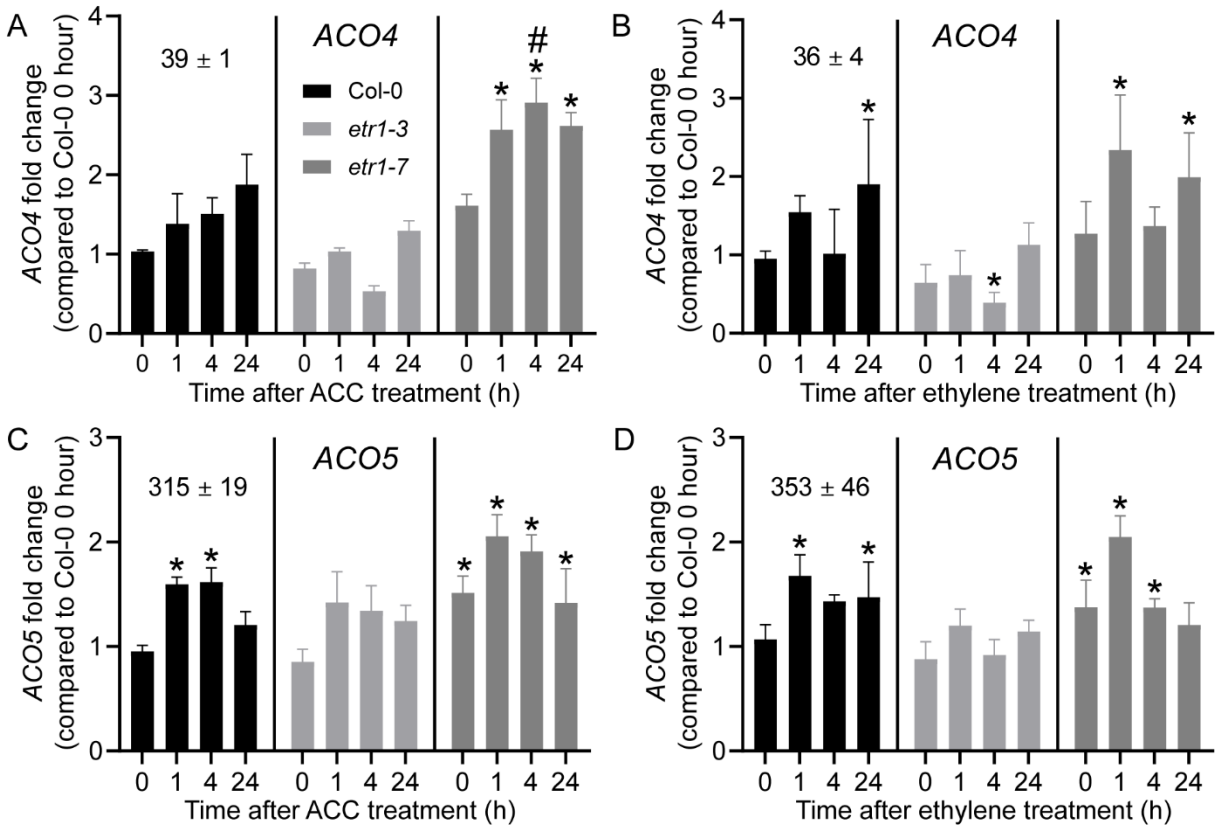

Supplemental Figure 8. Transcript abundance of *ACO4* and *ACO5* in the *etr1* mutant alleles. Transcript abundance (TPM) is reported relative to Col-0 time zero after ACC and ethylene treatment in our RNA-Seq dataset. Asterisks indicate statistical significance ($p < 0.01$) relative to untreated Col-0. Pound symbols indicate statistical significance ($p < 0.01$) compared to *etr1-7* time zero and are displayed only for the *etr1-7* data. Error bars represent SD.

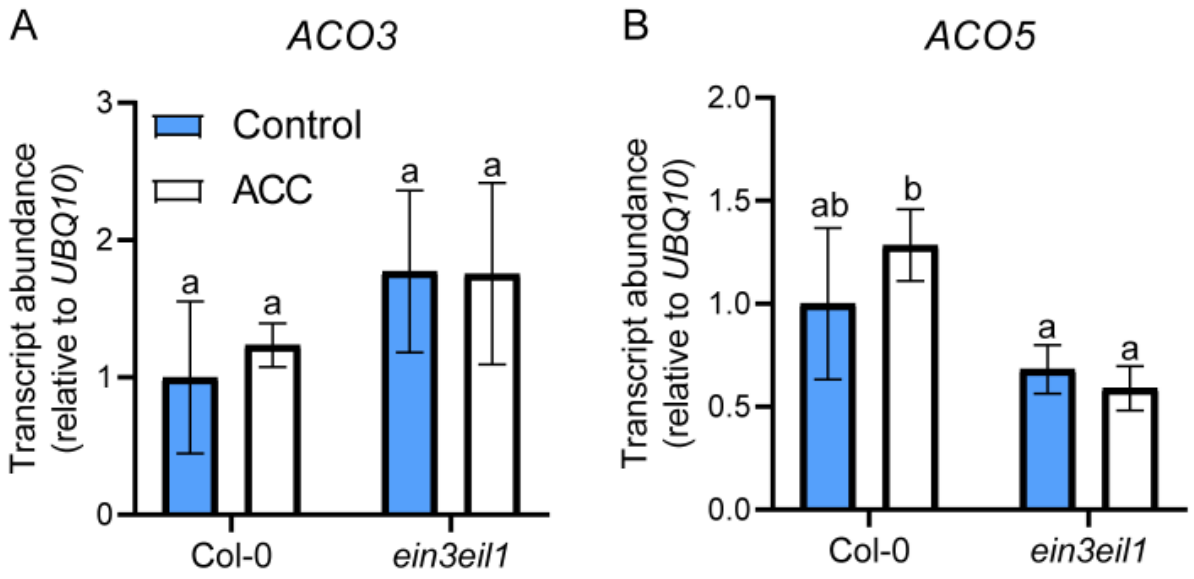

Supplemental Figure 9. *ACO3* and *ACO5* transcript abundance is not significantly different in an *ein3/eil1* mutantEIN3/EIL1. Transcript abundance in Col-0 and *ein3eil1* samples treated with and without 0.75 µM ACC for four hours. Error bars are SD. Statistical significance was defined as $p < 0.05$ according to Tukey's multiple comparisons test.

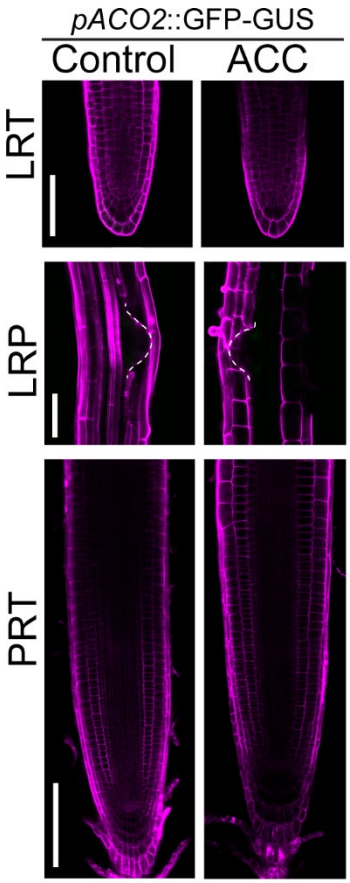

Supplemental Figure 10. *ACO*2 was not regulated by ACC in tissues that control lateral root or primary root development. 10-day-old *pACO2*::GFP-GUS seedlings treated with and without 0.75 µM ACC for five days. PRT, primary root tip. LRP, lateral root primordium. LRT, lateral root tip. Scale bar is 150 µm for PRT and LRT images and 100 µm for LRP images.

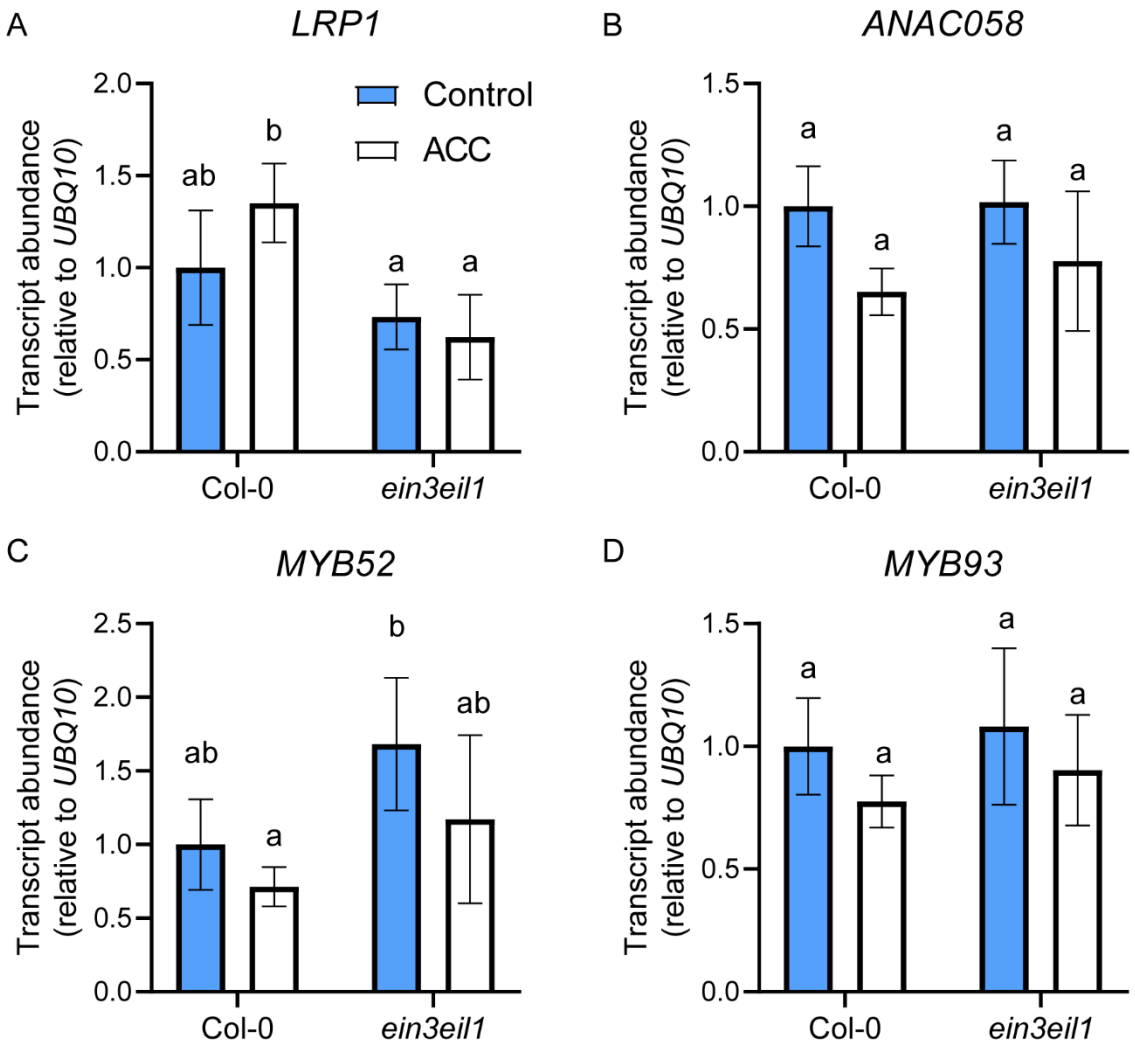

Supplemental Figure 11. Several ETR1-dependent transcripts encoding TFs did not have significant changes in the *ein3eil1* mutant. Transcript abundance in Col-0 and *ein3eil1* samples treated with and without 0.75 µM ACC for four hours. Error bars are SD. Statistical significance was defined as p-value < 0.05 according to Tukey's multiple comparisons test.

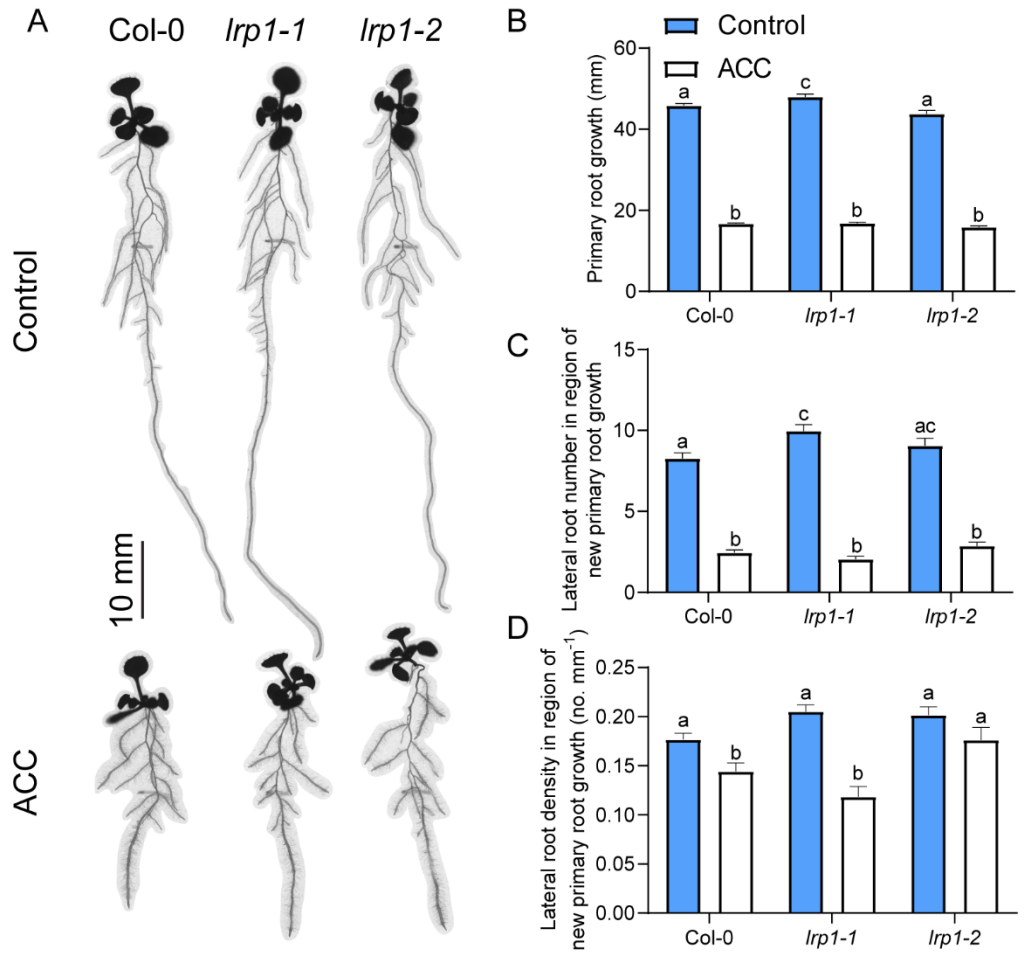

Supplemental Figure 12. The *lrp1-1* and *lrp1-2* mutants had weak and not consistent root phenotypes. (A) Representative images of 10-day-old Col-0, *lrp1-1*, and *lrp1-2* seedlings treated with and without 0.75 µM ACC for five days. Quantification of (B) primary root growth, (C) the number of lateral roots in the region of new root growth, and (C) and the lateral root density in the region of new root growth in Col-0, *lrp1-1*, and *lrp1-2* in the presence and absence of 0.75 µM ACC after five days. Error bars are SD. Statistical significance is defined as p-value < 0.05 according to Tukey's multiple comparisons test.

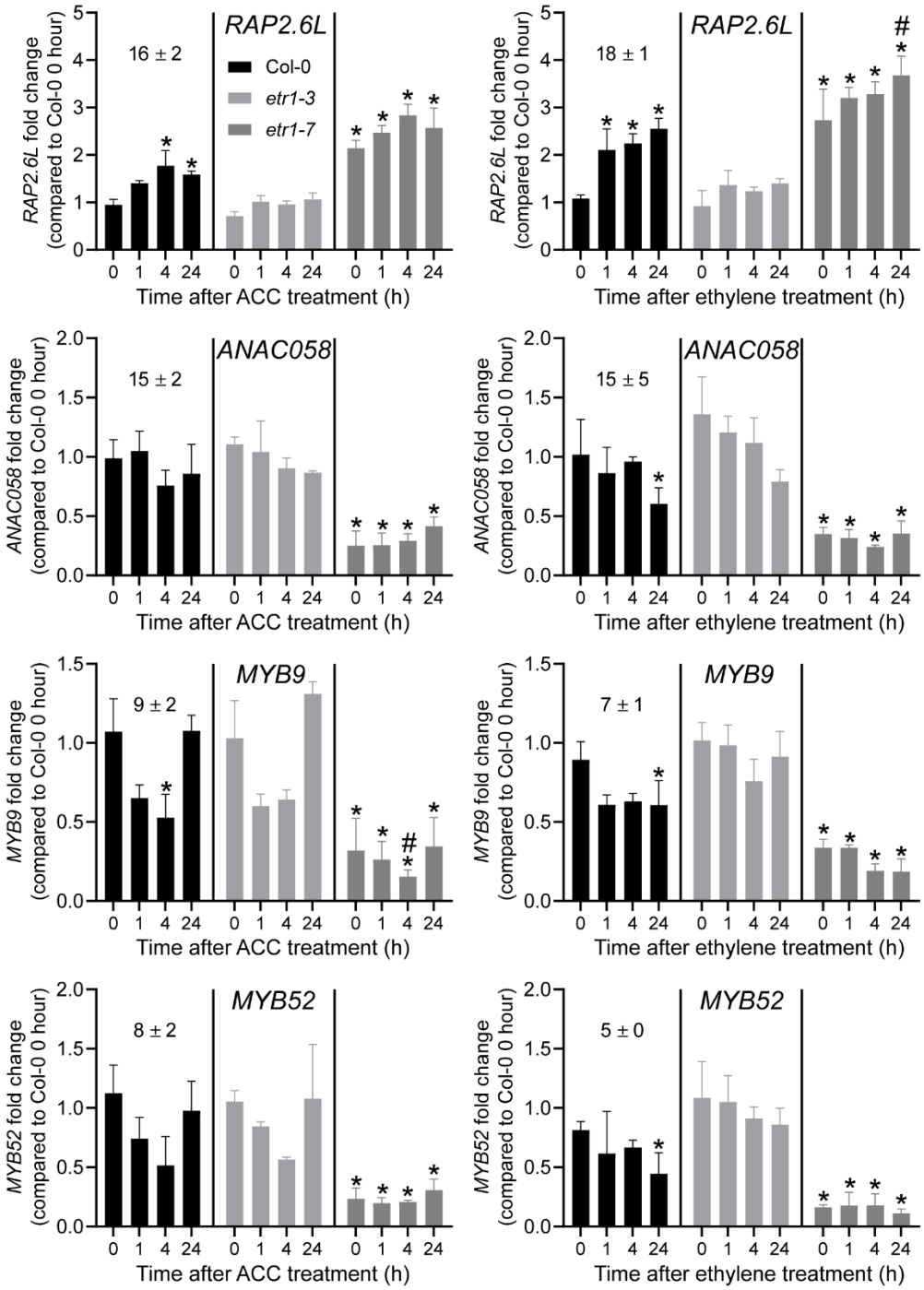

Supplemental Figure 13. Transcript abundance of the four downregulated ETR1-dependent transcripts encoding TFs. Transcript abundance (TPM) is reported relative to Col-0 time zero after ACC and ethylene treatment in our RNA Seq dataset. Asterisks indicate statistical significance (p-value < 0.01) relative to untreated Col-0. Pound symbols indicate statistical significance (p-value < 0.01) compared to *etr1-7* time zero and are displayed only for the *etr1-7* data. Error bars are SD.

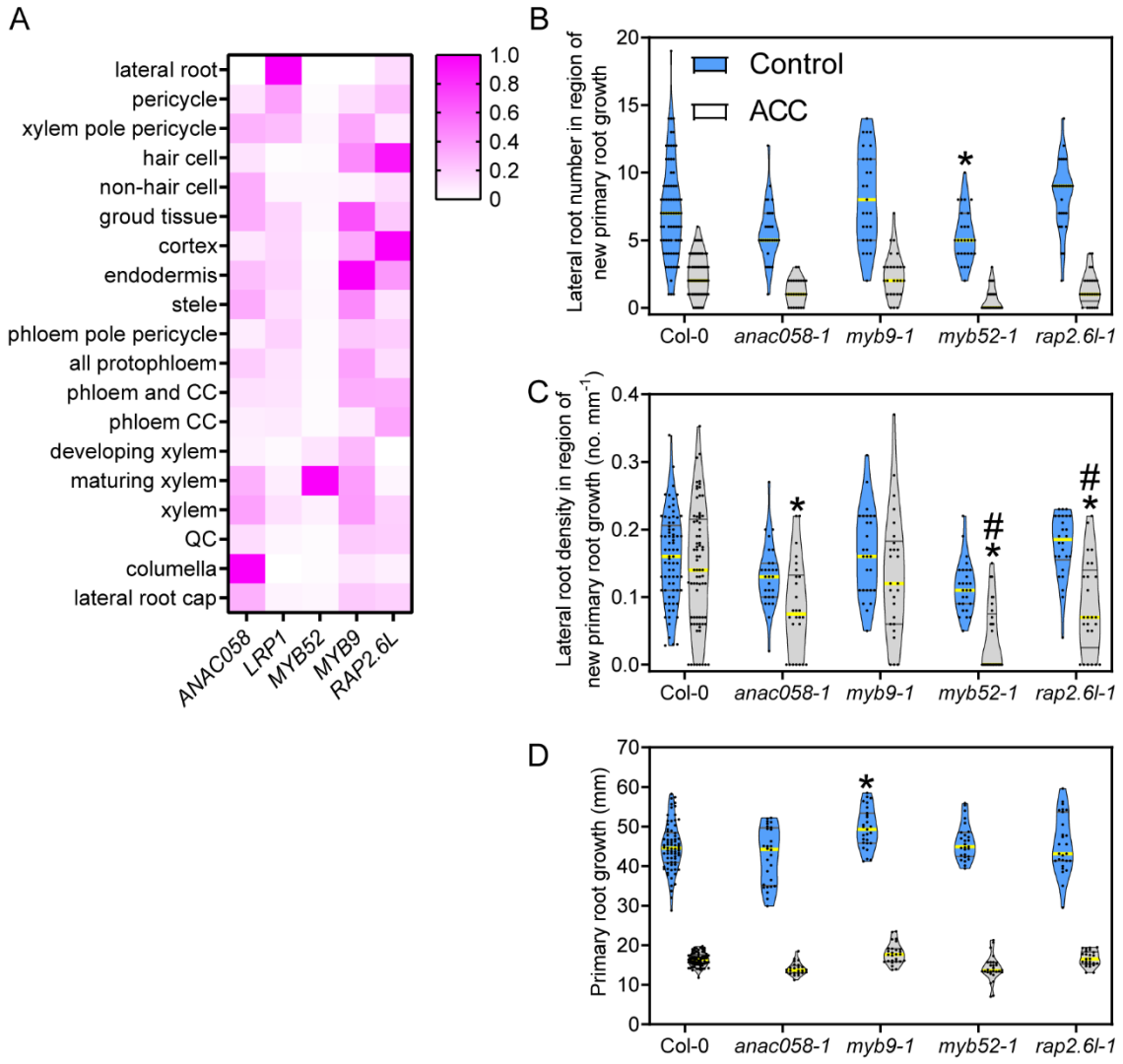

Supplemental Figure 14. Mutants in several ETR1-dependent TFs have alterations in lateral root formation or primary root growth. (A) Root cell type data reported as a heatmap (Brady et al. 2007). Data has been scaled and normalized to the tissue with the highest expression for each transcript. Violin plots of lateral root number in the region of new root growth (B), lateral root density in the region of new root growth (C), and primary root growth (D) for 10-day-old seedlings treated with and without 0.75 µM ACC for five days. Asterisks indicate significant differences from Col-0 under the same treatment conditions (p-value < 0.05). ACC effects within genotypes were significant for all genotypes in B and D (not shown on graphs). Pound symbols indicate significant differences within genotypes (p-value <0.05) for B. At least three biological replicates were performed. The median is illustrated in a thicker yellow line. The quartiles are illustrated in thinner gray lines.

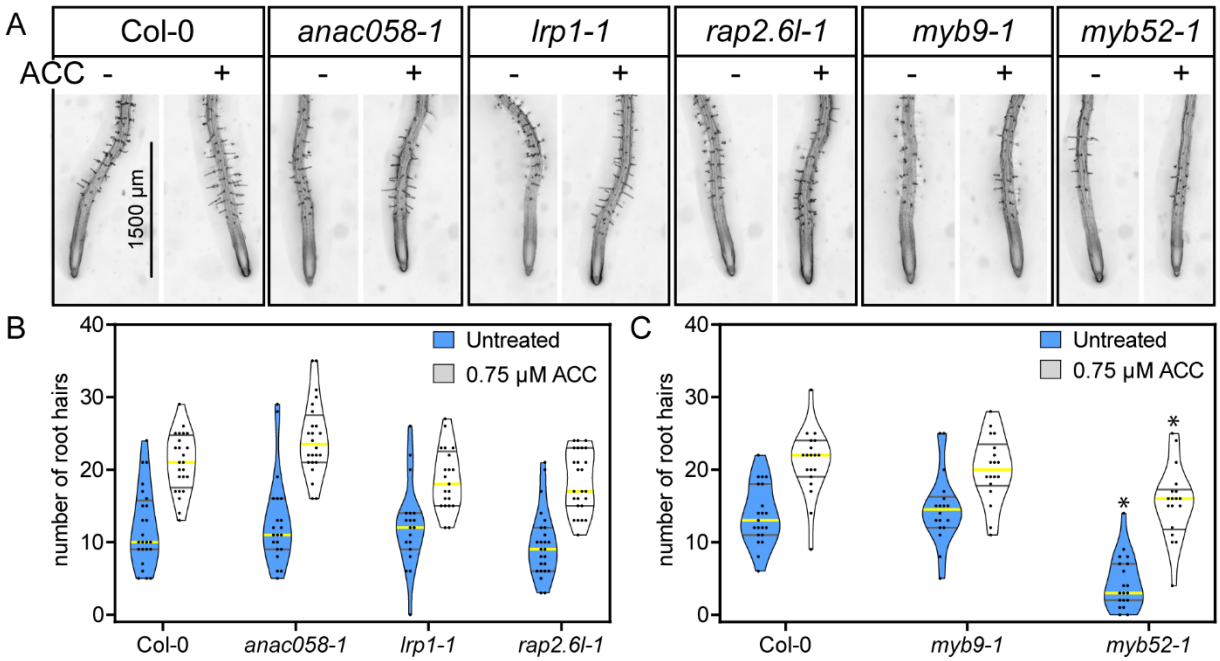

Supplemental Figure 15. A mutant in the ETR1-dependent *MYB52* has altered root hair initiation. (A) Representative images of five-day-old Col-0 and mutant seedlings treated with and without 0.75 µM ACC for four hours. Scale bar is 1,500 µm. (B,C) Violin plots of the number of root hairs in the region 0-1500 µm from the root tip in the absence and presence of 0.75 µM ACC. Asterisks indicate significant differences from Col-0 under the same condition, either untreated or with ACC (p-value < 0.05). ACC effects within genotypes were significant for all genotypes (p-value < 0.05). Three biological replicates were performed. The median is shown in a thicker yellow line. The quartiles are shown in thinner gray lines.

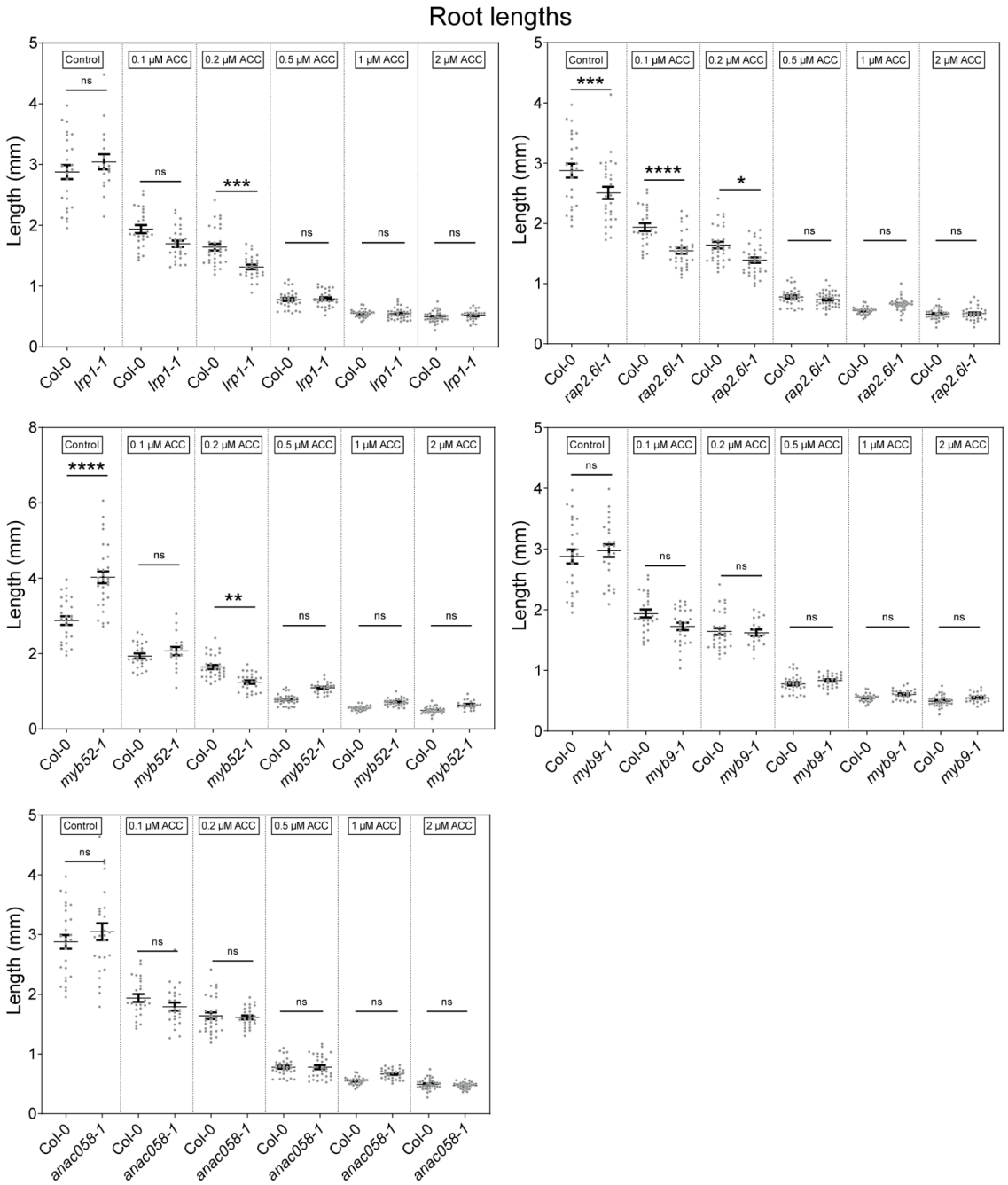

Supplemental Figure 16. Triple response assay results for the candidate ETR1-dependent genes that function in root hair or lateral root formation. Seedlings were incubated in the dark on control or ACC plates for four days before hypocotyl and root lengths were measured. Statistical significance was determined using a one-way ANOVA followed by a multiple comparisons test. * p-value < 0.05; ** p-value < 0.01; *** p-value < 0.001; **** p-value < 0.0001.

Supplemental Table 1. The number of differentially expressed genes between Wake Forest University- and University of Tennessee-prepared untreated samples for each genotype (with and without the untreated Col-0 outlier sample).

Genotype	With outlier	Outlier removed
Col-0	693	34
etr1-3	137	121
etr1-7	997	763

Supplemental Table 2. Number of DE genes in response to ethylene and ACC based on two $\log_2$FC cutoffs. Note that the small number of genes that were regulated in opposite directions in the two treatments were not shown here for simplicity.

Group of genes	0.25 cutoff	0.5 cutoff
Down in both	860	504
Down in ethylene	2,461	1,493
Down in ACC	317	182
Up in both	620	457
Up in ethylene	2,563	1,657
Up in ACC	255	213

Supplemental Table 3. Gene Ontology (GO) enrichment results for genes transcriptionally regulated by ethylene and/or ACC in Col-0. Transcripts were separated based on if they responded to one or both treatments and if they were down- or up-regulated by the treatment(s). The number of genes with each GO annotation, the p-value and false discovery rate (FDR) for each annotation are reported.

GO Term	# of genes	p-value	FDR
Up in both treatments			
regulation of transcription, DNA-dependent	36	7.80E-09	5.00E-07
response to chitin	14	1.20E-08	5.70E-07
regulation of gene expression	50	1.10E-06	2.60E-05
negative regulation of two-component signal transduction system (phosphorelay)	5	1.70E-06	3.60E-05
negative regulation of ethylene mediated signaling pathway	5	1.70E-06	3.60E-05
response to auxin stimulus	16	1.30E-05	0.00025
lipid localization	5	2.10E-05	0.00039
response to oxidative stress	14	7.40E-05	0.0013
response to osmotic stress	14	0.00056	0.0095
defense response to bacterium	8	0.0017	0.027
defense response, incompatible interaction	7	0.0021	0.034
response to external stimulus	13	0.0025	0.04
nitrogen compound metabolic process	65	0.0027	0.042
Down in both treatments			
lipid transport	14	9.5E-08	0.000016
hyperosmotic salinity response	7	0.000014	0.0011
response to cold	16	0.000014	0.0011
response to water deprivation	13	0.00002	0.0013
response to abscisic acid stimulus	17	0.00002	0.0013
response to nematode	7	0.000066	0.0029
phenylpropanoid biosynthetic process	9	0.00016	0.0064

response to oxidative stress	14	0.0002	0.0076
unidimensional cell growth	10	0.00027	0.0094
glycolysis	5	0.0013	0.028
terpenoid metabolic process	7	0.0018	0.036
Up in ethylene only			
chlorophyll biosynthetic process	19	1.3E-11	1.7E-09
cofactor biosynthetic process	33	2.7E-10	2.8E-08
chloroplast organization	20	1.1E-09	1.1E-07
response to high light intensity	16	3.8E-08	3.4E-06
lipid localization	11	9.7E-08	8.1E-06
photosynthesis, light harvesting	11	1.8E-07	0.000014
protein folding	34	2.5E-07	0.000018
response to red light	17	2.9E-07	0.00002
carbon fixation	9	3.9E-07	0.000027
photosynthetic electron transport in photosystem I	10	5.5E-07	0.000034
response to cold	37	5.9E-07	0.000036
response to blue light	15	1.7E-06	0.000089
embryonic development ending in seed dormancy	45	1.9E-06	0.000097
regulation of photosynthesis, light reaction	8	2.4E-06	0.00012
photosystem II assembly	7	2.8E-06	0.00014
response to far red light	13	5.2E-06	0.00024
protein import into chloroplast thylakoid membrane	6	0.000011	0.00049
response to other organism	49	0.000043	0.0017
response to hydrogen peroxide	11	0.000058	0.0023
defense response	58	0.000068	0.0026
thylakoid membrane organization	7	0.00018	0.0062
carotenoid biosynthetic process	8	0.00024	0.0075
positive regulation of development, heterochronic	5	0.00025	0.008
heat acclimation	6	0.00045	0.013

vitamin K biosynthetic process	5	0.00049	0.014
positive regulation of nitrogen compound metabolic process	11	0.0005	0.014
isopentenyl diphosphate biosynthetic process, mevalonate-independent pathway	5	0.00066	0.018
positive regulation of gene expression	10	0.00082	0.022
positive regulation of transcription	10	0.00082	0.022
positive regulation of cellular biosynthetic process	11	0.00091	0.023
xanthophyll metabolic process	5	0.0014	0.034
RNA metabolic process	98	0.0017	0.039
Down in ethylene only			
protein amino acid phosphorylation	76	1.5E-08	4.7E-06
oligopeptide transport	17	1.5E-08	4.7E-06
secondary cell wall biogenesis	9	5.2E-07	0.000089
glycoside metabolic process	18	7.2E-07	0.0001
plant-type cell wall organization	15	2.2E-06	0.00026
root hair cell differentiation	10	0.000033	0.0021
cell wall polysaccharide metabolic process	6	0.000068	0.004
transmembrane receptor protein tyrosine kinase signaling pathway	16	0.00027	0.012
glucosinolate metabolic process	10	0.00034	0.014
cell tip growth	11	0.00055	0.02
phenylpropanoid biosynthetic process	15	0.00081	0.028
lignin metabolic process	8	0.00097	0.031
multidrug transport	10	0.0011	0.034
isoprenoid biosynthetic process	14	0.0015	0.046
Up in ACC only			
regulation of biological quality	12	0.00034	0.022
defense response to bacterium	6	0.0005	0.026

protein amino acid phosphorylation	14	0.00078	0.036
transmembrane receptor protein tyrosine kinase signaling pathway	5	0.0012	0.038
response to inorganic substance	7	0.00098	0.038
response to hormone stimulus	14	0.0011	0.038
response to chitin	5	0.0016	0.046
Down in ACC only			
None significant			
Up in either treatment			
response to light intensity	22	3.20E-07	2.00E-05
cellular nitrogen compound biosynthetic process	50	4.00E-06	0.00019
fat-soluble vitamin biosynthetic process	9	2.20E-05	0.00091
toxin catabolic process	13	7.80E-05	0.0027
cellular response to chemical stimulus	48	0.00033	0.011
reductive pentose-phosphate cycle	5	0.00034	0.011
positive regulation of cellular metabolic process	16	0.00037	0.012
cellular response to stimulus	76	0.00075	0.022
quinone cofactor biosynthetic process	8	0.00097	0.027
response to iron ion	5	0.0011	0.03
cellular cation homeostasis	14	0.0013	0.034
Down in either treatment			
response to salt stress	41	0.000091	0.0045
lignin biosynthetic process	7	0.00015	0.0065
cell maturation	11	0.00016	0.0069
plant-type cell wall loosening	10	0.00028	0.011
sucrose biosynthetic process	6	0.00084	0.028
zinc ion transport	6	0.00084	0.028
fatty acid metabolic process	26	0.0011	0.035

glucosinolate biosynthetic process	9	0.0012	0.039
pentacyclic triterpenoid biosynthetic process	5	0.0016	0.049
alcohol metabolic process	29	0.0016	0.049
abscisic acid mediated signaling pathway	8	0.18	1
oligopeptide transporter activity	5	0.011	0.14

Supplemental Table 4. GO annotations enriched in genes which respond to ethylene or ACC via ETR1-dependent and -independent pathways. The number of genes with each GO annotation, the p-value and false discovery rate (FDR) for each annotation are reported.

GO Term	# of genes	p-value	FDR
ETR1 dependent (all)			
oligopeptide transport	7	0.000092	0.0097
lipid transport	10	0.00019	0.011
post-embryonic development	24	0.00013	0.011
response to water deprivation	12	0.00018	0.011
regulation of transcription, DNA-dependent	30	0.00014	0.011
response to abscisic acid stimulus	15	0.00053	0.021
ethylene mediated signaling pathway	6	0.00095	0.03
fatty acid metabolic process	10	0.002	0.048
ETR1 independent (all)			
response to heat	21	1.60E-11	8.30E-09
response to chitin	17	1.00E-08	3.20E-06
response to hydrogen peroxide	8	1.20E-05	0.0013
response to high light intensity	8	2.00E-05	0.0018
root hair cell differentiation	7	3.70E-05	0.0027
unidimensional cell growth	12	0.00025	0.013
protein folding	14	0.00076	0.036
inorganic anion transport	5	0.00087	0.04
nucleotide-sugar metabolic process	5	0.00097	0.043
cellular response to nutrient levels	7	0.0011	0.045
lipid metabolic process	29	0.0011	0.045
plant-type cell wall loosening	5	0.0012	0.048

ETR1 complex (all)			
response to light stimulus	180	1.4E-08	0.000004
response to chitin	64	1.1E-07	0.000026
phenylpropanoid biosynthetic process	60	2.4E-07	0.000051
toxin catabolic process	33	2.5E-07	0.000051
protein amino acid phosphorylation	244	2.6E-06	0.00044
oligopeptide transport	35	3.1E-06	0.00048
response to wounding	71	2.9E-06	0.00048
glucosinolate biosynthetic process	25	8.9E-06	0.0011
plant-type cell wall organization	37	8.7E-06	0.0011
monocarboxylic acid metabolic process	120	0.000009	0.0011
response to nematode	34	0.000011	0.0013
response to salt stress	107	0.000033	0.0037
post-embryonic morphogenesis	21	0.000054	0.0055
photosynthetic electron transport chain	24	0.000088	0.0086
multidrug transport	32	0.000091	0.0088
response to abscisic acid stimulus	107	0.000094	0.009
response to metal ion	74	0.00011	0.0097
intracellular signaling cascade	169	0.00011	0.0097
cell wall modification	45	0.00013	0.012
response to cold	94	0.00017	0.015
disaccharide biosynthetic process	21	0.00017	0.015
protein complex assembly	47	0.00021	0.017
heterocycle metabolic process	123	0.00022	0.018
defense response to fungus	40	0.00025	0.019
terpenoid biosynthetic process	36	0.00029	0.022
cellular carbohydrate catabolic process	44	0.00031	0.023
regulation of transcription	400	0.00039	0.028

response to ethylene stimulus	61	0.00055	0.034
cellular glucan metabolic process	33	0.00059	0.036
cation transport	97	0.00062	0.037
two-component signal transduction system (phosphorelay)	34	0.00071	0.042
cell wall macromolecule metabolic process	21	0.00074	0.044
chemical homeostasis	45	0.00078	0.045
response to water deprivation	67	0.00085	0.049
transition metal ion transmembrane transporter activity	16	0.022	0.43

Supplemental Table 5. Genotyping primers used in this study. Sequences are written 5' to 3'. L, left border primer. R, right border primer.

Genome Locus	Allele Name	T-DNA Insertion Line	Location of Insertion	Primer Sequences
AT3G18400	*anac058-1*	SALK_049205C	3' UTR	L:GTTCTGGCAGCAATTGTGATC R:CAACTCTTTGTTGCTCAAGGC
AT5G12330	*lrp1-1*	SAIL_402_G06/ CS873836	Promoter	L:TGTATGGCCAGTAAGCAATCC R:ACGTCGGTAGATTATGCCTCC
AT5G12330	*lrp1-2*	SALK_201247C	Exon	L:TGATAAGTGCATGAGAAAATGG R:ACACACCACCTCAAAGTTTCG
AT5G16770	*myb9-1*	SALK_149765C	Promoter	L:TGGAATCGCAGTTTTTCTAGC R:CGTGCATAAATATTTGCATGTG
AT1G17950	*myb52-1*	SALK_138624C	Exon	L:AAAAGGATGTTCATTTGGTGG R:TGCAAGTAAATGAGTAATGGTGC
AT5G13330	*rap2.6l-1*	SALK_051006C	5' UTR	L:AAAAGGTGGTACATACAGGCG R:TCGGTGGTTCAATTCAAAAAC

Supplemental Table 6. RT-qPCR primers used in this study. Sequences are written 5' to 3'. F, forward primer. R, reverse primer.

Genome Locus	Gene Symbol	Primer Sequences
AT2G19590	*ACO1*	F: TGGTCCAAAAGGTCCAGCTTT R: ATTCCCCCAGCATCCGTATG
AT1G62380	*ACO2*	F: TCTACGTTCGTCACCTCCCT R: AGTCTTTCATGGCCGTCCTG
AT1G12010	*ACO3*	F: ACAACGGGTCCAACTTTTGC R: TGTGAGCCCTAAGCCCTTTG
AT1G05010	*ACO4*	F: CTACCTCAAGCACCTTCCCG R: GCACAGCAGATCCAGTAGCT
AT1G77330	*ACO5*	F: AGTCAATGGCCTTCGAGCTC R: GATCCACTCGCCGTCTTTCA
AT3G18400	*ANAC058*	F: ACAACCTTTCAACCCCACGA R: TTTGCTGCCGTGCTCTTTTC
AT5G12330	*LRP1*	F: CTGTGGCTACAACGAGGAGG R: ACGGAAGCTGAGCCTAAACC
AT5G16770	*MYB9*	F: ACAAGTGGTCGTCGATAGCC R: GGCTATAAGCTGCGGGAGAG
AT1G17950	*MYB52*	F: CCGGTCGAACTGATAACGCT R: TAGCGGTTGTGGTTGCCAAT
AT1G34670	*MYB93*	F: ATCAACCCACCCAACCACTC R: GTCACCTTGCGATGGTAGCT
AT5G13330	*RAP2.6L*	F: CAAAGAAAGCAGCCCGTGTC R: GTTGTGGTGGTAGTAGGGCC
AT5G43175	*RSL5*	F: GCAATTTGGTTACCGAGCCT R: ATCCCTCTGTTGGCTTTCGC